

CHAPTER 18

NONRESIDENTIAL COOLING AND HEATING
LOAD CALCULATIONS

<i>Cooling Load Calculation Principles</i>	18.1	<i>Radiant Time Series (RTS) Method</i>	18.26
<i>Internal Heat Gains</i>	18.4	<i>Heating Load Calculations</i>	18.37
<i>Infiltration and Moisture Migration</i>		<i>System Heating and Cooling Load Effects</i>	18.46
<i>Heat Gains</i>	18.14	<i>Example Cooling and Heating Load Calculations</i>	18.49
<i>Fenestration Heat Gain</i>	18.19	<i>Previous Cooling Load Calculation Methods</i>	18.63
<i>Heat Balance Method</i>	18.20		

HEATING and cooling load calculations are the primary design basis for most heating and air-conditioning systems and components. These calculations affect the size of piping, ductwork, diffusers, air handlers, boilers, chillers, coils, compressors, fans, and every other component of systems that condition indoor environments. Cooling and heating load calculations can significantly affect first cost of building construction, comfort and productivity of occupants, and operating cost and energy consumption.

Simply put, heating and cooling loads are the rates of energy input (heating) or removal (cooling) required to maintain an indoor environment at a desired temperature and humidity condition. Heating and air conditioning systems are designed, sized, and controlled to accomplish that energy transfer. The amount of heating or cooling required at any particular time varies widely, depending on external (e.g., outdoor temperature) and internal (e.g., number of people occupying a space) factors.

Peak design heating and cooling load calculations, which are this chapter's focus, seek to determine the maximum rate of heating and cooling energy transfer needed to maintain the space conditions at the desired level (set point). Similar principles, but with different assumptions, data, and application, can be used to estimate building energy consumption, as described in Chapter 19.

This chapter discusses common elements of cooling and heating load calculation (e.g., internal heat gain, ventilation and infiltration, moisture migration, fenestration heat gain) and two methods of heating and cooling load estimation: heat balance (HB) and radiant time series (RTS).

1. COOLING LOAD CALCULATION PRINCIPLES

Cooling loads result from many conduction, convection, and radiation heat transfer processes through the building envelope and from internal sources and system components. Building components or contents that may affect cooling loads include the following:

- **External:** Walls, roofs, windows, skylights, doors, partitions, ceilings, and floors
- **Internal:** Lights, people, appliances, and equipment
- **Infiltration:** Air leakage and moisture migration
- **System:** Outdoor air, duct leakage and heat gain, reheat, fan and pump energy, and energy recovery

1.1 TERMINOLOGY

The variables affecting cooling load calculations are numerous, often difficult to define precisely, and always intricately interrelated.

The preparation of this chapter is assigned to TC 4.1, Load Calculation Data and Procedures.

Many cooling load components vary widely in magnitude, and possibly direction, during a 24 h period. Because these cyclic changes in load components often are not in phase with each other, each component must be analyzed to establish the maximum cooling load for a building or zone. A **zoned system** (i.e., one serving several independent areas, each with its own temperature control) needs to provide no greater total cooling load capacity than the largest hourly sum of simultaneous zone loads throughout a design day; however, it must handle the peak cooling load for each zone at its individual peak hour. At some times of day during heating or intermediate seasons, some zones may require heating while others require cooling. The zones' ventilation, humidification, or dehumidification needs must also be considered.

The current terminology presented here has been developed over time based on the assumption that heat will be removed from a space through a convective- (air system) based cooling process. ASHRAE research project RP-1729 (Moftakhari et al. 2020) shows that when cooling is provided through a predominantly radiant-based cooling system, conversion of heat gain to cooling load can differ from convective-based systems. It is always important to distinguish between room load and HVAC system load. This is true for both convective-based and radiant cooling systems. This chapter deals with calculation of the room cooling load. For radiant cooling systems, those room loads should be applied to calculation of HVAC system loads using principles described in Chapter 6 of the 2020 *ASHRAE Handbook—HVAC Systems and Equipment*. This current chapter is largely based on convective or air-system-based cooling, but some key differences that would exist with radiant systems will be pointed out.

Heat Flow Rates

In air-conditioning design, the following four related heat flow rates, each of which varies with time, must be differentiated.

Space Heat Gain. This instantaneous rate of heat gain is the rate at which heat enters into and/or is generated within a space. Heat gain is classified by its mode of entry into the space and whether it is sensible or latent. **Entry modes** include (1) solar radiation through transparent surfaces; (2) heat conduction through exterior walls and roofs; (3) heat conduction through ceilings, floors, and interior partitions; (4) heat generated in the space by occupants, lights, and appliances; (5) heat transfer through direct-with-space ventilation and infiltration of outdoor air; and (6) miscellaneous heat gains. **Sensible heat** is added directly to the conditioned space by conduction, convection, and/or radiation. **Latent heat** gain occurs when moisture is added to the space (e.g., from vapor emitted by occupants and equipment). To maintain a constant humidity ratio, water vapor must condense on the cooling apparatus and be removed at the same rate it is added to the space. The amount of energy required to offset latent heat gain essentially equals the product of the condensation rate and latent heat of condensation. In selecting cooling equipment, distinguish between sensible and latent heat gain: every cooling

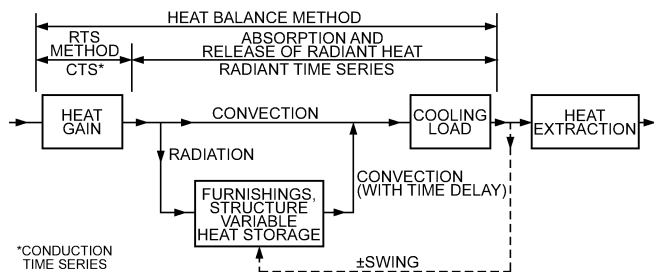


Fig. 1 Origin of Difference Between Magnitude of Instantaneous Heat Gain and Instantaneous Cooling Load

apparatus has different maximum removal capacities for sensible versus latent heat for particular operating conditions. In extremely dry climates, humidification may be required, rather than dehumidification, to maintain thermal comfort.

Radiant Heat Gain. Radiant heat gain will first be absorbed by surfaces that enclose the space (walls, floor, and ceiling) and objects in the space (furniture, etc.). With convective or air-based cooling systems, these surfaces and objects become warmer than the surrounding air and some of their heat transfers to the air by convection. The composite heat storage capacity of these surfaces and objects determines the rate at which their respective surface temperatures increase for a given radiant input, and thus governs the relationship between the radiant portion of heat gain and its corresponding conversion to space cooling load (Figure 1). The thermal storage effect is critical in differentiating between instantaneous heat gain for a given space and its cooling load at that moment. Predicting the nature and magnitude of this phenomenon to estimate a realistic cooling load for a particular set of circumstances has long been of interest to design engineers; the Bibliography lists some early work on the subject.

With radiant-based cooling systems, radiant gains are still absorbed by surfaces in the space but the process of conversion from radiant heat gains to cooling load can be very different than would occur with convective or air-based cooling systems. The first difference occurs if the radiant gain strikes the radiant cooling surface directly. In this case, the radiant gain is converted to cooling load immediately as the heat is absorbed directly by the active radiant cooling system. Other radiant gains are absorbed by nonactive surfaces in the space. In these cases, though, the heat gain could be converted to cooling load either by convection to the space air or through radiation exchange with the active radiant cooling surface. ASHRAE research project RP-1729 (Moftakhari et al. 2020) found that in general, the radiant system maintains nonactive surfaces at a temperature below the room air and that most absorbed radiant gains are converted to cooling load by exchange with the radiant cooling system. This resulted in less stored heat and less time lag between the heat gain and its conversion to cooling load as compared to conventional air based systems.

The heat transfer mechanics of the conversion of radiant heat gains to cooling load does not depend on the mass of the radiant cooling device. All radiant exchange between the cooling device and the space is through the exposed surface of the device. The position, configuration, and surface area of the device can result in different heat transfer dynamics. For example, a radiant cooling floor interacts differently with direct solar gain than a radiant ceiling would for a given space. The same might be true for radiant gain from ceiling-mounted lighting, though RP-1729 performed experiments only for the case of radiant ceiling panels. Computer modeling was done to explore the differences between ceiling- and floor-mounted radiant cooling devices, verifying these conclusions.

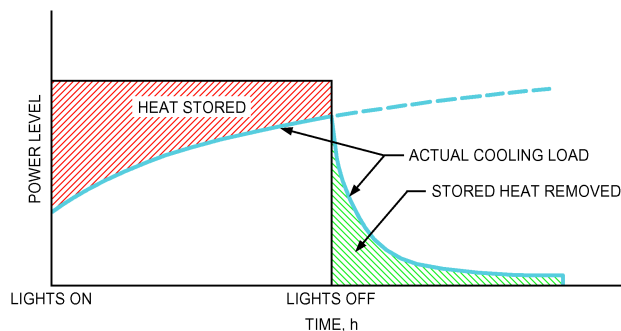


Fig. 2 Thermal Storage Effect in Cooling Load from Lights

Space Cooling Load. This is the rate at which sensible and latent heat must be removed from the space to maintain a constant space air temperature and humidity. The sum of all space instantaneous heat gains at any given time does not necessarily (or even frequently) equal the cooling load for the space at that same time because of the effect of radiant gains being stored in the building mass, as described previously.

Space Heat Extraction Rate. The rates at which sensible and latent heat are removed from the conditioned space equal the space cooling load when the room air temperature and humidity are constant. Along with the intermittent operation of cooling equipment, control systems usually allow a minor cyclic variation or swing in room temperature; humidity is often allowed to float, but it can be controlled. Therefore, proper simulation of the control system gives a more realistic value of energy removal over a fixed period than using values of the space cooling load. However, this is primarily important for estimating energy use over time; it is not needed to calculate design peak cooling load for equipment selection.

Cooling Coil Load. The rate at which energy is removed at a cooling coil serving one or more conditioned spaces equals the sum of instantaneous space cooling loads (or space heat extraction rate, if it is assumed that space temperature and humidity vary) for all spaces served by the coil, plus any system loads. System loads include fan heat gain, duct heat gain, and outdoor air heat and moisture brought into the cooling equipment to satisfy the ventilation air requirement.

Time Delay Effect

Heat gain absorbed by walls, floor, furniture, etc., contributes to space cooling load only after it has been converted to cooling load, as described previously. Some of this stored heat gain can still be present and converting to cooling load even after the heat gain sources have been switched off or removed, as shown in Figure 2.

For other than purely convective heat gains, there is some delay between the time a heat source is activated and the point when the rate of conversion to cooling load equals the rate of heat gain (steady-state). This time lag must be considered when calculating cooling load, because the load required for the space can be much lower than the instantaneous heat gain being generated, and the space's peak load may be significantly affected.

Accounting for the time delay effect is the major challenge in cooling load calculations. Several methods, including the two presented in this chapter, have been developed to take the time delay effect into consideration.

1.2 COOLING LOAD CALCULATION METHODS

This chapter presents two load calculation methods that vary significantly from previous methods. The technology involved, however (the principle of calculating a heat balance for a given space) is

not new. The first of the two methods is the **heat balance (HB) method**; the second is **radiant time series (RTS)**, which is a simplification of the HB procedure. Both methods are explained in their respective sections.

Cooling load calculation of an actual, multiple-room building requires a complex computer program implementing the principles of either method.

Cooling Load Calculations in Practice

Load calculations should accurately describe the building. All load calculation inputs should be as accurate as reasonable, without using safety factors. Introducing compounding safety factors at multiple levels in the load calculation results in an unrealistic and oversized load.

Variation in heat transmission coefficients of typical building materials and composite assemblies, differing motivations and skills of those who construct the building, unknown infiltration rates, and the manner in which the building is actually operated are some of the variables that make precise calculation impossible. Even if the designer uses reasonable procedures to account for these factors, the calculation can never be more than a good estimate of the actual load. Frequently, a cooling load must be calculated before every parameter in the conditioned space can be properly or completely defined. An example is a cooling load estimate for a new building with many floors of unleased spaces for which detailed partition requirements, furnishings, lighting, and layout cannot be predefined. Potential tenant modifications once the building is occupied also must be considered. Load estimating requires proper engineering judgment that includes a thorough understanding of heat balance fundamentals.

Perimeter spaces exposed to high solar heat gain often need cooling during sunlit portions of traditional heating months, as do completely interior spaces with significant internal heat gain. These spaces can also have significant heating loads during nonsunlit hours or after periods of nonoccupancy, when adjacent spaces have cooled below interior design temperatures. The heating loads involved can be estimated conventionally to offset or to compensate for them and prevent overheating, but they have no direct relationship to the spaces' design heating loads.

Correct design and sizing of air-conditioning systems require more than calculation of the cooling load in the space to be conditioned. The type of air-conditioning system, ventilation rate, reheat, fan energy, fan location, duct heat loss and gain, duct leakage, heat extraction lighting systems, type of return air system, and any sensible or latent heat recovery all affect system load and component sizing. Adequate system design and component sizing require that system performance be analyzed as a series of psychrometric processes.

System design could be driven by either sensible or latent load, and both need to be checked. In a sensible-load-driven space (the most common case), the cooling supply air has surplus capacity to dehumidify, but this is usually permissible. For a space driven by latent load (e.g., an auditorium), supply airflow based on sensible load is likely not to have enough dehumidifying capability, so subcooling and reheating or some other dehumidification process is needed.

This chapter is primarily concerned with a given space or zone in a building. When estimating loads for a group of spaces (e.g., for an air-handling system that serves multiple zones), the assembled zones must be analyzed to consider (1) the simultaneous effects taking place; (2) any diversification of heat gains for occupants, lighting, or other internal load sources; (3) ventilation; and/or (4) any other unique circumstances. With large buildings that involve more than a single HVAC system, simultaneous loads and any additional diversity also must be considered when designing the central equipment that serves the systems. Methods presented in this chapter are expressed as hourly load summaries, reflecting 24 h input schedules

and profiles of the individual load variables. Specific systems and applications may require different profiles.

1.3 DATA ASSEMBLY

Calculating space cooling loads requires detailed building design information and weather data at design conditions. Generally, the following information should be compiled.

Building Characteristics. Building materials, component size, external surface colors, and shape are usually determined from building plans and specifications.

Configuration. Determine building location, orientation, and external shading from building plans and specifications. Shading from adjacent buildings can be determined from a site plan or by visiting the proposed site, but its probable permanence should be carefully evaluated before it is included in the calculation. The possibility of abnormally high ground-reflected solar radiation (e.g., from adjacent water, sand, or parking lots) or solar load from adjacent reflective buildings should not be overlooked.

Outdoor Design Conditions. Obtain appropriate weather data, and select outdoor design conditions. Chapter 14 provides information for many weather stations; note, however, that these design dry-bulb and mean coincident wet-bulb temperatures may vary considerably from data traditionally used in various areas. Use judgment to ensure that results are consistent with expectations. Also, consider prevailing wind velocity and the relationship of a project site to the selected weather station.

Recent research projects have greatly expanded the amount of available weather data (e.g., ASHRAE 2012). In addition to the conventional dry bulb with mean coincident wet bulb, data are now available for wet bulb and dew point with mean coincident dry bulb. Peak space load generally coincides with peak solar or peak dry bulb, but peak system load often occurs at peak wet-bulb temperature. The relationship between space and system loads is discussed further in following sections of the chapter.

To estimate conductive heat gain through exterior surfaces and infiltration and outdoor air loads at any time, applicable outdoor dry- and wet-bulb temperatures must be used. Chapter 14 gives monthly cooling load design values of outdoor conditions for many locations. These are generally midafternoon conditions; for other times of day, the daily range profile method described in Chapter 14 can be used to estimate dry- and wet-bulb temperatures. Peak cooling load is often determined by solar heat gain through fenestration; this peak may occur in winter months and/or at a time of day when outdoor air temperature is not at its maximum.

Indoor Design Conditions. Select indoor dry-bulb temperature, indoor relative humidity, and ventilation rate. Include permissible variations and control limits. Consult ASHRAE *Standard* 90.1 for energy-savings conditions, and *Standard* 55 for ranges of indoor conditions needed for thermal comfort.

Internal Heat Gains and Operating Schedules. Obtain planned density and a proposed schedule of lighting, occupancy, internal equipment, appliances, and processes that contribute to the internal thermal load.

Areas. Use consistent methods for calculation of building areas. For fenestration, the definition of a component's area must be consistent with associated ratings.

Gross surface area. It is efficient and conservative to derive gross surface areas from outer building dimensions, ignoring wall and floor thicknesses and avoiding separate accounting of floor edge and wall corner conditions. Measure floor areas to the outside of adjacent exterior walls or to the centerline of adjacent partitions. When apportioning to rooms, façade area should be divided at partition centerlines. Wall height should be taken as floor-to-floor height.

Table 1 Representative Rates at Which Heat and Moisture Are Given Off by Human Beings in Different States of Activity

Degree of Activity	Location	Total Heat, W		Sensible Heat, W	Latent Heat, W	% Sensible Heat that is Radiant ^b	
		Adult Male	Adjusted, M/F ^a			Low V	High V
Seated at theater	Theater	114	103	72	31	60	27
Seated, very light work	Offices, hotels, apartments	132	117	72	45		
Moderately active office work	Offices, hotels, apartments	139	132	73	59		
Standing, light work; walking	Department store; retail store	161	132	73	59	58	38
Walking, standing	Drug store, bank	161	147	73	73		
Sedentary work	Restaurant ^c	144	161	81	81		
Light bench work	Factory	235	220	81	139		
Moderate dancing	Dance hall	264	249	89	160	49	35
Walking 3 mph; light machine work	Factory	293	293	110	183		
Bowling ^d	Bowling alley	440	425	170	255		
Heavy work	Factory	440	425	170	255	54	19
Heavy machine work; lifting	Factory	469	469	186	283		
Athletics	Gymnasium	587	528	208	320		

Notes:

1. Tabulated values are based on 23.9°C room dry-bulb temperature. For 26.7°C room dry bulb, total heat remains the same, but sensible heat values should be decreased by approximately 20%, and latent heat values increased accordingly.

2. Also see Table 4, Chapter 9, for additional rates of metabolic heat generation.

3. All values are rounded to nearest watt.

^aAdjusted heat gain is based on normal percentage of men, women, and children for the application listed, and assumes that gain from an adult female is 85% of that for an adult male, and gain from a child is 75% of that for an adult male.

^bValues approximated from data in Table 6, Chapter 9, where V is air velocity with limits shown in that table.

^cAdjusted heat gain includes 18 W for food per individual (9 W sensible and 9 W latent).

^dFigure one person per alley actually bowling, and all others as sitting (117 W) or standing or walking slowly (161 W).

The outer-dimension procedure is expedient for load calculations, but it is not consistent with rigorous definitions used in building-related standards. The resulting differences do not introduce significant errors in this chapter's procedures.

Fenestration area. As discussed in Chapter 15, fenestration ratings [U-factor and solar heat gain coefficient (SHGC)] are based on the entire product area, including frames. Thus, for load calculations, fenestration area is the area of the rough opening in the wall or roof.

Net surface area. Net surface area is the gross surface area less any enclosed fenestration area.

2. INTERNAL HEAT GAINS

Internal heat gains from people, lights, motors, appliances, and equipment can contribute the majority of the cooling load in a modern building. As building envelopes have improved in response to more restrictive energy codes, internal loads have increased because of factors such as increased use of computers and the advent of dense-occupancy spaces (e.g., call centers). Internal heat gain calculation techniques are identical for both heat balance (HB) and radiant time series (RTS) cooling-load calculation methods, so internal heat gain data are presented here independent of calculation methods.

2.1 PEOPLE

Table 1 gives representative rates at which sensible heat and moisture are emitted by humans in different states of activity. In high-density spaces, such as auditoriums, these sensible and latent heat gains comprise a large fraction of the total load. Even for short-term occupancy, the extra sensible heat and moisture introduced by people may be significant. See Chapter 9 for detailed information; however, Table 1 summarizes design data for common conditions.

The conversion of sensible heat gain from people to space cooling load is affected by the thermal storage characteristics of that space because some percentage of the sensible load is radiant energy. Latent heat gains are usually considered instantaneous, but

research is yielding practical models and data for the latent heat storage of and release from common building materials.

2.2 LIGHTING

Because lighting is often a major space cooling load component, an accurate estimate of the space heat gain it imposes is needed. Calculation of this load component is not straightforward; the rate of cooling load from lighting at any given moment can be quite different from the heat equivalent of power supplied instantaneously to those lights, because of heat storage.

Instantaneous Heat Gain from Lighting

The primary source of heat from lighting comes from light-emitting elements, or lamps, although significant additional heat may be generated from ballasts and other appurtenances in the luminaires. Generally, the instantaneous rate of sensible heat gain from electric lighting may be calculated from

$$q_{el} = WF_{ul}F_{sa} \quad (1)$$

where

q_{el} = heat gain, W

W = total light wattage, W

F_{ul} = lighting use factor

F_{sa} = lighting special allowance factor

The **total light wattage** is obtained from the ratings of all lamps installed, both for general illumination and for display use. Ballasts are not included, but are addressed by a separate factor. Wattages of magnetic ballasts are significant; the energy consumption of high-efficiency electronic ballasts might be insignificant compared to that of the lamps.

The **lighting use factor** is the ratio of wattage in use, for the conditions under which the load estimate is being made, to total installed wattage. For commercial applications such as stores, the use factor is generally 1.0.

The **special allowance factor** is the ratio of the lighting fixtures' power consumption, including lamps and ballast, to the nominal

power consumption of the lamps. For incandescent lights, this factor is 1. For fluorescent lights, it accounts for power consumed by the ballast as well as the ballast's effect on lamp power consumption. The special allowance factor can be less than 1 for electronic ballasts that lower electricity consumption below the lamp's rated power consumption. Use manufacturers' values for system (lamps + ballast) power, when available.

For high-intensity-discharge lamps (e.g. metal halide, mercury vapor, high- and low-pressure sodium vapor lamps), the actual lighting system power consumption should be available from the manufacturer of the fixture or ballast. Ballasts available for metal halide and high-pressure sodium vapor lamps may have special allowance factors from about 1.3 (for low-wattage lamps) down to 1.1 (for high-wattage lamps).

An alternative procedure is to estimate the lighting heat gain on a per-square-metre basis. Such an approach may be required when final lighting plans are not available. Table 2 shows the maximum lighting power density (LPD) (lighting heat gain per square metre) allowed by ASHRAE *Standard* 90.1-2019 for a range of space types.

In addition to determining the lighting heat gain, the fraction of lighting heat gain that enters the conditioned space may need to be distinguished from the fraction that enters an unconditioned space; of the former category, the distribution between radiative and convective heat gain must be established.

Fisher and Chantrasrisalai (2006) and Zhou et al. (2016) experimentally studied 12 luminaire types and recommended several categories of luminaires, as shown in Table 3. The table provides a range of design data for the conditioned space fraction, short-wave radiative fraction, and long-wave radiative fraction under typical operating conditions: airflow rate of 5 L/(s·m²), supply air temperature between 15 and 16.7°C, and room air temperature between 22 and 24°C. The recommended fractions in Table 3 are based on lighting heat input rates range of 9.7 to 28 W/m². For higher design power input, the lower bounds of the space and short-wave fractions should be used; for design power input below this range, the upper bounds of the space and short-wave fractions should be used. The **space fraction** in the table is the fraction of lighting heat gain that goes to the room; the fraction going to the plenum can be computed as 1 – the space fraction. The **radiative fraction** is the radiative part of the lighting heat gain that goes to the room. The convective fraction of the lighting heat gain that goes to the room is 1 – the radiative fraction. Using values in the middle of the range yields sufficiently accurate results. However, values that better suit a specific situation may be determined according to the notes for Table 3.

Table 3's data apply to both ducted and non-ducted returns. However, application of the data, particularly the ceiling plenum fraction, may vary for different return configurations. For instance, for a room with a ducted return, although a portion of the lighting energy initially dissipated to the ceiling plenum is quantitatively equal to the plenum fraction, a large portion of this energy would likely end up as the conditioned space cooling load and a small portion would end up as the cooling load to the return air.

If the space airflow rate is different from the typical condition [i.e., about 5 L/(s·m²)], Figure 3 can be used to estimate the lighting heat gain parameters. Design data shown in Figure 3 are only applicable for the recessed fluorescent luminaire without lens.

Although design data presented in Table 3 and Figure 3 can be used for a vented luminaire with side-slot returns, they are likely not applicable for a vented luminaire with lamp compartment returns, because in the latter case, all heat convected in the vented luminaire is likely to go directly to the ceiling plenum, resulting in zero convective fraction and a much lower space fraction. Therefore, the design data should only be used for a configuration where conditioned air is returned through the ceiling grille or luminaire side slots.

For other luminaire types, it may be necessary to estimate the heat gain for each component as a fraction of the total lighting heat

gain by using judgment to estimate heat-to-space and heat-to-return percentages.

Because of the directional nature of downlight luminaires, a large portion of the short-wave radiation typically falls on the floor. When converting heat gains to cooling loads in the RTS method, the solar **radiant time factors (RTFs)** may be more appropriate than nonsolar RTFs. (Solar RTFs are calculated assuming most solar radiation is intercepted by the floor; nonsolar RTFs assume uniform distribution by area over all interior surfaces.) This effect may be significant for rooms where lighting heat gain is high and for which solar RTFs are significantly different from nonsolar RTFs.

2.3 ELECTRIC MOTORS

Instantaneous sensible heat gain from equipment operated by electric motors in a conditioned space is calculated as

$$q_{em} = 2545(P/E_M)F_{UM}F_{LM} \quad (2)$$

where

q_{em} = heat equivalent of equipment operation, W

P = motor power rating, W

E_M = motor efficiency, decimal fraction <1.0

F_{UM} = motor use factor, 1.0 or decimal fraction <1.0

F_{LM} = motor load factor, 1.0 or decimal fraction <1.0

The motor use factor may be applied when motor use is known to be intermittent, with significant nonuse during all hours of operation (e.g., overhead door operator). For conventional applications, its value is 1.0.

The motor load factor is the fraction of the rated load delivered under the conditions of the cooling load estimate. Equation (2) assumes that both the motor and driven equipment are in the conditioned space. If the motor is outside the space or airstream,

$$q_{em} = 2545PF_{UM}F_{LM} \quad (3)$$

When the motor is inside the conditioned space or airstream but the driven machine is outside,

$$q_{em} = P \left(\frac{1.0 - E_M}{E_M} \right) F_{UM}F_{LM} \quad (4)$$

Equation (4) also applies to a fan or pump in the conditioned space that exhausts air or pumps fluid outside that space.

Table 4A and 4B gives minimum efficiencies and related data representative of typical electric motors from ASHRAE *Standard*

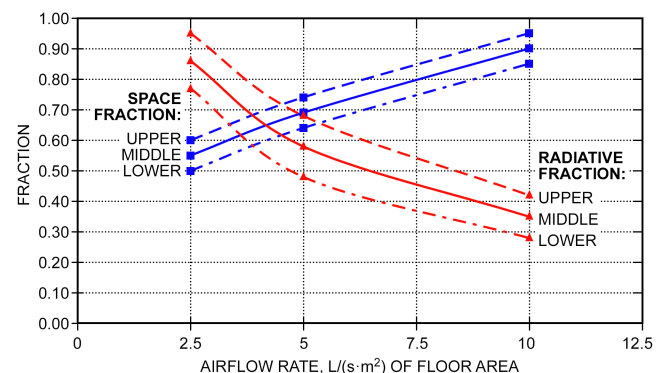


Fig. 3 Lighting Heat Gain Parameters for Recessed Fluorescent Luminaire Without Lens

(Fisher and Chantrasrisalai 2006)

Table 2 Lighting Power Densities Using Space-by-Space Method

Common Space Types*	LPD, W/m ²	Common Space Types ^a	LPD, W/m ²	Building-Specific Space Types*	LPD, W/m ²
Atrium		Lobby		Playing area	9.2
<6.1 m in height	4.6	Facility for the visually impaired (and not used primarily by staff) ^c	18.2	Health Care Facility	
≥6.1 m and ≤12.2 m in height	5.2	Elevator	7.0	In exam/treatment room	15.1
>12.2 m in height	6.5	Hotel	5.4	In imaging room	10.1
Audience Seating Area		Motion picture theater	2.5	Medical supply room	6.7
Auditorium	6.5	Performing arts theater	13.5	Nursery	9.9
Gymnasium	2.5	All other lobbies	9.0	Nurses' station	12.6
Motion picture theater	2.9	Locker Room	5.6	Operating room	24.3
Penitentiary	7.2	Lounge/Breakroom		Patient room	7.3
Performing arts theater	12.5	Health care facility	4.5	Physical therapy room	9.8
Religious building	7.8	All other lounges/breakrooms	6.3	Recovery room	13.5
Sports arena	3.5	Office		Library	
All other audience seating areas	2.5	Enclosed and ≤23.2 m ²	8.0	Reading area	10.3
Banking Activity Area	6.5	Enclosed and >23.2 m ²	7.1	Stacks	12.7
Breakroom (See Lounge/Breakroom)		Open plan	6.6	Manufacturing Facility	
Classroom/Lecture Hall/Training Room		Parking Area, Interior	1.6	Detailed manufacturing area	8.6
Penitentiary	9.5	Pharmacy Area	17.9	Equipment room	8.2
All other classrooms/lecture halls/training rooms	7.6	Restroom		Extra-high-bay area (15.2 m floor-to-ceiling height)	15.3
Conference/Meeting/Multipurpose Room	10.5	Facility for the visually impaired (and not used primarily by staff) ^c	13.5	High-bay area (7.6 to 15.2 m floor-to-ceiling height)	13.4
Confinement Cells	7.5	All other restrooms	6.8	Low-bay area (<7.6 m floor-to-ceiling height)	9.3
Copy/Print Room	3.3	Sales Area^d	11.3	Museum	
Corridor^b		Seating Area, General	2.5	General exhibition area	3.3
Facility for visually impaired (and not used primarily by staff) ^c	7.7	Stairway		Restoration room	11.9
Hospital	7.7	Space containing stairway determines LPD and control requirements for stairway.		Performing Arts Theater, Dressing Room	4.4
All other corridors	4.4	Stairwell	5.3	Post Office, Sorting Area	8.1
Courtroom	12.9	Storage Room		Religious Buildings	
Computer Room	10.1	<4.6 m ²	5.5	Fellowship hall	5.8
Dining Area		>4.6 m ²	4.1	Worship/pulpit/choir area	9.2
Penitentiary	4.5	Vehicular Maintenance Area	6.5	Retail Facilities	
Facility for visually impaired (and not used primarily by staff) ^c	13.7	Workshop	13.5	Dressing/fitting room	5.4
Bar/lounge or leisure dining	9.3			Mall concourse	8.8
Cafeteria or fast food dining	4.3	Building-Specific Space Types* LPD, W/m²		Sports Arena, Playing Area^g	
Family dining	6.5	Facility for Visually Impaired^c		Class I facility	31.6
All other dining areas	4.7	Chapel (used primarily by residents)	7.5	Class II facility	21.6
Electrical/Mechanical Room^f	4.6	Recreation room/common living room (and not used primarily by staff)	19.0	Class III facility	13.9
Emergency Vehicle Garage	5.6	Automotive (See Vehicular Maintenance Area)		Class IV facility	9.3
Food Preparation Area	11.7	Convention Center: Exhibit Space	6.6	Transportation Facility	
Guest Room	4.4	Dormitory/Living Quarters	5.4	Baggage/carousel area	4.2
Laboratory		Fire Station: Sleeping Quarters	2.5	Airport concourse	2.7
In or as classroom	11.9	Gymnasium/Fitness Center		Ticket counter	5.5
All other laboratories	14.3	Exercise area	9.6	Warehouse—Storage Area	
Laundry/Washing Area	5.7			Medium to bulky, palletized items	3.6
Loading Dock, Interior	9.5			Smaller, hand-carried items ^e	7.4

Source: ASHRAE Standard 90.1-2019, Table 9.6.1.

^aIn cases where both a common space type and a building-specific type are listed, the building-specific space type applies.^bIn corridors, the extra lighting power density allowance is granted when corridor width is <2.4 m and is not based on room/corridor ratio (RCR).^cA "Facility for the Visually Impaired" is a facility that can be documented as being designed to comply with light levels in ANSI/IES RP-28 and is licensed or will be licensed by local/state authorities for either senior long-term care, adult daycare, senior support, and/or people with special visual needs.^dFor accent lighting, see section 9.6.2(b) of ASHRAE Standard 90.1-2019.^eSometimes called a "Picking Area".^fAn additional 5.6 W/m² shall be allowed, provided that the additional lighting is controlled separately from the base allowance of 4.6 W/m². The additional 5.6 W/m² allowance shall not be used for any other purpose.^gClass of play as defined by IES RP-6.

Table 3 Lighting Heat Gain Parameters for Typical Operating Conditions

Luminaire Category	Space Fraction	Radiative Fraction	Notes
Recessed fluorescent luminaire without lens	0.64 to 0.74	0.48 to 0.68	Use middle values in most situations May use higher space fraction, and lower radiative fraction for luminaire with side-slot returns May use lower values of both fractions for direct/indirect luminaire May use higher values of both fractions for ducted returns
Recessed fluorescent luminaire with lens	0.40 to 0.50	0.61 to 0.73	May adjust values in the same way as for recessed fluorescent luminaire without lens
Downlight compact fluorescent luminaire	0.12 to 0.24	0.95 to 1.0	Use middle or high values if detailed features are unknown Use low value for space fraction and high value for radiative fraction if there are large holes in luminaire's reflector
Downlight incandescent luminaire	0.70 to 0.80	0.95 to 1.0	Use middle values if lamp type is unknown Use low value for space fraction if standard lamp (i.e. A-lamp) is used Use high value for space fraction if reflector lamp (i.e. BR-lamp) is used
Non-in-ceiling fluorescent luminaire	1.0	0.5 to 0.57	Use lower value for radiative fraction for surface-mounted luminaire Use higher value for radiative fraction for pendant luminaire
Recessed LED troffer partial aperture diffuser	0.49 to 0.64	0.37 to 0.47	Use middle value in most cases May use higher space fraction for ducted return configuration and lower space fraction for high supply air temperature May use higher radiant value for ducted return configuration and lower value for large supply airflow rate
Recessed LED troffer uniform diffuser	0.44 to 0.66	0.32 to 0.41	Use middle value in most cases. May use higher space fraction for smaller supply airflow rate and lower value for larger supply airflow rate. May use higher radiant value for ducted return configuration and lower value for larger supply airflow rate.
Recessed high-efficacy LED troffer	0.59	0.51	
Recessed LED downlight	0.40 to 0.56	0.15 to 0.18	Use middle value in most cases. May use higher space fraction value for high supply air temperature and lower value for smaller air flowrate. May use higher radiant value for dimming control and lower value for large supply air flowrate.
Recessed LED retrofit kit 2×4	0.41 to 0.53	0.31 to 0.42	Use middle value in most cases. May use higher space fraction value for large supply air flowrate and lower value for ducted return configuration. May use higher radiant value for ducted return configuration and lower value for larger supply airflow rate.
Recessed LED color tuning fixture	0.53 to 0.56	0.40 to 0.42	Use middle value in most cases.
High-bay LED fixture	1.0	0.42 to 0.51	Use middle value in most cases.
Linear pendant LED fixture	1.0	0.55 to 0.60	Use middle value in most cases.

Sources: Fisher and Chantrasrisalai (2006); Zhou et al. (2016).

90.1-2019. If electric motor load is an appreciable portion of cooling load, the motor efficiency should be obtained from the manufacturer. Also, depending on design, maximum efficiency might occur anywhere between 75 to 110% of full load; if under- or overloaded, efficiency could vary from the manufacturer's listing.

Overloading or Underloading

Heat output of a motor is generally proportional to motor load, within rated overload limits. Because of typically high no-load motor current, fixed losses, and other reasons, F_{LM} is generally assumed to be unity, and no adjustment should be made for underloading or overloading unless the situation is fixed and can be accurately established, and reduced-load efficiency data can be obtained from the motor manufacturer.

Radiation and Convection

Unless the manufacturer's technical literature indicates otherwise, motor heat gain normally should be equally divided between

radiant and convective components for the subsequent cooling load calculations.

2.4 APPLIANCES

A cooling load estimate should take into account heat gain from all appliances (electrical, gas, or steam). Because of the variety of appliances, applications, schedules, use, and installations, estimates can be very subjective. Often, the only information available about heat gain from equipment is that on its nameplate, which can overestimate actual heat gain for many types of appliances, as discussed in the section on Office Equipment.

Cooking Appliances

These appliances include common heat-producing cooking equipment found in conditioned commercial kitchens.

Fundamental Principles. In commercial kitchens, appliances are typically turned on at the beginning of each operating period and are not turned off until closing time. Although the appliances are

Table 4A Minimum Nominal Full-Load Efficiency for NEMA Design A, NEMA Design B, and IEC Design N Motors (excluding Fire Pump Electric Motors) at 60 Hz^{a,b}

Number of Poles ⇒	2	2	4	4	6	6	8	8
Motor Type ⇒	Enclosed	Open	Enclosed	Open	Enclosed	Open	Enclosed	Open
<i>Motor Kilowatts</i>								
0.75	77.0	77.0	85.5	85.5	82.5	82.5	75.5	75.5
1.1	84.0	84.0	86.5	86.5	87.5	86.5	78.5	77.0
1.5	85.5	85.5	86.5	86.5	88.5	87.5	84.0	86.5
2.2	86.5	85.5	89.5	89.5	89.5	88.5	85.5	87.5
3.7	88.5	86.5	89.5	89.5	89.5	89.5	86.5	88.5
5.5	89.5	88.5	91.7	91.0	91.0	90.2	86.5	89.5
7.5	90.2	89.5	91.7	91.7	91.0	91.7	89.5	90.2
11	91.0	90.2	92.4	93.0	91.7	91.7	89.5	90.2
15	91.0	91.0	93.0	93.0	91.7	92.4	90.2	91.0
18.5	91.7	91.7	93.6	93.6	93.0	93.0	90.2	91.0
22	91.7	91.7	93.6	94.1	93.0	93.6	91.7	91.7
30	92.4	92.4	94.1	94.1	94.1	94.1	91.7	91.7
37	93.0	93.0	94.5	94.5	94.1	94.1	92.4	92.4
45	93.6	93.6	95.0	95.0	94.5	94.5	92.4	93.0
55	93.6	93.6	95.4	95.0	94.5	94.5	93.6	94.1
75	94.1	93.6	95.4	95.4	95.0	95.0	93.6	94.1
90	95.0	94.1	95.4	95.4	95.0	95.0	94.1	94.1
110	95.0	94.1	95.8	95.8	95.8	95.4	94.1	94.1
150	95.4	95.0	96.2	95.8	95.8	95.4	94.5	94.1
186	95.8	95.0	96.2	95.8	95.8	95.8	95.0	95.0
224	95.8	95.4	96.2	95.8	95.8	95.8	NA	NA
261	95.8	95.4	96.2	95.8	95.8	95.8	NA	NA
298	95.8	95.8	96.2	95.8	NA	NA	NA	NA
336	95.8	96.2	96.2	96.2	NA	NA	NA	NA
373	95.8	96.2	96.2	96.2	NA	NA	NA	NA

Source: ASHRAE Standard 90.1-2019, Table 10.8-1

^a Nominal efficiencies shall be established in accordance with 10 CFR 431.

^b For purposes of determining the required minimum nominal full-load efficiency of an electric motor that has a horsepower or kilowatt rating between two horsepower or two kilowatt ratings listed in this table, each such motor shall be deemed to have a listed horsepower or kilowatt rating, determined as follows:

1. A horsepower at or above the midpoint between the two consecutive horsepower shall be rounded up to the higher of the two horsepower.
2. A horsepower below the midpoint between the two consecutive horsepower shall be rounded down to the lower of the two horsepower.
3. A kilowatt rating shall be directly converted from kilowatts to horsepower using the formula 1 kilowatt = (1/0.746) horsepower. The conversion should be calculated to three significant decimal places, and the resulting horsepower shall be rounded in accordance with paragraph (1) or (2), whichever applies.

“up to temperature” all of the time, they may be used to cook food less than 25% of the time. The “up to temperature” condition is referred to as the “idle (ready to cook)” condition, while “cooking” condition is when the appliance is being used to cook food. Due to this operation, idle (ready to cook) heat gain measurements provide a good estimate of heat gain for calculating cooling load (Swierczyna et al. 2008). In estimating appliance heat gains, probabilities of simultaneous use and operation for different appliances located in the same space should be considered.

Cooking appliances generate three types of heat gain to the kitchen space: sensible radiant, sensible convective, and latent heat gain. For unhooded appliances, all three types of heat gain contribute to cooling load in the kitchen space. For hooded appliances, Marn (1962) determined that, where appliances are installed under an effective hood, only sensible radiant gain adds to the cooling load of the kitchen space. Convective and latent heat from cooking and combustion products are exhausted and do not enter the kitchen

space. Gordon et al. (1994) and Smith et al. (1995) substantiated these findings. Chapter 35 of the 2019 ASHRAE *Handbook—HVAC Applications* has more information on kitchen ventilation. Marn (1962) also concluded that appliance surfaces contributed most of the heat to commercial kitchens and that when appliances were installed under an effective hood, the cooling load was independent of the fuel or energy used for similar unhooded equipment performing the same operations.

Radiant heat gain from hooded cooking equipment can range from 15 to 45% of the actual appliance energy consumption (Gordon et al. 1994; Smith et al. 1995; Swierczyna et al. 2008; Talbert et al. 1973). This ratio of heat gain to appliance energy consumption may be expressed as a radiation factor, F_R , and it is a function of both appliance type and fuel source. The radiation factor is applied to the average rate of appliance energy consumption, determined by applying usage factor F_U to the nameplate or rated energy input:

Table 4B Minimum Average Full-Load Efficiency for Polyphase Small Electric Motors^a

Full-Load Efficiency, %				
Number of Poles ⇒ Synchronous Speed (RPM) ⇒		Open Motors		
		2	4	6
		3600	1800	1200
Motor Kilowatts				
0.19	65.6	69.5	67.5	
0.25	69.5	73.4	71.4	
0.37	73.4	78.2	75.3	
0.56	76.8	81.1	81.7	
0.75	77.0	83.5	82.5	
1.1	84.0	86.5	83.8	
1.5	85.5	86.5	N/A	
2.2	85.5	86.9	N/A	

Source: ASHRAE Standard 90.1-2019, Table 10.8-3.

^aAverage full-load efficiencies shall be established in accordance with 10 CFR 431.

$$q_s = q_{input} F_U F_R \quad (5)$$

or

$$q_s = q_{input} F_L \quad (6)$$

where F_L is the ratio of sensible heat gain to the manufacturer's rated energy input.

ASHRAE research (Swierczyna et al. 2008, 2009) showed the design value for heat gain from a hooded appliance at idle (ready-to-cook) conditions based on its energy consumption rate is, at best, a rough estimate. When appliance heat gain measurements during idle conditions were regressed against energy consumption rates for gas and electric appliances, the appliances' emissivity, insulation, and surface cooling (e.g., through ventilation rates) scattered the data points widely, with large deviations from the average values. Because large errors could occur in the heat gain calculation for specific appliance types by using a general non-appliance-specific radiation factor, the appliance-specific radiation factors or heat gain values in Tables 5C through 5E should be applied in HVAC design rather than calculating heat gain using a non-appliance-specific radiation factor.

Gordon et al. (1994) and Smith et al. (1995) found that gas appliances may exhibit slightly higher heat gains than their electric counterparts under wall-canopy hoods operated at typical ventilation rates. This is because heat contained in combustion products exhausted from a gas appliance may increase the temperatures of the appliance and surrounding surfaces, as well as the hood above the appliance, more so than the heat produced by its electric counterpart. These higher-temperature surfaces radiate heat to the kitchen, adding moderately to the radiant gain directly associated with the appliance cooking surface.

Marn (1962) found that radiant heat temperature rise can be substantially reduced by shielding the fronts of cooking appliances. Although this approach may not always be practical in a commercial kitchen, radiant gains can also be reduced by adding side panels or partial enclosures that are integrated with the exhaust hood.

Heat Gain from Unhooded Cooking Appliances. Use the sensible radiant, sensible convective, and latent heat gains tabulated for unhooded appliances at idle (ready to cook) conditions in Table 5A, or at cooking conditions tabulated in Table 5B.

Heat Gain from Hooded Cooking Appliances. For specified or existing appliances where the actual nameplate rating is available, sensible radiant heat gain can be estimated using Equation (5) and the appliance-specific radiation and usage factors in Tables 5C, 5D, and 5E. When the appliance is not yet specified or the nameplate rat-

ing is not available, use the appliance-specific sensible radiant heat gains tabulated in Tables 5C, 5D, and 5E.

Warewashing Applications. Typically, hot-water sanitizing and conveyor-type dish machines have either a dishwasher/condensing hood or direct-connected ductwork. If the ventilation is not operating properly, there are significant sensible and latent gains to the space. Chemical sanitizing and vapor reduction models are typically unhooded; consequently, the dish machines produce internal gains that must be accounted for and managed by the building HVAC system.

Sensible radiant and convective gains are affected by dishwasher insulation, and latent convective gains are affected by door seals. Heat loads may vary.

Recirculating Systems. Cooking appliances ventilated by recirculating systems or "ductless" hoods should be treated as unhooded appliances when estimating heat gain. In other words, all energy consumed by the appliance and all moisture produced by cooking is introduced to the kitchen as a sensible or latent cooling load.

Recommended Heat Gain Values. Table 5 lists recommended rates of heat gain from typical commercial cooking appliances. Data in the "hooded" columns assume installation under a properly designed exhaust hood connected to a mechanical fan exhaust system operating at an exhaust rate for complete capture and containment of the thermal and effluent plume. Improperly operating hood systems load the space with a significant convective component of the heat gain.

Hospital and Laboratory Equipment

Hospital and laboratory equipment items are major sources of sensible and latent heat gains in conditioned spaces. Care is needed in evaluating the probability and duration of simultaneous usage when many components are concentrated in one area, such as a laboratory, an operating room, etc. Commonly, heat gain from equipment in a laboratory ranges from 50 to 220 W/m² or, in laboratories with outdoor exposure, as much as four times the heat gain from all other sources combined.

Medical Equipment. It is more difficult to provide generalized heat gain recommendations for medical equipment than for general office equipment because medical equipment is much more varied in type and in application. Some heat gain testing has been done, but the equipment included represents only a small sample of the type of equipment that may be encountered.

Data presented for medical equipment in Table 6 are relevant for portable and bench-top equipment. Medical equipment is very specific and can vary greatly from application to application. The data

Table 5A Recommended Rates of Radiant and Convective Heat Gain from Unhooded Electric Appliances During Idle (Ready-to-Cook) Conditions

Appliance	Energy Rate, W		Rate of Heat Gain, W				Usage Factor F_U	Radiation Factor F_R
	Rated	Standby	Sensible Radiant	Sensible Convective	Latent	Total		
Cabinet: hot serving (large), insulated ^a	1993	352	117	234	0	352	0.18	0.33
hot serving (large), uninsulated	1993	1026	205	821	0	1026	0.51	0.20
proofing (large) ^a	5099	410	352	0	59	410	0.08	0.86
proofing (small-15 shelf)	4191	1143	0	264	879	1143	0.27	0.00
Cheesemelter ^b	2400	976	443	533	0	976	0.41	0.45
Coffee brewing urn	3810	352	59	88	205	352	0.08	0.17
Drawer warmers, 2-drawer (moist holding) ^a	1202	147	0	0	59	59	0.12	0.00
Egg cooker ^b	2380	249	65	184	0	249	0.10	0.26
Espresso machine ^a	2403	352	117	234	0	352	0.15	0.33
Food warmer: steam table (2-well-type)	1495	1026	88	176	762	1026	0.69	0.08
Freezer (small)	791	322	147	176	0	322	0.41	0.45
Fryer, countertop, open deep fat ^b	4600	431	202	229	0	431	0.09	0.47
Griddle, countertop ^b	8000	1771	848	923	0	1771	0.22	0.48
Hot dog roller ^b	1600	1240	267	973	0	1240	0.77	0.22
Hot plate: single element, high speed ^b	1100	982	314	668	0	982	0.89	0.32
Hot-food case (dry holding) ^a	9115	733	264	469	0	733	0.08	0.36
Hot-food case (moist holding) ^a	9115	967	264	528	176	967	0.11	0.27
Induction hob, countertop ^b	5000	0	0	0	0	0	0.00	0.00
Microwave oven: commercial ^b	1700	0	0	0	0	0	0	0.00
Oven: countertop conveyorized bake/finishing ^b	5000	3932	718	3214	0	3932	0.79	0.18
Panini ^b	1800	673	195	478	0	673	0.37	0.29
Popcorn popper ^b	850	115	28	87	0	115	0.14	0.24
Rapid-cook oven (quartz-halogen) ^a	12 016	0	0	0	0	0	0	0.00
Rapid-cook oven (microwave/convection) ^b	5700	1141	96	1045	0	1141	0.20	0.08
Reach-in refrigerator ^a	1407	352	88	264	0	352	0.25	0.25
Refrigerated prep table ^a	586	264	176	88	0	264	0.45	0.67
Rice cooker ^b	1550	82	14	68	0	82	0.05	0.17
Soup warmer ^b	800	390	0	53	337	390	0.49	0.00
Steamer (bun) ^b	1500	200	32	168	0	200	0.13	0.16
Steamer, countertop ^b	8300	344	0	248	96	344	0.04	0.00
Toaster: 4-slice pop up (large): cooking	1788	879	59	410	293	762	0.49	0.07
contact (vertical) ^b	2600	759	180	579	0	759	0.29	0.24
conveyor (large)	9613	3019	879	2139	0	3019	0.31	0.29
small conveyor ^b	1745	1702	358	1344	0	1702	0.98	0.21
Tortilla grill ^b	2200	1034	254	780	0	1034	0.47	0.25
Waffle iron ^b	2700	267	60	207	0	267	0.10	0.22

Sources: Swierczyna et al. (2008, 2009), with the following exceptions as noted.

^aSwierczyna et al. (2009) only.

^bAdditions and updates from ASHRAE research project RP-1631 (Kong and Zhang 2016; Zhang et al. 2016).

are presented to provide guidance in only the most general sense. For large equipment, such as MRI, heat gain must be obtained from the manufacturer.

Laboratory Equipment. Equipment in laboratories is similar to medical equipment in that it varies significantly from space to space. Chapter 17 of the 2019 *ASHRAE Handbook—HVAC Applications* discusses heat gain from equipment, which may range from 50 to 270 W/m² in highly automated laboratories. Table 7 lists some values for laboratory equipment, but, as with medical equipment, it is for general guidance only. Wilkins and Cook (1999) also examined laboratory equipment heat gains.

Office Equipment

Computers, printers, copiers, etc., can generate very significant heat gains, sometimes greater than all other gains combined. ASHRAE research project RP-822 developed a method to measure the actual heat gain from equipment in buildings and the radiant/convective percentages (Hosni et al. 1998; Jones et al. 1998). This methodology was then incorporated into ASHRAE research project RP-1055 and applied to a wide range of equipment

(Hosni et al. 1999) as a follow-up to independent research by Wilkins and McGaffin (1994) and Wilkins et al. (1991). Komor (1997) found similar results. Analysis of measured data showed that results for office equipment could be generalized, but results from laboratory and hospital equipment proved too diverse. The following general guidelines for office equipment are a result of these studies.

Nameplate Versus Measured Energy Use. Nameplate data rarely reflect the actual power consumption of office equipment. Actual power consumption is assumed to equal total (radiant plus convective) heat gain, but its ratio to the nameplate value varies widely. ASHRAE research project RP-1055 (Hosni et al. 1999) found that, for general office equipment with nameplate power consumption of less than 1000 W, the actual ratio of total heat gain to nameplate ranged from 25 to 50%, but when all tested equipment is considered, the range is broader. Generally, if the nameplate value is the only information known and no actual heat gain data are available for similar equipment, it is conservative to use 50% of nameplate as heat gain and more nearly correct if 25% of nameplate is used. Much better results can be obtained, however, by considering

Table 5B Recommended Rates of Radiant and Convective Heat Gain from Unhooded Electric Appliances during Cooking Conditions

Appliance	Energy Rate, W		Rate of Heat Gain, W				Usage Factor F_U	Radiation Factor F_R
	Rated	Cooking	Sensible Radiant	Sensible Convective	Latent	Total		
Cheesemelter	2400	2714	443	1094	599	2136	1.13	0.16
Egg cooker	2380	1191	65	369	630	1065	0.50	0.05
Fryer, countertop, open deep fryer	4600	3818	202	492	1629	2323	0.83	0.05
Griddle, countertop	8000	3280	848	631	1277	2757	0.41	0.26
Hot dog roller	1600	1577	267	611	679	1556	0.99	0.17
Hot plate, single burner	1100	985	313	627	44	985	0.90	0.32
Induction hob, countertop	5000	653	0	318	335	653	0.13	0.00
Oven, conveyor	5000	4292	718	2454	193	3365	0.86	0.17
Microwave	1700	2363	0	934	995	1929	1.39	0.00
Rapid cook	5700	2310	96	1234	771	2102	0.41	0.04
Panini grill	1800	1374	195	718	150	1062	0.76	0.14
Popcorn popper	850	576	28	236	192	457	0.68	0.05
Rice cooker	1550	1159	14	95	44	153	0.75	0.01
Soup warmer	800	842	0	85	716	801	1.05	0.00
Steamer (bun)	1500	791	32	240	511	783	0.53	0.04
Steamer, countertop	8300	7731	0	499	6934	7433	0.93	0.00
Toaster, conveyor	1745	1705	358	974	373	1705	0.98	0.21
Vertical	2600	1841	180	715	322	1218	0.71	0.10
Tortilla grill	2200	2194	254	1267	673	2194	1.00	0.12
Waffle maker	2700	1180	60	357	559	975	0.44	0.05

Source: ASHRAE research project RP-1631 (Zhang et al. 2015).

Table 5C Recommended Rates of Radiant Heat Gain from Hooded Electric Appliances During Idle (Ready-to-Cook) Conditions

Appliance	Energy Rate, W		Rate of Heat Gain, W		Usage Factor F_U	Radiation Factor F_R
	Rated	Standby	Sensible Radiant			
Broiler: underfired 900 mm	10 814	9 056	3165		0.84	0.35
Cheesemelter*	3 605	3 488	1348		0.97	0.39
Fryer, kettle	29 014	528	147		0.02	0.28
Open deep-fat, 1-vat	14 008	821	293		0.06	0.36
Pressure	13 511	791	147		0.06	0.19
Griddle, double-sided 900 mm (clamshell down)*	21 218	2 022	410		0.10	0.20
(Clamshell up)*	21 218	3 370	1055		0.16	0.31
Flat 900 mm	17 115	3 370	1319		0.20	0.39
Small 900 mm*	8 997	1 788	791		0.20	0.44
Induction cooktop*	21 013	0	0		0.00	0.00
Induction wok*	3 488	0	0		0.00	0.00
Oven, combi: combi-mode*	16 411	1 612	234		0.10	0.15
Combi: convection mode	16 412	1 612	410		0.10	0.25
Oven, convection full-size	12 103	1 964	440		0.16	0.22
Convection half-size*	5 510	1 084	147		0.20	0.14
Pasta cooker*	22 010	2 491	0		0.11	0.00
Range top, top off/oven on*	4 865	1 172	293		0.24	0.25
3 elements on/oven off	15 005	4 513	1846		0.30	0.41
6 elements on/oven off	15 005	9 730	4074		0.65	0.42
6 elements on/oven on	19 870	10 668	4250		0.54	0.40
Range, hot-top	15 826	15 035	3458		0.95	0.23
Rotisserie*	11 107	4 044	1319		0.36	0.33
Salamander*	7 004	6 829	2051		0.97	0.30
Steam kettle, large (225 L), simmer lid down*	32 414	762	29		0.02	0.04
small (150 L), simmer lid down*	21 599	528	88		0.02	0.17
Steamer, compartment, atmospheric*	9 789	4 484	59		0.46	0.01
Tilting skillet/braising pan	9 642	1 553	0		0.16	0.00

*Items with an asterisk appear only in Swierczyna et al. (2009); all others appear in both Swierczyna et al. (2008) and (2009).

heat gain to be predictable based on the type of equipment. However, if the device has a mainly resistive internal electric load (e.g., a space heater), the nameplate rating may be a good estimate of its peak energy dissipation.

Computers. Based on tests by Hosni et al. (1999) and Wilkins and McGaffin (1994), nameplate values on computers should be ignored when performing cooling load calculations. Tables 8A, 8B, and 8C (Bach and Sarfraz 2018) present typical heat gain values for computers of varying types and models.

Table 5D Recommended Rates of Radiant Heat Gain from Hooded Gas Appliances during Idle (Ready-to-Cook) Conditions

Appliance	Standby Energy Rate, W		Rate of Heat Sensible Gain, W	Usage Factor F_U	Radiation Factor F_R
Broiler: batch*	27 842	20 280	2374	0.73	0.12
Chain (conveyor)	38 685	28 340	3869	0.73	0.14
Overfired (upright)*	29 307	25 761	733	0.88	0.03
Underfired 900 mm	28 135	21 658	2638	0.77	0.12
Fryer: doughnut	12 895	3634	850	0.28	0.23
Open deep-fat, 1 vat	23 446	1377	322	0.06	0.23
Pressure	23 446	2638	234	0.11	0.09
Griddle: double sided 900 mm, clamshell down*	31 710	2345	528	0.07	0.23
Clamshell up*	31 710	4308	1436	0.14	0.33
Flat 900 mm	26 376	5979	1084	0.23	0.18
Oven: combi: combi-mode*	22 185	1758	117	0.08	0.07
Convection mode	22 185	1700	293	0.08	0.17
Convection, full-size	12 895	3488	293	0.27	0.08
Conveyor (pizza)	49 822	20 017	2286	0.40	0.11
Deck	30 772	6008	1026	0.20	0.17
Rack mini-rotating*	16 500	1319	322	0.08	0.24
Pasta cooker*	23 446	6946	0	0.30	0.00
Range top: top off/oven on*	7327	2169	586	0.30	0.27
3 burners on/oven off	35 169	17 614	2081	0.50	0.12
6 burners on/oven off	35 169	35 403	3370	1.01	0.10
6 burners on/oven on	42 495	36 018	3986	0.85	0.11
Range: wok*	29 014	25 614	1524	0.88	0.06
Rethermalizer*	26 376	6829	3370	0.26	0.49
Rice cooker*	10 257	147	88	0.01	0.60
Salamander*	10 257	9759	1553	0.95	0.16
Steam kettle: large (225 L) simmer lid down*	42 495	1583	0	0.04	0.00
Small (38 L) simmer lid down*	15 240	967	88	0.06	0.09
Medium (150 L) simmer lid down	29 307	1260	0	0.04	0.00
Steamer: compartment: atmospheric*	7620	2432	0	0.32	0.00
Tilting skillet/braising pan	30 479	3048	117	0.10	0.04

*Items with an asterisk appear only in Swierczyna et al. (2009); all others appear in both Swierczyna et al. (2008) and (2009).

Table 5E Recommended Rates of Radiant Heat Gain from Hooded Solid-Fuel Appliances during Idle (Ready-to-Cook) Conditions

Appliance	Rated	Standby Energy Rate, W	Rate of Sensible Heat Gain, W	Usage Factor F_U	Radiation Factor F_R
Broiler: solid fuel: charcoal	18 kg	12 309	1817	N/A	0.15
Broiler: solid fuel: wood (mesquite)	18 kg	14 536	2051	N/A	0.14

Source: Swierczyna et al. (2008).

Monitors. Table 8D shows typical values for various sizes and types.

Flat-panel monitors have replaced CRT monitors in almost all workplaces. Power consumption, and thus heat gain, for flat-panel displays are significantly lower than for CRTs.

Laser Printers. Hosni et al. (1999) found that power consumption, and therefore the heat gain, of laser printers depended largely on the level of throughput for which the printer was designed. Smaller printers tend to be used more intermittently, and larger printers may run continuously for longer periods.

Table 9 presents data on typical printers. These data can be applied by taking the value for continuous operation and then applying an appropriate diversity factor. This would likely be most appropriate for larger open office areas. Another approach, which may be appropriate for a single room or small area, is to take the value that most closely matches the expected operation of the printer with no diversity.

Copiers. Bach and Sarfraz (2018) also tested photocopy machines, including desktop and office (freestanding high-volume copiers) models. Larger machines used in production environments were not addressed. Table 9 summarizes the results. Desktop copi-

ers rarely operate continuously, but office copiers frequently operate continuously for periods of an hour or more. Large, high-volume photocopiers often include provisions for exhausting air outdoors; if so equipped, the direct-to-space or system makeup air heat gain needs to be included in the load calculation. Also, when the air is dry, humidifiers are often operated near copiers to limit static electricity; if this occurs during cooling mode, their load on HVAC systems should be considered.

Miscellaneous Office Equipment. Table 10 presents data on miscellaneous office equipment such as vending machines and other equipment tested by Bach and Sarfraz (2018).

Diversity. The ratio of measured peak electrical load at equipment panels to the sum of the maximum electrical load of each individual item of equipment is the usage diversity. A small, one- or two-person office containing equipment listed in Tables 8 to 10 usually contributes heat gain to the space at the sum of the appropriate listed values. Progressively larger areas with many equipment items always experience some degree of usage diversity resulting from whatever percentage of such equipment is not in operation at any given time.

Wilkins and McGaffin (1994) measured diversity in 23 areas within five different buildings totaling over 25 600 m². Diversity

Table 5F Recommended Rates of Sensible and Latent Heat Gain to Space from Warewashing Equipment

Equipment Type	Supply Water Flow Rate, L/s	Operating Water Temperature, °C	Rate of Heat Gain to Space, W ^a				Usage Factor F_U ^c
			Sensible Radiant ^b	Sensible Convective	Latent	Total	
Pre-Rinse Equipment							
Pre-rinse spray valve	0.04	49	0	59	2403	2462	1
Pre-rinse spray valve	0.08	49	0	88	3429	3517	1
Pre-rinse spray valve	0.25	49	0	322	4044	4367	1
3-Compartment sink, rinsing	NA	49	0	264	1436	1700	1
Idle	NA	NA	0	205	586	791	NA
Power wash sink, rinsing	NA	49	0	586	909	1495	1
Idle	NA	NA	0	440	469	909	NA
Scrapper	1.14 ^d	49	0	352	3224	3575	1
Scrapper with trough	4.42 ^d	49	0	821	4074	4894	1
Unhooded Dishwashers							
Under-counter dishwasher, low temperature	0.05	60	0	645	1436	2081	1
Under-counter dishwasher, high temperature	0.05	82	0	1172	1348	2520	1
Under-counter dishwasher, high temperature with heat recovery	0.04	82	0	645	322	967	1
Upright door type, low temperature dump and fill	0.06	49	0	938	1026	1964	1
Upright door type, low temperature with tank	0.04	60	0	1143	3869	5012	1
Upright door type, high temperature	0.06	82	0	2345	6272	8616	1
Upright door type, high temperature with heat recovery	0.06	82	0	1407	3810	5217	1
Pot and pan washer	0.15	82	0	1758	6887	8646	1
Pot and pan washer with heat recovery	0.15	82	0	1612	5568	7180	1
1120 mm Conveyor dishwasher, unvented	0.11	82	0	2931	17379	20310	1
1680 mm Conveyor dishwasher, unvented	0.11	82	0	4718	13188	17907	1
Hooded or Ducted High-Temperature Dishwashers							
Upright door type, high temperature under a 0.9 × 0.9 m hood at 142 L/s	NA	82	0	1026	3810	4836	1
Upright door type, high temperature under a 1.5 × 1.2 m hood at 236 L/s	NA	82	0	469	2315	2784	1
1120 mm conveyor, high temperature under a 0.9 m hood at 472 L/s	0.11	88	0	293	5861	6154	1
Ducted Conveyor Dishwashers							
Ducted 1680 mm conveyor dishwasher	0.11	82	0	3107	1846	4953	1
Ducted flight type conveyor dishwasher	0.06	88	0	3927	2608	6535	1
Ducted flight type conveyor dishwasher with heat recovery	0.06	88	0	3605	1055	4660	1
Ducted flight type conveyor dishwasher with blow dryer	0.06	88	0	6213	4601	10814	1

Source: Livchak and Swierczyna (2020)

^a Heat gain rates for pre-rinse equipment and unhooded dishwashers are for unhooded appliances only. For these equipment items the total appliance heat gain affects the space directly. If an appliance is hooded or vented, the heat gain rates in the hooded and ducted sections of the table must be used. Hooded and ducted line items account for the heat gain captured by the hood or duct and therefore only list the portion of heat gain affecting the space.

^b Average surface temperature of pre-rinse equipment does not exceed 49°C which is the maximum temperature of water flowing through these devices. Average surface temperatures of the dishwashers are less than the wash tank temperature of 75°C. The surfaces are stainless steel and produce negligible radiant heat gain.

^c Values given are for continuous rinsing or washing and are peak values. Rinse and wash times usually extend 1 to 3 hours after each meal period served by the food service facility. Duration of heat gains will vary based on the operating schedule of the food service.

^d For scraper equipment the recirculation flow rate is listed.

was found to range between 37 and 78%, with the average (normalized based on area) being 46%. Figure 4 shows the relationship between nameplate, sum of peaks, and actual electrical load with diversity accounted for, based on the average of the total area tested. Data on actual diversity can be used as a guide, but diversity varies significantly with occupancy. The proper diversity factor for an office of call center operators is different from that for an office of sales representatives who travel regularly.

ASHRAE research project RP-1093 derived diversity profiles for use in energy calculations (Abushakra et al. 2004; Claridge et al. 2004). Those profiles were derived from available measured data sets for a variety of office buildings, and indicated a range of peak weekday diversity factors for lighting ranging from 70 to 85% and for receptacles (appliance load) between 42 and 89%.

Heat Gain per Unit Area. Bach and Sarfraz (2018), Wilkins and Hosni (2000, 2011) and Wilkins and McGaffin (1994) summarized research on a heat gain per unit area basis. Early diversity testing by Wilkins and McGaffin showed that the actual heat gain per unit area, or load factor, ranged from 4.7 to 11.6 W/m², with an average (normalized based on area) of 8.7 W/m². Spaces tested were fully occupied and highly automated, comprising 21 unique areas in five buildings, with a computer and monitor at every workstation. These data are from a time when equipment was primarily desktop computers with cathode ray tube (CRT) monitors, but the relative values for nameplate, sum of peaks, and actual are still applicable today. Table 11 presents more recent data from Bach and Sarfraz indicating a range of load factors with a subjective description of the type of space to which they would apply. This represents more

Table 6 Recommended Heat Gain from Typical Medical Equipment

Equipment	Nameplate, W	Peak, W	Average, W
Anesthesia system	250	177	166
Blanket warmer	500	504	221
Blood pressure meter	180	33	29
Blood warmer	360	204	114
ECG/RESP	1440	54	50
Electrosurgery	1000	147	109
Endoscope	1688	605	596
Harmonical scalpel	230	60	59
Hysteroscopic pump	180	35	34
Laser sonics	1200	256	229
Optical microscope	330	65	63
Pulse oximeter	72	21	20
Stress treadmill	N/A	198	173
Ultrasound system	1800	1063	1050
Vacuum suction	621	337	302
X-ray system	968		82
	1725	534	480
	2070		18

Source: Hosni et al. (1999).

Table 7 Recommended Heat Gain from Typical Laboratory Equipment

Equipment	Nameplate, W	Peak, W	Average, W
Analytical balance	7	7	7
Centrifuge	138	89	87
	288	136	132
	5500	1176	730
Electrochemical analyzer	50	45	44
	100	85	84
Flame photometer	180	107	105
Fluorescent microscope	150	144	143
	200	205	178
Function generator	58	29	29
Incubator	515	461	451
	600	479	264
	3125	1335	1222
Orbital shaker	100	16	16
Oscilloscope	72	38	38
	345	99	97
Rotary evaporator	75	74	73
	94	29	28
Spectronics	36	31	31
Spectrophotometer	575	106	104
	200	122	121
	N/A	127	125
Spectro fluorometer	340	405	395
Thermocycler	1840	965	641
	N/A	233	198
Tissue culture	475	132	46
	2346	1178	1146

Source: Hosni et al. (1999).

current laptop equipment with LED or LCD monitors. The medium load density is likely to be appropriate for most standard office spaces. Medium/heavy or heavy load densities may be encountered but can be considered extremely conservative estimates even for densely populated and highly automated spaces. Table 12 indicates applicable diversity factors.

Radiant/Convective Split. ASHRAE research project RP-1482 (Hosni and Beck 2008) examined the radiant/convective split for common office equipment; the most important differentiating feature is whether the equipment had a cooling fan. Footnotes in Tables 8 and 9 summarize those results.

3. INFILTRATION AND MOISTURE MIGRATION HEAT GAINS

Two other load components contribute to space cooling load directly without time delay from building mass: (1) infiltration, and (2) moisture migration through the building envelope.

3.1 INFILTRATION

Principles of estimating infiltration in buildings, with emphasis on the heating season, are discussed in Chapter 16. When eco-

Table 8A Recommended Heat Gain for Typical Desktop Computers

Description	Nameplate Power, ^a W	Peak Heat Gain, ^{b, d} W
Manufacturer 1		
3.0 GHz processor, 4 GB RAM, $n = 1$	NA	83
3.3 GHz processor, 8 GB RAM, $n = 8$	NA	50
3.5 GHz processor, 8 GB RAM, $n = 2$	NA	42
3.6 GHz processor, 16 GB RAM, $n = 2$	NA	66
3.3 GHz processor, 16 GB RAM, $n = 2$	NA	52
4.0 GHz processor, 16 GB RAM, $n = 1$	NA	83
3.3 GHz processor, 8 GB RAM, $n = 1$	NA	84
3.7 GHz processor, 32 GB RAM, $n = 1$	750	116
3.5 GHz processor, 16 GB RAM, $n = 3^c$	NA	102
	550	144
	NA	93
Manufacturer 2		
3.6 GHz processor, 32 GB RAM, $n = 8$	NA	80
3.6 GHz processor, 16 GB RAM, $n = 1$	NA	78
3.4 GHz processor, 32 GB RAM, $n = 1$	NA	72
3.4 GHz processor, 24 GB RAM, $n = 1$	NA	86
3.50 GHz processor, 4 GB RAM, $n = 1$	NA	26
3.3 GHz processor, 8 GB RAM, $n = 1$	NA	78
3.20 GHz processor, 8 GB RAM, $n = 1$	NA	61
3.20 GHz processor, 4 GB RAM, $n = 1$	NA	44
2.93 GHz processor, 16 GB RAM, $n = 1$	NA	151
2.67 GHz processor, 8 GB RAM, $n = 1$	NA	137
Average 15-min peak power consumption (range)	82 (26-151)	

Source: Bach and Sarfraz (2018)

n = number of tested equipment of same configuration.

^aNameplate for desktop computer is present on its power supply, which is mounted inside desktop, hence not accessible for most computers, where NA = not available.

^bFor equipment peak heat gain value, highest 15-min interval of recorded data is listed in tables.

^cFor tested equipment with same configuration, increasing power supply size does not increase average power consumption.

^dApproximately 90% convective heat gain and 10% radiative heat gain.

Table 8B Recommended Heat Gain for Typical Laptops and Laptop Docking Station

Equipment	Description	Nameplate Power, ^a W	Peak Heat Gain, ^{b, c} W
Laptop computer	Manufacturer 1, 2.6 GHz processor, 8 GB RAM, $n = 1$	NA	46
	Manufacturer 2, 2.4 GHz processor, 4 GB RAM, $n = 1$	NA	59
Average 15-min peak power consumption (range)		53 (46-59)	
Laptop with docking station	Manufacturer 1, 2.7 GHz processor, 8 GB RAM, $n = 1$	NA	38
	1.6 GHz processor, 8 GB RAM, $n = 2$	NA	45
	2.0 GHz processor, 8 GB RAM, $n = 1$	NA	50
	2.6 GHz processor, 4 GB RAM, $n = 1$	NA	51
	2.4 GHz processor, 8 GB RAM, $n = 1$	NA	40
	2.6 GHz processor, 8 GB RAM, $n = 1$	NA	35
	2.7 GHz processor, 8 GB RAM, $n = 1$	NA	59
	3.0 GHz processor, 8 GB RAM, $n = 3$	NA	70
	2.9 GHz processor, 32 GB RAM, $n = 3$	NA	58
	3.0 GHz processor, 32 GB RAM, $n = 1$	NA	128
	3.7 GHz processor, 32 GB RAM, $n = 1$	NA	63
	3.1 GHz processor, 32 GB RAM, $n = 1$	NA	89
Average 15-min peak power consumption (range)		61 (26-151)	

Source: Bach and Sarfraz (2018)

n = number of tested equipment of same configuration.

^aVoltage and amperage information for laptop computer and laptop docking station is available on power supply nameplates; however, nameplate does not provide information on power consumption, where NA = not available.

^bFor equipment peak heat gain value, the highest 15-min interval of recorded data is listed in tables.

^cApproximately 75% convective heat gain and 25% radiative heat gain.

nomically feasible, somewhat more outdoor air may be introduced to a building than the total of that exhausted, to create a slight overall positive pressure in the building relative to the outdoors.

Under these conditions, air usually exfiltrates, rather than infiltrates, through the building envelope and thus effectively eliminates infiltration sensible and latent heat gains. However, there is

Table 8C Recommended Heat Gain for Typical Tablet PC

Description	Nameplate Power, ^a W	Peak Heat Gain, ^b W
1.7 GHz processor, 4 GB RAM, $n = 1$	NA	42
2.2 GHz processor, 16 GB RAM, $n = 1$	NA	40
2.3 GHz processor, 8 GB RAM, $n = 1$	NA	30
2.5 GHz processor, 8 GB RAM, $n = 1$	NA	31
Average 15-min peak power consumption (range)	36 (31-42)	

Source: Bach and Sarfraz (2018)

n = number of tested equipment of same configuration.

^aVoltage and amperage information for tablet PC is available on power supply nameplate; however, nameplate does not provide information on power consumption, where NA = not available.

^bFor equipment peak heat gain value, highest 15-min interval of recorded data is listed in tables.

Table 8D Recommended Heat Gain for Typical Monitors

Description ^a	Nameplate Power, W	Peak Heat Gain, ^{b, c} W
Manufacturer 1		
1397 mm LED flat screen, $n = 1$ (excluded from average because atypical size)	240	50
686 mm LED flat screen, $n = 2$	40	26
546 mm LED flat screen, $n = 2$	29	25
Manufacturer 2		
1270 mm 3D LED flat screen, $n = 1$ (excluded from average because atypical size)	94	49
Manufacturer 3		
864 mm LCD curved screen, $n = 1$ (excluded from average because atypical size and curved)	130	48
584 mm LED flat screen, $n = 3$	50	17
584 mm LED flat screen, $n = 1$	38	21
584 mm LED flat screen, $n = 1$	38	14
Manufacturer 4		
610 mm LED flat screen, $n = 1$	42	25
Manufacturer 5		
600 mm LED flat screen, $n = 1$	26	17
546 mm LED flat screen, $n = 1$	29	22
Manufacturer 6		
546 mm LED flat screen, $n = 1$	28	24
Average 15-min peak power consumption (range)	21 (14-26)	

Source: Bach and Sarfraz (2018)

n = number of tested equipment of same configuration.

^aScreens with atypical size and shape are excluded for calculating average 15-min peak power consumption.

^bFor equipment peak heat gain value, highest 15-min interval of recorded data is listed in tables.

^cApproximately 60% convective heat gain and 40% radiative heat gain.

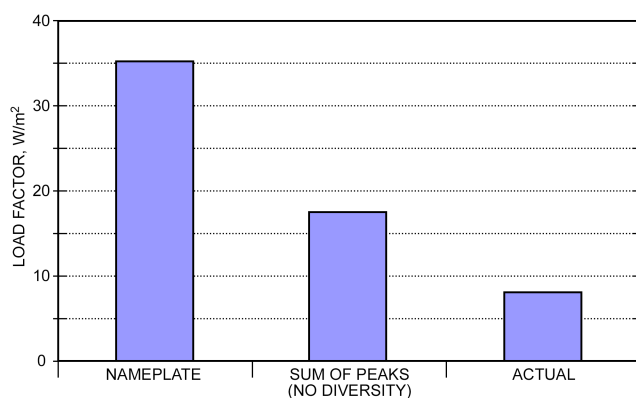


Fig. 4 Office Equipment Load Factor Comparison
(Wilkins and McGaffin 1994)

concern, especially in some climates, that water may condense within the building envelope; actively managing space air pressures to reduce this condensation problem, as well as infiltration, may be needed. When positive air pressure is assumed, most designers do not include infiltration in cooling load calculations

for commercial buildings. However, including some infiltration for spaces such as entry areas or loading docks may be appropriate, especially when those spaces are on the windward side of buildings. But the downward stack effect, as occurs when indoor air is denser than the outdoor, might eliminate infiltration to these entries on lower floors of tall buildings; infiltration may occur on the upper floors during cooling conditions if makeup air is not sufficient.

Infiltration also depends on wind direction and magnitude, temperature differences, construction type and quality, and occupant use of exterior doors and operable windows. As such, it is impossible to accurately predict infiltration rates. Designers usually predict overall rates of infiltration using the number of **air changes per hour (ACH)**. A common guideline for climates and buildings typical of at least the central United States is to estimate the ACHs for winter heating conditions, and then use half that value for the cooling load calculations.

Standard Air Volumes

Because the specific volume of air varies appreciably, calculations are more accurate when made on the basis of air mass instead of volume. However, volumetric flow rates are often required for selecting coils, fans, ducts, etc.; basing volumes on measurement at standard conditions may be used for accurate results. One standard

Table 9 Recommended Heat Gain for Typical Printers

		Max. Printing Speed, Pages per Minute	Nameplate Power, W	Peak Heat Gain, ^a W
Equipment	Description			
Multifunction printer (copy, print, scan)	Large, multiuser, office type	40	1010	540 (Idle 29 W)
		30	1300	303 (Idle 116 W)
		28	1500	433 (Idle 28 W)
Average 15-min peak power consumption (range)			425 (303-540)	
	Multiuser, medium-office type	35	900	732 (Idle 18 W)
	Desktop, small-office type	25	470	56 (Idle 3 W)
Monochrome printer	Desktop, medium-office type	55	1000	222
		45	680	61
Average 15-min peak power consumption (range)			142 (61-222)	
Color printer	Desktop, medium-office type	40	620	120
Laser printer	Desktop, small-office type	14	310	89
		24	495	67
		26	1090	65
Average 15-min peak power consumption (range)			74 (65-89)	
Plotter	Manufacturer 1		1600	571
	Manufacturer 2		270	173
Average 15-min peak power consumption (range)			372 (173-571)	
Fax machine	Medium		1090	92
	Small		600	46
Average 15-min peak power consumption (range)			69 (46-92)	

Source: Bach and Sarfraz (2018)

^aApproximately 70% convective heat gain and 30% radiative heat gain.

Table 10 Recommended Heat Gain for Miscellaneous Equipment

Equipment	Nameplate Power, ^a W	Peak Heat Gain, ^b W
Vending machine		
Drinks, 280 to 400 items	NA	940
Snacks	NA	54
Food (e.g., for sandwiches)	NA	465
Thermal binding machine, 2 single documents up to 340 pages	350	28.5
Projector, resolution 1024 × 768	340	308
Paper shredder, up to 28 sheets	1415	265
Electric stapler, up to 45 sheets	NA	1.5
Speakers	220	15
Temperature-controlled electronics soldering station	95	16
Cell phone charger	NA	5
Battery charger		
40 V	NA	19
AA	NA	5.5
Microwave oven, 25 to 34 L	1000 to 1550	713 to 822
Coffee maker		
Single cup	1400	385
Up to 12 cups	950	780
With grinder	1350	376
Coffee grinder, up to 12 cups	NA	73
Tea kettle, up to 6 cups	1200	1200
Dorm fridge, 88 L	NA	57
Freezer, 510 L	130	125
Fridge, 510 L	NA	387 to 430
Ice maker and dispenser, 9 kg bin capacity	NA	658
Top mounted bottled water cooler	NA	114 to 350
Cash register	25	9
Touch screen computer, 380 mm standard LCD and 2.2 GHz processor	NA	58
Self-checkout machine	NA	15

Source: Bach and Sarfraz (2018)

^aFor some equipment, nameplate power consumption is not available, where NA = not available.^bFor equipment peak heat gain value, highest 15-min interval of recorded data is listed in tables.

value is $1.2 \text{ kg}_{da}/\text{m}^3$ ($0.833 \text{ m}^3/\text{kg}$). This density corresponds to about 16°C at saturation and 21°C dry air (at 101.325 kPa). Because

air usually passes through the equipment at a density close to standard for locations below about 300 m, the accuracy desired nor-

Table 11 Recommended Load Factors for Various Types of Offices

Type of Use	Load Factor,* W/m ²	Description
100% laptop, docking station		
light	3.67	15.5 m ² /workstation, all laptop docking station use, 1 printer per 10
medium	4.91	11.6 m ² /workstation, all laptop docking station use, 1 printer per 10
50% laptop, docking station		
light	4.75	15.5 m ² /workstation, 50% laptop docking station/50% desktop, 1 printer per 10
medium	6.35	11.6 m ² /workstation, 50% laptop docking station/50% desktop, 1 printer per 10
100% desktop		
light	5.83	15.5 m ² /workstation, all desktop use, 1 printer per 10
medium	7.79	11.6 m ² /workstation, all desktop use, 1 printer per 10
100% laptop, docking station		
2 screens	7.44	11.6 m ² /workstation, all laptop docking station use, 2 screens, 1 printer per 10
100% desktop		
2 screens	9.06	11.6 m ² /workstation, all laptop use, 2 screens, 1 printer per 10
3 screens	10.33	11.6 m ² /workstation, all desktop use, 3 screens, 1 printer per 10
100% desktop		
heavy, 2 screens	11.00	7.9 m ² /workstation, all desktop use, 2 screens, 1 printer per 8
heavy, 3 screens	12.49	7.9 m ² /workstation, all desktop use, 3 screens, 1 printer per 8
100% laptop, docking station		
full on, 2 screens	12.23	7.9 m ² /workstation, all laptop docking use, 2 screens, 1 printer per 8, no diversity
100% desktop		
full on, 2 screens	14.35	7.9 m ² /workstation, all desktop use, 2 screens, 1 printer per 8, no diversity
full on, 3 screens	16.48	7.9 m ² /workstation, all desktop use, 3 screens, 1 printer per 8, no diversity

Source: Bach and Sarfraz (2018)

*Medium office type monochrome printer is used for load factor calculator with 15-min peak power consumption of 142 W.

Table 12 Diversity Factor for Different Equipment

Equipment	Diversity Factor, %	Diversity Factor, ^a %
Desktop PC	75	75
Laptop docking station	70	NA
Notebook computer	75 ^b	75
Screen	70	60
Printer	45	NA

Source: Bach and Sarfraz (2017)

^a2013 ASHRAE Handbook—Fundamentals^bInsufficient data from RP-1742; values based on previous data from 2013 ASHRAE Handbook—Fundamentals and judgment of Bach and Sarfraz (2017).

mally requires no correction. When airflow is to be measured at a particular condition or point, such as at a coil entrance or exit, the corresponding specific volume can be read from the sea-level psychrometric chart. For higher elevations, the mass flow rates of air must be adjusted and higher-elevation psychrometric charts or algorithms must be used.

Heat Gain Calculations Using Standard Air Values

Air-conditioning design often requires the following information:

1. Total heat

Total heat gain q_t corresponding to the change of a given standard flow rate Q_s through an enthalpy difference Δh is

$$q_t = 1.2 Q_s \Delta h \quad (7)$$

where 60 = min/h, 1.2 = kg_{da}/m³.

This total heat equation can also be expressed as

$$q_t = C_t Q_s \Delta h$$

where $C_t = 1.2$ is the air total heat factor, in kg_{da}/m³.

2. Sensible heat

Sensible heat gain q_s corresponding to the change of dry-bulb temperature Δt for given airflow (standard conditions) Q_s is

$$q_s = 1.2(1005 + 1884W)Q_s \Delta t \quad (8)$$

where

1005 = specific heat of dry air, J/(kg·K)

W = humidity ratio, kg_w/kg_{da}

1884 = specific heat of water vapor, J/(kg·K)

The specific heats are for a range from about –75 to 90°C. When $W = 0$, the value of $1.20(1005 + 1884W) = 1210$; when $W = 0.01$, the value is 1230; when $W = 0.02$, the value is 1250; and when $W = 0.03$, the value is 1270. Because a value of $W = 0.01$ approximates conditions found in many air-conditioning problems, the sensible heat change (in watts) has traditionally been found as

$$q_s = 1230 Q_s \Delta t \quad (9)$$

This sensible heat equation can also be expressed as

$$q_s = C_s Q_s \Delta t$$

where $C_s = 1230$ is the air sensible heat factor, in (W·s)/(m³·K).

3. Latent heat

Latent heat gain q_l corresponding to the change of humidity ratio ΔW (in kg_w/kg_{da}) for given airflow (standard conditions) Q_s is

$$q_l = 1.20 \times 2500 Q_s \Delta W = 3000 Q_s \Delta W \quad (10)$$

where 2500 is the approximate heat content of 50% rh vapor at 24°C less the heat content of water at 10°C. A common design condition for the space is 50% rh at 24°C, and 10°C is normal condensate temperature from cooling and dehumidifying coils.

This latent heat equation can also be expressed as

$$q_l = C_l Q_s \Delta W$$

where $C_l = 3000$ is the air latent heat factor, in (W·s)/m³.

4. Elevation correction for total, sensible, and latent heat equations

The constants 1200, 1230, and 3000 are useful in air-conditioning calculations at sea level (101.325 kPa) and for normal temperatures and moisture ratios. For other conditions, more precise values should be used. For an elevation of 1525 m (84.1 kPa), appropriate values are 998, 1023, and 2496. Equations (8) to (10) can be corrected for elevations other than sea level by multiplying them by the ratio of pressure at sea level divided by the pressure at actual altitude. This can be derived from Equation (3) in Chapter 1 as

$$C_{x,alt} = C_{x,0}P/P_0$$

where $C_{x,0}$ is any sea-level C value and $P/P_0 = [1 - (\text{elevation} \times 2.25577 \times 10^{-5})]^{5.2559}$, where elevation is in metres.

Elevation Correction Examples

To correct the C values for El Paso, Texas, the elevation listed in the appendix of Chapter 14 is 1194 m. C values for Equations (7) to (10) can be corrected using Equation (3) in Chapter 1 as follows:

$$C_{t,1194} = 1200 \times [1 - (1194 \times 2.25577 \times 10^{-5})]^{5.2559} = 1040$$

$$C_{s,1194} = 1230 \times [1 - (1194 \times 2.25577 \times 10^{-5})]^{5.2559} = 1066$$

$$C_{l,1194} = 3000 \times [1 - (1194 \times 2.25577 \times 10^{-5})]^{5.2559} = 2599$$

To correct the C values for Albuquerque, New Mexico, the elevation listed in the appendix of Chapter 14 is 1619 m. C values for Equations (7) to (10) can be corrected as follows:

$$C_{t,1619} = 1200 \times [1 - (1619 \times 2.25577 \times 10^{-5})]^{5.2559} = 987$$

$$C_{s,1619} = 1230 \times [1 - (1619 \times 2.25577 \times 10^{-5})]^{5.2559} = 1012$$

$$C_{l,1619} = 3000 \times [1 - (1619 \times 2.25577 \times 10^{-5})]^{5.2559} = 2467$$

3.2 LATENT HEAT GAIN FROM MOISTURE DIFFUSION

Diffusion of moisture through building materials is a natural phenomenon that is always present. Chapters 25 to 27 cover principles, materials, and specific methods used to control moisture. Moisture transfer through walls and roofs is often neglected in comfort air conditioning because the actual rate is quite small and the corresponding latent heat gain is insignificant. Permeability and permeance values for various building materials are given in Chapter 26. Vapor retarders should be specified and installed in the proper location to keep moisture transfer to a minimum, and to minimize condensation within the envelope. Moisture migration up through slabs-on-grade and basement floors has been found to be significant, but has historically not been addressed in cooling load calculations. Under-slab continuous moisture retarders and drainage can reduce upward moisture flow.

Some industrial applications require low moisture to be maintained in a conditioned space. In these cases, the latent heat gain accompanying moisture transfer through walls and roofs may be greater than any other latent heat gain. This gain is computed by

$$q_{l_m} = MA\Delta p_v (h_g - h_f) \quad (11)$$

where

q_{l_m} = latent heat gain from moisture transfer, W

M = permeance of wall or roof assembly, ng/(s·m²·Pa)

A = area of wall or roof surface, m²

Δp_v = vapor pressure difference, Pa

h_g = enthalpy at room conditions, kJ/kg

h_f = enthalpy of water condensed at cooling coil, kJ/kg

$h_g - h_f$ = 2500 kJ/kg when room temperature is 24°C and condensate off coil is 10°C

3.3 OTHER LATENT LOADS

Moisture sources within a building (e.g., shower areas, swimming pools or natatoriums, arboretums) can also contribute to latent load. Unlike sensible loads, which correlate to supply air quantities required in a space, latent loads usually only affect cooling coils sizing or refrigeration load. Because air from showers and some other moisture-generating areas is exhausted completely, those airborne latent loads do not reach the cooling coil and thus do not contribute to cooling load. However, system loads associated with ventilation air required to make up exhaust air must be recognized, and any recirculated air's moisture must be considered when sizing the dehumidification equipment.

For natatoriums, occupant comfort and humidity control are critical. In many instances, size, location, and environmental requirements make complete exhaust systems expensive and ineffective. Where recirculating mechanical cooling systems are used, evaporation (latent) loads are significant. Chapter 6 of the 2019 *ASHRAE Handbook—HVAC Applications* provides guidance on natatorium load calculations.

4. FENESTRATION HEAT GAIN

For spaces with neutral or positive air pressurization, the primary weather-related variable affecting cooling load is solar radiation. The effect of solar radiation is more pronounced and immediate on exposed, nonopaque surfaces. Chapter 14 includes procedures for calculating clear-sky solar radiation intensity and incidence angles for weather conditions encountered at specific locations. That chapter also includes some useful solar equations. Calculation of solar heat gain and conductive heat transfer through various glazing materials and associated mounting frames, with or without interior and/or exterior shading devices, is discussed in Chapter 15. This chapter covers application of such data to overall heat gain evaluation, and conversion of calculated heat gain into a composite cooling load for the conditioned space.

4.1 FENESTRATION DIRECT SOLAR, DIFFUSE SOLAR, AND CONDUCTIVE HEAT GAINS

For fenestration heat gain, use the following equations:

Direct beam solar heat gain q_b :

$$q_b = AE_{t,b} \text{SHGC}(\theta) \text{IAC}(\theta, \Omega) \quad (12)$$

Diffuse solar heat gain q_d :

$$q_d = A(E_{t,d} + E_{t,r}) \langle \text{SHGC} \rangle_D \text{IAC}_D \quad (13)$$

Conductive heat gain q_c :

$$q_c = UA(T_{out} - T_{in}) \quad (14)$$

Total fenestration heat gain Q :

$$Q = q_b + q_d + q_c \quad (15)$$

where

A = window area, m²

$E_{t,b}$, $E_{t,d}$, and $E_{t,r}$ = beam, sky diffuse, and ground-reflected diffuse irradiance, calculated using equations in Chapter 14

SHGC(θ)=beam solar heat gain coefficient as a function of incident angle θ ; may be interpolated between values in Table 10 of Chapter 15
 (SHGC) $_D$ =diffuse solar heat gain coefficient (also referred to as hemispherical SHGC); from Table 10 of Chapter 15

T_{in} = indoor temperature, °C

T_{out} = outdoor temperature, °C

U = overall U-factor, including frame and mounting orientation from Table 4 of Chapter 15, W/(m²·K)

IAC(θ, Ω)=indoor solar attenuation coefficient for beam solar heat gain coefficient; = 1.0 if no indoor shading device. IAC(θ, Ω) is a function of shade type and, depending on type, may also be a function of beam solar angle of incidence θ and shade geometry

IAC $_D$ = indoor solar attenuation coefficient for diffuse solar heat gain coefficient; = 1.0 if no indoor shading device. IAC $_D$ is a function of shade type and, depending on type, may also be a function of shade geometry

If specific window manufacturer's SHGC and U-factor data are available, those should be used. For fenestration equipped with indoor shading (blinds, drapes, or shades), the indoor solar attenuation coefficients IAC(θ, Ω) and IAC $_D$ are listed in Tables 14A to 14G of Chapter 15.

Note that, as discussed in Chapter 15, fenestration ratings (U-factor and SHGC) are based on the entire product area, including frames. Thus, for load calculations, fenestration area is the area of the entire opening in the wall or roof.

4.2 EXTERIOR SHADING

Nonuniform exterior shading, caused by roof overhangs, side fins, or building projections, requires separate hourly calculations for the externally shaded and unshaded areas of the window in question, with the indoor shading SHGC still used to account for any internal shading devices. The areas, shaded and unshaded, depend on the location of the shadow line on a surface in the plane of the glass. Sun (1968) developed fundamental algorithms for analysis of shade patterns. McQuiston and Spitler (1992) provide graphical data to facilitate shadow line calculation.

Equations for calculating shade angles [Chapter 15, Equations (34) to (37)] can be used to determine the shape and area of a moving shadow falling across a given window from external shading elements during the course of a design day. Thus, a subprofile of heat gain for that window can be created by separating its sunlit and shaded areas for each hour.

5. HEAT BALANCE METHOD

Cooling load estimation involves calculating a surface-by-surface conductive, convective, and radiative heat balance for each room surface and a convective heat balance for the room air. These principles form the foundation for all methods described in this chapter. The heat balance (HB) method solves the problem using the most fundamental principles and the fewest simplifications. The advantages are that it contains the fewest parameters and general assumptions.

Some computations required by this rigorous approach require the use of computers. The heat balance procedure is not new. Many energy calculation programs have used it in some form for many years. The first implementation that incorporated all the elements to form a complete method was NBSLD (Kusuda 1967). The heat balance procedure is also implemented in both the BLAST and TARP energy analysis programs (Walton 1983). Before ASHRAE research project RP-875, the method had never been described completely or in a form applicable to cooling load calculations. The papers resulting from RP-875 describe the heat balance procedure in detail (Liesen and Pedersen 1997; McClellan and Pedersen 1997; Pedersen et al. 1997).

The HB method is codified in the software called Hbfort that accompanies *Cooling and Heating Load Calculation Principles* (Pedersen et al. 1998).

ASHRAE research project RP-1117 constructed two model rooms for which cooling loads were physically measured using extensive instrumentation (Chantrasrisalai et al. 2003; Eldridge et al. 2003; Lu et al. 2003). HB calculations closely approximated measured cooling loads when provided with detailed data for the test rooms.

5.1 ASSUMPTIONS

All calculation procedures involve some kind of model; all models require simplifying assumptions and, therefore, are approximate. The most fundamental assumption inherent in the traditional heat balance solution is that air in the thermal zone can be modeled as **well mixed**, meaning its temperature is uniform throughout the zone. ASHRAE research project RP-664 (Fisher and Pedersen 1997) established that this assumption is valid over a wide range of conditions. This assumption remains the same for both convective air system-based cooling systems and radiant cooling systems.

The next major assumption is that the surfaces of the room (walls, windows, floor, etc.) can be treated as having

1. Uniform surface temperatures
2. Uniform long-wave (LW) and short-wave (SW) irradiation
3. Diffuse radiating surfaces
4. One-dimensional heat conduction within

The resulting formulation is called the **heat balance (HB) model**. Note that the assumptions, although common, set certain limits on the information that can be obtained from the model. When using heat balance to solve for the cooling load in a space with radiant cooling, not all of the assumptions 1-4 above will apply. In particular, not all surfaces will have uniform surface temperatures.

ASHRAE research project RP-1729 (Moftakhari et al. 2020) developed modifications to the current implementation of heat balance to allow for solution when radiant cooling is the primary cooling system. The principles of heat balance still apply. Radiant and convective exchanges of heat are all modeled based on the same fundamental principles. Similar considerations are required when using heat balance for load calculation with under-floor air distribution (UFAD) systems. With UFAD, the floor is maintained at a lower temperature due to the below-floor air supply, so the resulting heat exchange interactions mimic radiant systems more than convective systems. The discussion that follows is primarily focused on the use of heat balance with convective air system based cooling systems.

5.2 ELEMENTS

Within the framework of the assumptions, the HB can be viewed as four distinct processes:

1. Outdoor-face heat balance
2. Wall conduction process
3. Indoor-face heat balance
4. Air heat balance

Figure 5 shows the relationship between these processes for a single opaque surface. The top part of the figure, inside the shaded box, is repeated for each surface enclosing the zone. The process for transparent surfaces is similar, but the absorbed solar component appears in the conduction process block instead of at the outdoor face, and the absorbed component splits into inward- and outward-flowing fractions. These components participate in the surface heat balances.

Outdoor-Face Heat Balance

The heat balance on the outdoor face of each surface is

$$q''_{\text{sol}} + q''_{\text{LWR}} + q''_{\text{conv}} - q''_{\text{ko}} = 0 \quad (16)$$

where

q''_{sol} = absorbed direct and diffuse solar radiation flux (q/A), W/m^2

q''_{LWR} = net long-wave radiation flux exchange with air and surroundings, W/m^2

q''_{conv} = convective exchange flux with outdoor air, W/m^2

q''_{ko} = conductive flux (q/A) into wall, W/m^2

All terms are positive for net flux to the face except q''_{ko} , which is traditionally taken to be positive from outdoors to inside the wall.

Each term in Equation (16) has been modeled in several ways, and in simplified methods the first three terms are combined by using the sol-air temperature.

Wall Conduction Process

The wall conduction process has been formulated in more ways than any of the other processes. Techniques include

- Numerical finite difference
- Numerical finite element
- Transform methods
- Time series methods

This process introduces part of the time dependence inherent in load calculation. Figure 6 shows surface temperatures on the indoor and outdoor faces of the wall element, and corresponding conductive heat fluxes away from the outer face and toward the indoor face.

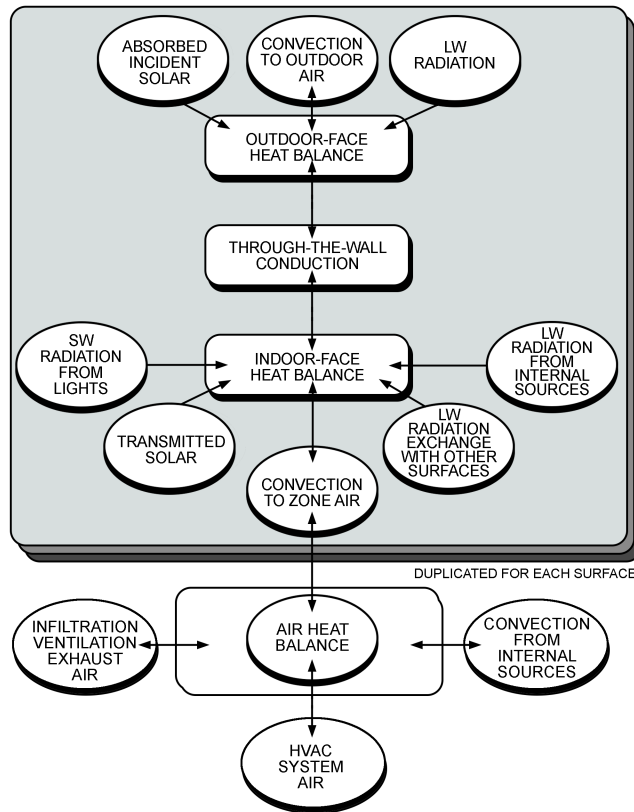


Fig. 5 Schematic of Heat Balance Processes in Zone

All four quantities are functions of time. Direct formulation of the process uses temperature functions as input or known quantities, and heat fluxes as outputs or resultant quantities.

In some models, surface heat transfer coefficients are included as part of the wall element, making the temperatures in question the indoor and outdoor air temperatures. This is not a desirable formulation, because it hides the heat transfer coefficients and prohibits changing them as airflow conditions change. It also prohibits treating the internal long-wave radiation exchange appropriately.

Because heat balances on both sides of the element induce both the temperature and heat flux, the solution must deal with this simultaneous condition. Two computational methods that have been used widely are finite difference and conduction transfer function methods. Because of the computational time advantage, the conduction transfer function formulation has been selected for presentation here.

Indoor-Face Heat Balance

The heart of the HB method is the internal heat balance involving the inner faces of the zone surfaces. This heat balance has many heat transfer components, and they are all coupled. Both long-wave (LW) and short-wave (SW) radiation are important, as well as wall conduction and convection to the air. The indoor-face heat balance for each surface can be written as follows:

$$q''_{\text{LWX}} + q''_{\text{SW}} + q''_{\text{LWS}} + q''_{\text{ki}} + q''_{\text{sol}} + q''_{\text{conv}} = 0 \quad (17)$$

where

q''_{LWX} = net long-wave radiant flux exchange between zone surfaces, W/m^2

q''_{SW} = net short-wave radiation flux to surface from lights, W/m^2

q''_{LWS} = long-wave radiation flux from equipment in zone, W/m^2

q''_{ki} = conductive flux through wall, W/m^2

q''_{sol} = transmitted solar radiative flux absorbed at surface, W/m^2

q''_{conv} = convective heat flux to zone air, W/m^2

These terms are explained in the following paragraphs.

LW Radiation Exchange Among Zone Surfaces. The limiting cases for modeling internal LW radiation exchange are

- Zone air is completely transparent to LW radiation
- Zone air completely absorbs LW radiation from surfaces in the zone

Most HB models treat air as completely transparent and not participating in LW radiation exchange among surfaces in the zone. The second model is attractive because it can be formulated simply using a combined radiative and convective heat transfer coefficient from each surface to the zone air and thus decouples radiant

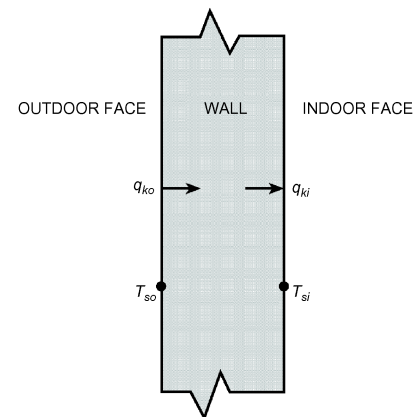


Fig. 6 Schematic of Wall Conduction Process

Table 13 Single-Layer Glazing Data Produced by WINDOW 7.7.10

Parameter	Incident Angle										Diffuse (Hemis.)
	0	10	20	30	40	50	60	70	80	90	
V_{tc}	0.899	0.899	0.898	0.896	0.889	0.870	0.822	0.705	0.441	0	0.822
R_{fv}	0.083	0.083	0.083	0.085	0.091	0.109	0.156	0.272	0.536	1	0.148
R_{bv}	0.083	0.083	0.083	0.085	0.091	0.109	0.156	0.272	0.536	1	0.148
T_{sol}	0.834	0.833	0.831	0.827	0.818	0.797	0.749	0.637	0.389	0	0.753
R_f	0.075	0.075	0.075	0.077	0.082	0.099	0.143	0.253	0.506	1	0.136
R_b	0.075	0.075	0.075	0.077	0.082	0.099	0.143	0.253	0.506	1	0.136
A_{bs1}	0.091	0.092	0.094	0.096	0.100	0.104	0.108	0.110	0.105	0	0.101
SHGC	0.861	0.860	0.859	0.855	0.847	0.827	0.781	0.669	0.424	0	0.783

Source: LBNL (2019).

exchange among surfaces in the zone. However, because the transparent air model allows radiant exchange and is more realistic, the second model is inferior.

Furniture in a zone increases the amount of surface area that can participate in radiative and convective heat exchanges. It also adds thermal mass to the zone. These two changes can affect the time response of the zone cooling load.

SW Radiation from Lights. The short-wavelength radiation from lights is usually assumed to be distributed over the surfaces in the zone in some manner. The HB procedure retains this approach but allows the distribution function to be changed.

LW Radiation from Internal Sources. The traditional model for this source defines a radiative/convective split for heat introduced into a zone from equipment. The radiative part is then distributed over the zone's surfaces in some manner. This model is not completely realistic, and it departs from HB principles. In a true HB model, equipment surfaces are treated just as other LW radiant sources in the zone. However, because information about the surface temperature of equipment is rarely known, it is reasonable to keep the radiative/convective split concept even though it ignores the true nature of the radiant exchange. ASHRAE research project RP-1055 (Hosni et al. 1999) determined radiative/convective splits for many additional equipment types, as listed in footnotes for Tables 8 and 9.

Transmitted Solar Heat Gain. Chapter 15's calculation procedure for determining transmitted solar energy through fenestration uses the solar heat gain coefficient (SHGC) directly rather than relating it to double-strength glass, as is done when using a shading coefficient (SC). The difficulty with this plan is that the SHGC includes both transmitted solar and inward-flowing fraction of the solar radiation absorbed in the window. With the HB method, this latter part should be added to the conduction component so it can be included in the indoor-face heat balance.

Transmitted solar radiation is also distributed over surfaces in the zone in a prescribed manner. It is possible to calculate the actual position of beam solar radiation, but this involves partial surface irradiation, which is inconsistent with the rest of the zone model, which assumes uniform conditions over an entire surface.

Using SHGC to Calculate Solar Heat Gain

The total solar heat gain through fenestration consists of directly transmitted solar radiation plus the inward-flowing fraction of solar radiation that is absorbed in the glazing system. Both parts contain beam and diffuse contributions. Transmitted radiation goes directly onto surfaces in the zone and is accounted for in the surface indoor heat balance. The zone heat balance model accommodates the resulting heat fluxes without difficulty. The second part, the inward-flowing fraction of the absorbed solar radiation, interacts with other surfaces of the enclosure through long-wave radiant exchange and with zone air through convective heat transfer. As such, it depends

both on geometric and radiative properties of the zone enclosure and convection characteristics inside and outside the zone. The **solar heat gain coefficient (SHGC)** combines the transmitted solar radiation and the inward-flowing fraction of the absorbed radiation. The SHGC is defined as

$$\text{SHGC} = \tau + \sum_{k=1}^n \alpha_k N_k \quad (18)$$

where

τ = solar transmittance of glazing

α_k = solar absorptance of the k th layer of the glazing system

n = number of layers

N_k = inward-flowing fraction of absorbed radiation in the k th layer

Note that Equation (18) is written generically. It can be written for a specific incidence angle and/or radiation wavelength and integrated over the wavelength and/or angle, but the principle is the same in each case. Refer to Chapter 15 for the specific expressions.

Unfortunately, the inward-flowing fraction N interacts with the zone in many ways. This interaction can be expressed as

$$N = f(\text{indoor convection coefficient, outdoor convection coefficient, glazing system overall heat transfer coefficient, zone geometry, zone radiation properties})$$

The only way to model these interactions correctly is to combine the window model with the zone heat balance model and solve both simultaneously. This has been done recently in some energy analysis programs, but is not generally available in load calculation procedures. In addition, the SHGC used for rating glazing systems is based on specific values of the indoor, outdoor, and overall heat transfer coefficients and does not include any zonal long-wavelength radiation considerations. So, the challenge is to devise a way to use SHGC values within the framework of heat balance calculation in the most accurate way possible, as discussed in the following paragraphs.

Using SHGC Data. The normal incidence SHGC used to rate and characterize glazing systems is not sufficient for determining solar heat gain for load calculations. These calculations require solar heat gain as a function of the incident solar angle to determine the hour-by-hour gain profile. Thus, it is necessary to use angular SHGC values and also diffuse SHGC values. These can be obtained from the WINDOW 7.7.10 program (LBNL 2019). This program does a detailed optical and thermal simulation of a glazing system and, when applied to a single clear layer, produces the information shown in Table 13.

Table 13 shows the parameters as a function of incident solar angle and also the diffuse values. The specific parameters shown are

V_{tc} = transmittance in visible spectrum
 R_{fv} and R_{bv} = front and back surface visible reflectances

T_{sol} = solar transmittance [τ in Equations (18), (19), and (20)]
 R_f and R_b = front and back surface solar reflectances
 A_{bs1} = solar absorptance for layer 1, which is the only layer in this case
 [α in Equations (18), (19), and (20)]
 SHGC = solar heat gain coefficient at center of glazing

The parameters used for heat gain calculations are T_{sol} , A_{bs} , and SHGC. For the specific convective conditions assumed in WINDOW 7.7.10 program, the inward-flowing fraction of the absorbed solar can be obtained by rearranging Equation (18) to give

$$N_k \alpha_k = \text{SHGC} - \tau \quad (19)$$

This quantity, when multiplied by the appropriate incident solar intensity, provides the amount of absorbed solar radiation that flows inward. In the heat balance formulation for zone loads, this heat flux is combined with that caused by conduction through glazing and included in the surface heat balance.

The outward-flowing fraction of absorbed solar radiation is used in the heat balance on the outdoor face of the glazing and is determined from

$$(1 - N_k) \alpha_k = \alpha_k - N_k \alpha_k = \alpha_k - (\text{SHGC} - \tau) \quad (20)$$

If there is more than one layer, the appropriate summation of absorptances must be done.

There is some potential inaccuracy in using the WINDOW 7.7.10 SHGC values because the inward-flowing fraction part was determined under specific conditions for the indoor and outdoor heat transfer coefficients. However, the program can be run with indoor and outdoor coefficients of one's own choosing. Normally, however, this effect is not large, and only in highly absorptive glazing systems might cause significant error.

For solar heat gain calculations, then, it seems reasonable to use the generic window property data that comes from WINDOW 7.7.10. Considering Table 13, the procedure is as follows:

1. Determine angle of incidence for the glazing.
2. Determine corresponding SHGC.
3. Evaluate $N_k \alpha_k$ using Equation (18).
4. Multiply T_{sol} by incident beam radiation intensity to get transmitted beam solar radiation.
5. Multiply $N_k \alpha_k$ by incident beam radiation intensity to get inward-flowing absorbed heat.
6. Repeat steps 2 to 5 with diffuse parameters and diffuse radiation.
7. Add beam and diffuse components of transmitted and inward-flowing absorbed heat.

This procedure is incorporated into the HB method so the solar gain is calculated accurately for each hour.

Table 10 in Chapter 15 contains SHGC information for many additional glazing systems. That table is similar to Table 13 but is slightly abbreviated. Again, the information needed for heat gain calculations is T_{sol} , SHGC, and A_{bs} .

The same caution about the indoor and outdoor heat transfer coefficients applies to the information in Table 10 in Chapter 15. Those values were also obtained with specific indoor and outdoor heat transfer coefficients, and the inward-flowing fraction N is dependent upon those values.

Convection to Zone Air. Indoor convection coefficients presented in past editions of this chapter and used in most load calculation procedures and energy programs are based on very old, natural convection experiments and do not accurately describe heat transfer coefficients in a mechanically ventilated zone. In previous load calculation procedures, these coefficients were buried in the procedures and could not be changed. A heat balance formulation keeps them as working parameters. In this way, research results such as those from ASHRAE research project RP-664 (Fisher 1998) can

be incorporated into the procedures. It also allows determining the sensitivity of the load calculation to these parameters.

Air Heat Balance

In HB formulations aimed at determining cooling loads, the capacitance of air in the zone is neglected and the air heat balance is done as a quasisteady balance in each time period. Four factors contribute to the air heat balance:

$$q_{conv} + q_{CE} + q_{IV} + q_{sys} = 0 \quad (21)$$

where

q_{conv} = convective heat transfer from surfaces, W
 q_{CE} = convective parts of internal loads, W
 q_{IV} = sensible load caused by infiltration and ventilation air, W
 q_{sys} = heat transfer to/from HVAC system, W

Convection from zone surfaces q_{conv} is the sum of all the convective heat transfer quantities from the indoor-surface heat balance. This comes to the air through the convective heat transfer coefficient on the surfaces.

The **convective parts of the internal loads** q_{CE} is the companion to q''_{LWS} , the radiant contribution from internal loads [Equation (17)]. It is added directly to the air heat balance. This also violates the tenets of the HB approach, because surfaces producing internal loads exchange heat with zone air through normal convective processes. However, once again, this level of detail is generally not included in the heat balance, so it is included directly into the air heat balance instead.

In keeping with the well-mixed model for zone air, any air that enters directly to a space through **infiltration or ventilation** q_{IV} is immediately mixed with the zone's air. The amount of infiltration or natural ventilation air is uncertain. Sometimes it is related to the indoor/outdoor temperature difference and wind speed; however it is determined, it is added directly to the air heat balance.

Conditioned air that enters the zone from the HVAC system and provides q_{sys} is also mixed directly with the zone air. For commercial HVAC systems, ventilation air is most often provided using outdoor air as part of this mixed-in conditioned air; ventilation air is thus normally a system load rather than a direct-to-space load. An exception is where infiltration or natural ventilation is used to provide all or part of the ventilation air, as discussed in Chapter 16.

5.3 GENERAL ZONE FOR LOAD CALCULATION

The HB procedure is tailored to a single thermal zone, shown in Figure 7. The definition of a thermal zone depends on how the fixed temperature is controlled. If air circulated through an entire building or an entire floor is uniformly well stirred, the entire building or floor could be considered a thermal zone. On the other hand, if each room has a different control scheme, each room may need to be considered as a separate thermal zone. The framework needs to be flexible enough to accommodate any zone arrangement, but the heat balance aspect of the procedure also requires that a complete zone be described. This zone consists of four walls, a roof or ceiling, a floor, and a "thermal mass surface" (described in the section on Input Required). Each wall and the roof can include a window (or skylight in the case of the roof). This makes a total of 12 surfaces, any of which may have zero area if it is not present in the zone to be modeled.

The heat balance processes for this general zone are formulated for a 24 h steady-periodic condition. The variables are the indoor and outdoor temperatures of the 12 surfaces plus either the HVAC system energy required to maintain a specified air temperature or the air temperature, if system capacity is specified. This makes a total of $25 \times 24 = 600$ variables. Although it is possible to set up the problem for a simultaneous solution of these variables, the relatively weak coupling of the problem from one hour to the next allows a

double iterative approach. One iteration is through all the surfaces in each hour, and the other is through the 24 h of a day. This procedure automatically reconciles nonlinear aspects of surface radiative exchange and other heat flux terms.

5.4 MATHEMATICAL DESCRIPTION

Conduction Process

Because it links the outdoor and indoor heat balances, the wall conduction process regulates the cooling load's time dependence. For the HB procedure presented here, wall conduction is formulated using **conduction transfer functions (CTFs)**, which relate conductive heat fluxes to current and past surface temperatures and past heat fluxes. The general form for the indoor heat flux is

$$q''_{ki}(t) = -Z_o T_{si,0} - \sum_{j=1}^{nz} Z_j T_{si,0-j\delta} + Y_o T_{so,0} + \sum_{j=1}^{nz} Y_j T_{so,0-j\delta} + \sum_{j=1}^{nq} \Phi_j q''_{ki,0-j\delta} \quad (22)$$

For outdoor heat flux, the form is

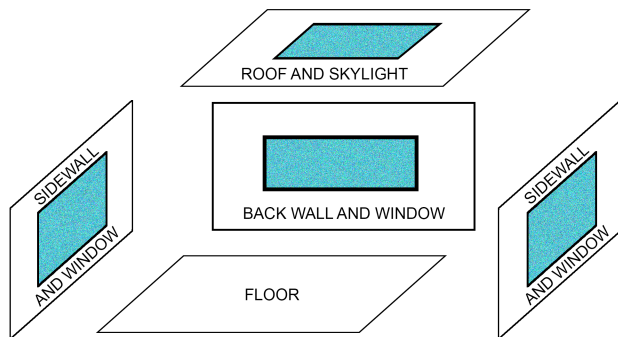
$$q''_{ko}(t) = -Y_o T_{si,0} - \sum_{j=1}^{nz} Y_j T_{si,0-j\delta} + X_o T_{so,0} + \sum_{j=1}^{nz} X_j T_{so,0-j\delta} + \sum_{j=1}^{nq} \Phi_j q''_{ko,0-j\delta} \quad (23)$$

where

- X_j = outdoor CTF, $j = 0, 1, \dots, nz$
- Y_j = cross CTF, $j = 0, 1, \dots, nz$
- Z_j = indoor CTF, $j = 0, 1, \dots, nz$
- Φ_j = flux CTF, $j = 1, 2, \dots, nq$
- θ = time
- δ = time step
- T_{si} = indoor-face temperature, °C
- T_{so} = outdoor-face temperature, °C
- q''_{ki} = conductive heat flux on indoor face, W/m²
- q''_{ko} = conductive heat flux on outdoor face, W/m²

The subscript following the comma indicates the time period for the quantity in terms of time step δ . Also, the first terms in the series have been separated from the rest to facilitate solving for the current temperature in the solution scheme.

The two summation limits nz and nq depend on wall construction and also somewhat on the scheme used for calculating the CTFs. If $nq = 0$, the CTFs are generally referred to as **response factors**, but then theoretically nz is infinite. Values for nz and nq are generally set to minimize the amount of computation. A development of CTFs can be found in Hittle and Pedersen (1981).



Front Wall/Window and Thermal Mass are not shown.

Fig. 7 Schematic View of General Heat Balance Zone

Heat Balance Equations

The primary variables in the heat balance for the general zone are the 12 indoor face temperatures and the 12 outdoor face temperatures at each of the 24 h, assigning i as the surface index and j as the hour index, or, in the case of CTFs, the sequence index. Thus, the primary variables are

$$T_{soij} = \text{outdoor face temperature, } i = 1, 2, \dots, 12; j = 1, 2, \dots, 24$$

$$T_{sij} = \text{indoor face temperature, } i = 1, 2, \dots, 12; j = 1, 2, \dots, 24$$

In addition, q_{sysj} = cooling load, $j = 1, 2, \dots, 24$.

Equations (16) and (23) are combined and solved for T_{so} to produce 12 equations applicable in each time step:

$$T_{soij} = \left(\sum_{k=1}^{nz} T_{si,j-k} Y_{i,k} - \sum_{k=1}^{nz} T_{so,j-k} Z_{i,k} - \sum_{k=1}^{nq} \Phi_{i,k} q''_{ko,j-k} + q''_{asol,i,j} + q''_{LWR,i,j} + T_{si,j} Y_{i,0} + T_{o,j} h_{co,i,j} \right) / (X_{i,0} + h_{co,i,j}) \quad (24)$$

where

T_o = outdoor air temperature

h_{co} = outdoor convection coefficient, introduced by using $q''_{conv} = h_{co}(T_o - T_{so})$

Equation (24) shows the need to separate $X_{i,0}$, because the contribution of current surface temperature to conductive flux cannot be collected with the other historical terms involving that temperature.

Equations (17) and (22) are combined and solved for T_{si} to produce the next 12 equations:

$$T_{soij} = \left(T_{so,i,j} Y_{i,0} + \sum_{k=1}^{nz} T_{so,j-k} Y_{i,k} - \sum_{k=1}^{nz} T_{si,j-k} Z_{i,k} + \sum_{k=1}^{nq} \Phi_{i,k} q''_{ki,j-k} + T_{a,j} h_{ci,j} + q''_{LWS} + q''_{LWX} + q''_{SW} + q''_{sol,e} \right) / (Z_{i,0} + h_{ci,i,j}) \quad (25)$$

where

T_a = zone air temperature

h_{ci} = convective heat transfer coefficient indoors, obtained from $q''_{conv} = h_{ci}(T_a - T_{si})$

Note that in Equations (24) and (25), the opposite surface temperature at the current time appears on the right-hand side. The two equations could be solved simultaneously to eliminate those variables. Depending on the order of updating the other terms in the equations, this can have a beneficial effect on solution stability.

The remaining equation comes from the air heat balance, Equation (21). This provides the cooling load q_{sys} at each time step:

$$q_{sysj} = \sum_{i=1}^{12} A_i h_{ci} (T_{si,j} - T_{a,j}) + q_{CE} + q_{IV} \quad (26)$$

In Equation (26), the convective heat transfer term is expanded to show the interconnection between the surface temperatures and the cooling load.

Overall HB Iterative Solution

The iterative HB procedure consists of a series of initial calculations that proceed sequentially, followed by a double iteration loop, as shown in the following steps:

1. Initialize areas, properties, and face temperatures for all surfaces, 24 h.
2. Calculate incident and transmitted solar flux for all surfaces and hours.
3. Distribute transmitted solar energy to all indoor faces, 24 h.
4. Calculate internal load quantities for all 24 h.
5. Distribute LW, SW, and convective energy from internal loads to all surfaces for all hours.
6. Calculate infiltration and direct-to-space ventilation loads for all hours.
7. Iterate the heat balance according to the following scheme:

```

For Day = 1 to Maxdays
  For j = 1 to 24           {hours in the day}
    For Surfacelter = 1 to Maxlter
      For i = 1 to 12       {The twelve zone surfaces}
        Evaluate Equations (33) and (34)
      Next i
      Next Surfacelter
      Evaluate Equation (35)
    Next j
  If not converged, Next Day

```

8. Display results.

Generally, four or six surface iterations are sufficient to provide convergence. The convergence check on the day iteration should be based on the difference between the indoor and outdoor conductive heat flux terms q_k . A limit, such as requiring the difference between all indoor and outdoor flux terms to be less than 1% of either flux, works well.

5.5 INPUT REQUIRED

Previous methods for calculating cooling loads attempted to simplify the procedure by precalculating representative cases and grouping the results with various correlating parameters. This generally tended to reduce the amount of information required to apply the procedure. With heat balance, no precalculations are made, so the procedure requires a fairly complete description of the zone.

Global Information. Because the procedure incorporates a solar calculation, some global information is required, including latitude, longitude, time zone, month, day of month, directional orientation of the zone, and zone height (floor to floor). Additionally, to take full advantage of the flexibility of the method to incorporate, for example, variable outdoor heat transfer coefficients, things such as wind speed, wind direction, and terrain roughness may be specified. Normally, these variables and others default to some reasonable set of values, but the flexibility remains.

Wall Information (Each Wall). Because the walls are involved in three of the fundamental processes (external and internal heat balance and wall conduction), each wall of the zone requires a fairly large set of variables. They include

- Facing angle with respect to solar exposure
- Tilt (degrees from horizontal)
- Area
- Solar absorptivity outdoors
- Long-wave emissivity outdoors
- Short-wave absorptivity indoors
- Long-wave emissivity indoors
- Exterior boundary temperature condition (solar versus nonsolar)
- External roughness
- Layer-by-layer construction information

Again, some of these parameters can be defaulted, but they are changeable, and they indicate the more fundamental character of the HB method because they are related to true heat transfer processes.

Window Information (Each Window). The situation for windows is similar to that for walls, but the windows require some additional information because of their role in the solar load. Necessary parameters include

- Area
- Normal solar transmissivity
- Normal SHGC
- Normal total absorptivity
- Long-wave emissivity outdoors
- Long-wave emissivity indoor
- Surface-to-surface thermal conductance
- Reveal (for solar shading)
- Overhang width (for solar shading)
- Distance from overhang to window (for solar shading)

Roof and Floor Details. The roof and floor surfaces are specified similarly to walls. The main difference is that the ground outdoor boundary condition will probably be specified more often for a floor.

Thermal Mass Surface Details. An “extra” surface, called a thermal mass surface, can serve several functions. It is included in radiant heat exchange with the other surfaces in the space but is only exposed to the indoor air convective boundary condition. As an example, this surface would be used to account for movable partitions in a space. Partition construction is specified layer by layer, similar to specification for walls, and those layers store and release heat by the same conduction mechanism as walls. As a general definition, the extra thermal mass surface should be sized to represent all surfaces in the space that are exposed to the air mass, except the walls, roof, floor, and windows. In the formulation, both sides of the thermal mass participate in the exchange.

Internal Heat Gain Details. The space can be subjected to several internal heat sources: people, lights, electrical equipment, and infiltration. Infiltration energy is assumed to go immediately into the air heat balance, so it is the least complicated of the heat gains. For the others, several parameters must be specified. These include the following fractions:

- Sensible heat gain
- Latent heat gain
- Short-wave radiation
- Long-wave radiation
- Energy that enters the air immediately as convection
- Activity level of people
- Lighting heat gain that goes directly to the return air

Radiant Distribution Functions. As mentioned previously, the generally accepted assumptions for the HB method include specifying the distribution of radiant energy from several sources to surfaces that enclose the space. This requires a distribution function that specifies the fraction of total radiant input absorbed by each surface. The types of radiation that require distribution functions are

- Long-wave, from equipment and lights
- Short-wave, from lights
- Transmitted solar

Other Required Information. Additional flexibility is included in the model so that results of research can be incorporated easily. This includes the capability to specify such things as

- Heat transfer coefficients/convection models
- Solar coefficients
- Sky models

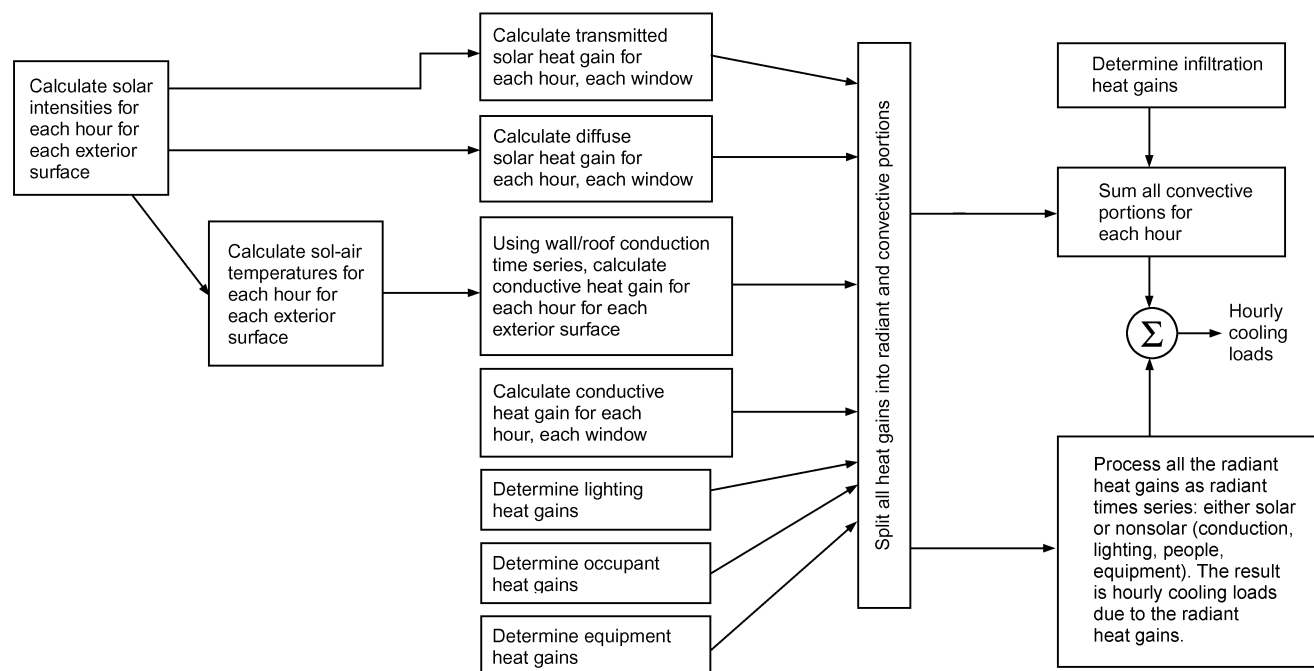


Fig. 8 Overview of Radiant Time Series Method

The amount of input information required may seem extensive, but many parameters can be set to default values in most routine applications. However, all parameters listed can be changed when necessary to fit unusual circumstances or when additional information is obtained.

6. RADIANT TIME SERIES (RTS) METHOD

The radiant time series (RTS) method is a simplified method for performing design cooling load calculations that is derived from the heat balance (HB) method. It is intended as a more up-to-date alternative to other simplified (non-heat-balance) methods, such as the transfer function method (TFM), the cooling load temperature difference/cooling load factor (CLTD/CLF) method, and the total equivalent temperature difference/time averaging (TETD/TA) method.

This method was developed to offer an approach that is rigorous, yet does not require iterative calculations, and that quantifies each component's contribution to the total cooling load. In addition, it is desirable for the user to be able to inspect and compare the coefficients for different construction and zone types in a form showing their relative effect on the result. These characteristics of the RTS method make it easier to apply engineering judgment during cooling load calculation.

The RTS method is suitable for peak design load calculations, but it should not be used for annual energy simulations because of its inherent limiting assumptions. Although simple in concept, RTS involves too many calculations for practical use as a manual method, although it can easily be implemented in a simple computerized spreadsheet, as shown in the examples. For a manual cooling load calculation method, refer to the CLTD/CLF method in Chapter 28 of the 1997 *ASHRAE Handbook—Fundamentals*.

6.1 ASSUMPTIONS AND PRINCIPLES

Design cooling loads are based on the assumption of **steady-periodic conditions** (i.e., the design day's weather, occupancy, and

heat gain conditions are identical to those for preceding days such that the loads repeat on an identical 24 h cyclical basis). Thus, the heat gain for a particular component at a particular hour is the same as 24 h prior, which is the same as 48 h prior, etc. This assumption is the basis for the RTS derivation from the HB method.

Cooling load calculations must address two time-delay effects inherent in building heat transfer processes:

- Delay of conductive heat gain through opaque massive exterior surfaces (walls, roofs, or floors)
- Delay of radiative heat gain conversion to cooling loads.

Exterior walls and roofs conduct heat because of temperature differences between outdoor and indoor air. In addition, solar energy on exterior surfaces is absorbed, then transferred by conduction to the building interior. Because of the mass and thermal capacity of the wall or roof construction materials, there is a substantial time delay in heat input at the exterior surface becoming heat gain at the interior surface.

As described in the section on Cooling Load Principles, most heat sources transfer energy to a room by a combination of convection and radiation. The convective part of heat gain immediately becomes cooling load. The radiative part must first be absorbed by the finishes and mass of the interior room surfaces, and becomes cooling load only when it is later transferred by convection from those surfaces to the room air. Thus, radiant heat gains become cooling loads over a delayed period of time.

6.2 OVERVIEW

Figure 8 gives an overview of the RTS method. When calculating solar radiation, transmitted solar heat gain through windows, sol-air temperature, and infiltration, RTS is exactly the same as previous simplified methods (TFM and TETD/TA). Important areas that differ from previous simplified methods include

- Computation of conductive heat gain
- Splitting of all heat gains into radiant and convective portions
- Conversion of radiant heat gains into cooling loads

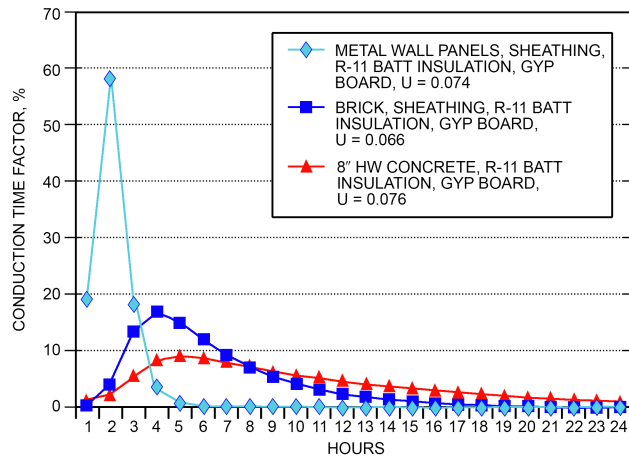


Fig. 9 CTS for Light to Heavy Walls

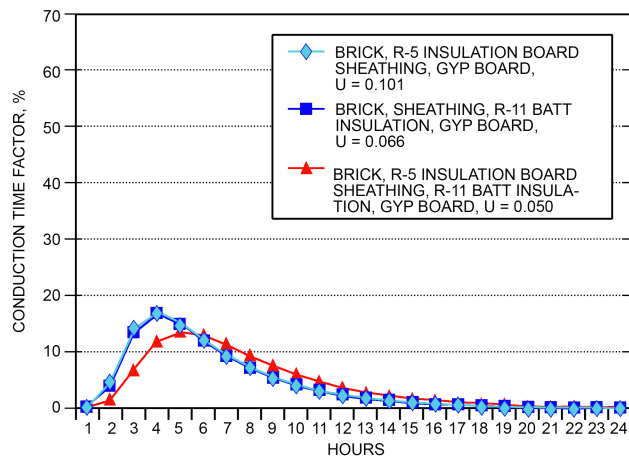


Fig. 10 CTS for Walls with Similar Mass and Increasing Insulation

The RTS method accounts for both conduction time delay and radiant time delay effects by multiplying hourly heat gains by 24 h time series. The time series multiplication, in effect, distributes heat gains over time. Series coefficients, which are called **radiant time factors** and **conduction time factors**, are derived using the HB method. Radiant time factors reflect the percentage of an earlier radiant heat gain that becomes cooling load during the current hour. Likewise, conduction time factors reflect the percentage of an earlier heat gain at the exterior of a wall or roof that becomes heat gain indoors during the current hour. By definition, each radiant or conduction time series must total 100%.

These series can be used to easily compare the time-delay effect of one construction versus another. This ability to compare choices is of particular benefit during design, when all construction details may not have been decided. Comparison can show the magnitude of difference between the choices, allowing the engineer to apply judgment and make more informed assumptions in estimating the load.

Figure 9 shows conduction time series (CTS) values for three walls with similar U-factors but with light to heavy construction. Figure 10 shows CTS for three walls with similar construction but with different amounts of insulation, thus with significantly different U-factors. Figure 11 shows RTS values for zones varying from light to heavy construction.

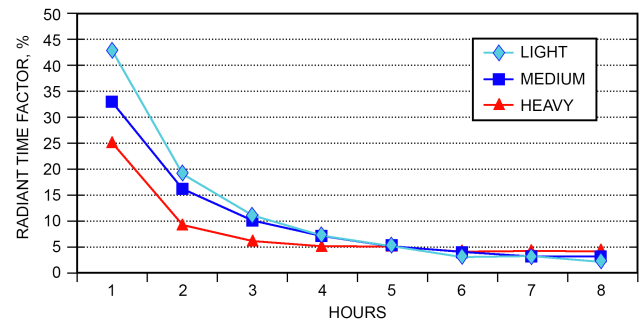


Fig. 11 RTS for Light to Heavy Construction

Note that the RTS and CTS factors presented in this section were derived using heat balance method solutions with an air-based system assumed. Specific values have not been developed that would take into account radiant cooling systems. In the case of the CTS factors, conduction through an exterior opaque wall is not expected to be meaningfully different whether a radiant or convective cooling system is used. In reality, the radiant cooling system alters inside surface temperature of the exterior wall, so there will be differences in the resulting heat exchange mechanics. However, based on modeling and testing completed as part of ASHRAE RP-1729 (Moftakhari et al. 2020), the impact on the timing and magnitude of conduction heat gains is small (5 to 10%) in relation to the overall space load.

RTS factors are used to model the conversion of stored radiant heat gains to cooling loads. There is a difference in the conversion of these heat gains for radiant systems compared to convective or air-based systems. RP-1729 found that the radiant time series method could be used with radiant cooling systems but only if RTS factors for radiantly cooled spaces were derived. To date, RTS factors based on radiant cooling systems have not been developed beyond the pilot examples developed for RP-1729.

6.3 RTS PROCEDURE

The general procedure for calculating cooling load for each load component (lights, people, walls, roofs, windows, appliances, etc.) with RTS is as follows:

1. Calculate 24 h profile of component heat gains for design day (for conduction, first account for conduction time delay by applying conduction time series).
2. Split heat gains into radiant and convective parts (see Table 14 for radiant and convective fractions).
3. Apply appropriate radiant time series to radiant part of heat gains to account for time delay in conversion to cooling load.
4. Sum convective part of heat gain and delayed radiant part of heat gain to determine cooling load for each hour for each cooling load component.

After calculating cooling loads for each component for each hour, sum those to determine the total cooling load for each hour and select the hour with the peak load for design of the air-conditioning system. Repeat this process for multiple design months to determine the month when the peak load occurs, especially with windows on southern exposures (northern exposure in southern latitudes), which can result in higher peak room cooling loads in winter months than in summer.

6.4 HEAT GAIN THROUGH EXTERIOR SURFACES

Heat gain through exterior opaque surfaces is derived from the same elements of solar radiation and thermal gradient as that for fenestration areas. It differs primarily as a function of the mass and nature of the wall or roof construction, because those elements affect the rate of conductive heat transfer through the composite assembly to the interior surface.

Sol-Air Temperature

Sol-air temperature is the outdoor air temperature that, in the absence of all radiation changes gives the same rate of heat entry into the surface as would the combination of incident solar radiation, radiant energy exchange with the sky and other outdoor surroundings, and convective heat exchange with outdoor air.

Heat Flux into Exterior Sunlit Surfaces. The heat balance at a sunlit surface gives the heat flux into the surface q/A as

$$\frac{q}{A} = \alpha E_t + h_o(t_o - t_s) - \varepsilon \Delta R \quad (27)$$

where

α = absorptance of surface for solar radiation

E_t = total solar radiation incident on surface, W/m^2

h_o = coefficient of heat transfer by long-wave radiation and convection at outer surface, $W/(m^2 \cdot K)$

t_o = outdoor air temperature, $^{\circ}C$

t_s = surface temperature, $^{\circ}C$

ε = hemispherical emittance of surface

ΔR = difference between long-wave radiation incident on surface from sky and surroundings and radiation emitted by blackbody at outdoor air temperature, W/m^2

Assuming the rate of heat transfer can be expressed in terms of the sol-air temperature t_e ,

$$\frac{q}{A} = h_o(t_e - t_s) \quad (28)$$

and from Equations (27) and (28),

$$t_e = t_o + \frac{\alpha E_t}{h_o} - \frac{\varepsilon \Delta R}{h_o} \quad (29)$$

For **horizontal surfaces** that receive long-wave radiation from the sky only, an appropriate value of ΔR is about $63 W/m^2$, so that if $\varepsilon = 1$ and $h_o = 17 W/(m^2 \cdot K)$, the long-wave correction term is about 4 K (Bliss 1961).

Because **vertical surfaces** receive long-wave radiation from the ground and surrounding buildings as well as from the sky, accurate ΔR values are difficult to determine. When solar radiation intensity is high, surfaces of terrestrial objects usually have a higher temperature than the outdoor air; thus, their long-wave radiation compensates to some extent for the sky's low emittance. Therefore, it is common practice to assume $\varepsilon \Delta R = 0$ for vertical surfaces.

Tabulated Temperature Values. The sol-air temperatures in Example Cooling and Heating Load Calculations section have been calculated based on $\varepsilon \Delta R/h_o$ values of 4 K for horizontal surfaces and 0 K for vertical surfaces; total solar intensity values used for the calculations were calculated using equations in Chapter 14.

Surface Colors. Sol-air temperature values are given in the Example Cooling and Heating Load Calculations section for two values of the parameter α/h_o ; the value of 0.026 is appropriate for a light-colored surface, whereas 0.052 represents the usual maximum value for this parameter (i.e., for a dark-colored surface or any surface for which the permanent lightness cannot reliably be anticipated). Solar absorptance values of various surfaces are included in Table 15.

This procedure was used to calculate the sol-air temperatures included in the Examples section. Because of the tedious solar angle and intensity calculations, using a simple computer spreadsheet or other software for these calculations can reduce the effort involved.

Calculating Conductive Heat Gain Using Conduction Time Series

In the RTS method, conduction through exterior walls and roofs is calculated using CTS values. Wall and roof conductive heat input at the exterior is defined by the familiar conduction equation as

$$q_{i,0-n} = UA(t_{e,0-n} - t_{rc}) \quad (30)$$

where

$q_{i,0-n}$ = conductive heat input for surface n hours ago, W

U = overall heat transfer coefficient for surface, $W/(m^2 \cdot K)$

A = surface area, m^2

$t_{e,0-n}$ = sol-air temperature n hours ago, $^{\circ}C$

t_{rc} = presumed constant room air temperature, $^{\circ}C$

Conductive heat gain through walls or roofs can be calculated using conductive heat inputs for the current hours and past 23 h and conduction time series:

Table 14 Recommended Radiative/Convective Splits for Internal Heat Gains

Heat Gain Type	Recommended Radiative Fraction	Recommended Convective Fraction	Comments
Occupants, typical office conditions	0.60	0.40	See Table 1 for other conditions.
Equipment	0.1 to 0.8	0.9 to 0.2	See Tables 6 to 12 for details of equipment heat gain and recommended radiative/convective splits for motors, cooking appliances, laboratory equipment, medical equipment, office equipment, etc.
Office, with fan	0.10	0.90	
Without fan	0.30	0.70	
Lighting			Varies; see Table 3.
Conduction heat gain			
Through walls and floors	0.46	0.54	
Through roof	0.60	0.40	
Through windows	0.33 (SHGC > 0.5) 0.46 (SHGC < 0.5)	0.67 (SHGC > 0.5) 0.54 (SHGC < 0.5)	
Solar heat gain through fenestration			
Without interior shading	1.00	0.00	
With interior shading			Varies; see Tables 14A to 14G in Chapter 15.
Infiltration	0.00	1.00	

Source: Nigusse (2007).

Table 15 Solar Absorptance Values of Various Surfaces

Surface	Absorptance
Brick, red (Purdue) ^a	0.63
Paint	
Red ^b	0.63
Black, matte ^b	0.94
Sandstone ^b	0.50
White acrylic ^a	0.26
Sheet metal, galvanized	
New ^a	0.65
Weathered ^a	0.80
Shingles	
Gray ^b	0.82
Brown ^b	0.91
Black ^b	0.97
White ^b	0.75
Concrete ^{a,c}	0.60 to 0.83

^aIncropera and DeWitt (1990).^bParker et al. (2000). ^cMiller (1971).

$$q_0 = c_0 q_{i,0} + c_1 q_{i,0-1} + c_2 q_{i,0-2} + c_3 q_{i,0-3} + \dots + c_{23} q_{i,0-23} \quad (31)$$

where

 q_0 = hourly conductive heat gain for surface, W $q_{i,0}$ = heat input for current hour $q_{i,0-n}$ = heat input n hours ago c_0, c_1 , etc. = conduction time factors

Conduction time factors for representative wall and roof types are included in Tables 16 and 17. Those values were derived by first calculating conduction transfer functions for each example wall and roof construction. Assuming steady-periodic heat input conditions for design load calculations allows conduction transfer functions to be reformulated into periodic response factors, as demonstrated by Spitler and Fisher (1999a). The periodic response factors were further simplified by dividing the 24 periodic response factors by the respective overall wall or roof U-factor to form the conduction time series. The conduction time factors can then be used in Equation (31) and provide a way to compare time delay characteristics between different wall and roof constructions. Construction material data used in the calculations for walls and roofs in Tables 16 and 17 are listed in Table 18.

Heat gains calculated for walls or roofs using periodic response factors (and thus CTS) are identical to those calculated using conduction transfer functions for the steady periodic conditions assumed in design cooling load calculations. The methodology for calculating periodic response factors from conduction transfer functions was originally developed as part of ASHRAE research project RP-875 (Spitler and Fisher 1999b; Spitler et al. 1997). For walls and roofs that are not reasonably close to the representative constructions in Tables 16 and 17, CTS coefficients may be computed with a computer program such as that described by Iu and Fisher (2004). For walls and roofs with thermal bridges, the procedure described by Karambakkam et al. (2005) may be used to determine an equivalent wall construction, which can then be used as the basis for finding the CTS coefficients. When considering the level of detail needed to make an adequate approximation, remember that, for buildings with windows and internal heat gains, the conduction heat gains make up a relatively small part of the cooling load. For heating load calculations, the conduction heat loss may be more significant.

The tedious calculations involved make a simple computer spreadsheet or other computer software a useful labor saver.

6.5 HEAT GAIN THROUGH INTERIOR SURFACES

Whenever a conditioned space is adjacent to a space with a different temperature, heat transfer through the separating physical section must be considered. The heat transfer rate is given by

$$q = UA(t_b - t_i) \quad (32)$$

where

 q = heat transfer rate, W U = coefficient of overall heat transfer between adjacent and conditioned space, W/(m²·K) A = area of separating section concerned, m² t_b = average air temperature in adjacent space, °C t_i = air temperature in conditioned space, °C

U-values can be obtained from Chapter 27. Temperature t_b may differ greatly from t_i . The temperature in a kitchen or boiler room, for example, may be as much as 8 to 28 K above the outdoor air temperature. Actual temperatures in adjoining spaces should be measured, when possible. Where nothing is known except that the adjacent space is of conventional construction, contains no heat sources, and itself receives no significant solar heat gain, $t_b - t_i$ may be considered the difference between the outdoor air and conditioned space design dry-bulb temperatures minus 3 K. In some cases, air temperature in the adjacent space corresponds to the outdoor air temperature or higher.

Floors

For floors directly in contact with the ground or over an underground basement that is neither ventilated nor conditioned, sensible heat transfer may be neglected for cooling load estimates because usually there is a heat loss rather than a gain. An exception is in hot climates (i.e., where average outdoor air temperature exceeds indoor design condition), where the positive soil-to-indoor temperature difference causes sensible heat gains (Rock 2005). In many climates and for various temperatures and local soil conditions, moisture transport up through slabs-on-grade and basement floors is also significant, and contributes to the latent heat portion of the cooling load.

6.6 CALCULATING COOLING LOAD

The **instantaneous cooling load** is the rate at which heat energy is convected to the zone air at a given point in time. Computation of cooling load is complicated by the radiant exchange between surfaces, furniture, partitions, and other mass in the zone. Most heat gain sources transfer energy by both convection and radiation. Radiative heat transfer introduces a time dependency to the process that is not easily quantified. Radiation is absorbed by thermal masses in the zone and then later transferred by convection into the space. This process creates a time lag and dampening effect. The convective portion, on the other hand, is assumed to immediately become cooling load in the hour in which that heat gain occurs.

Heat balance procedures calculate the radiant exchange between surfaces based on their surface temperatures and emissivities, but they typically rely on estimated "radiative/convective splits" to determine the contribution of internal loads, including people, lighting, appliances, and equipment, to the radiant exchange. RTS further simplifies the HB procedure by also relying on an estimated radiative/convective split of wall and roof conductive heat gain instead of simultaneously solving for the instantaneous convective and radiative heat transfer from each surface, as in the HB procedure.

Thus, the cooling load for each load component (lights, people, walls, roofs, windows, appliances, etc.) for a particular hour is the sum of the convective portion of the heat gain for that hour plus the

Table 16 Wall Conduction Time Series (CTS)

	Curtainwalls						Studwalls			
	Spandrel Glass, R-1.8 Insulation Board, Gyp. Board	Spandrel Glass, R-3.5 Insulation Board, Gyp. Board	Metal Wall Panel, R-1.8 Insulation Board, Gyp. Board	Metal Wall Panel, R-3.5 Insulation Board, Gyp. Board	25 mm Stone, R-1.8 Insulation Board, Gyp. Board	25 mm Stone, R-3.5 Insulation Board, Gyp. Board	Metal Wall Panel, Sheathing, R-9 Batt Insulation, Gyp. Board	Metal Wall Panel, Sheathing, R-3.9 Batt Insulation, Gyp. Board	25 mm Stone, Sheathing, R-1.9 Batt Insulation, Gyp. Board	25 mm Stone, Sheathing, R-3.9 Batt Insulation, Gyp. Board
Wall Number	1	2	3	4	5	6	7	8	9	10
U , W/ (m ² ·K)	0.428	0.244	0.429	0.244	0.427	0.244	0.419	0.231	0.417	0.231
Total R	2.34	4.10	2.33	4.09	2.34	4.10	2.39	4.33	2.40	4.34
Hour	Conduction Time Factors, %						Conduction Time Factors, %			
0	16.4	2.5	23.0	4.1	7.5	1.0	26.1	16.3	9.4	5.3
1	56.7	31.6	56.3	36.5	42.8	19.1	56.3	57.5	44.3	39.0
2	21.3	37.1	16.5	34.9	32.2	34.6	14.5	20.9	29.9	34.0
3	4.5	18.1	3.3	15.6	12.3	24.5	2.6	4.3	11.3	14.5
4	0.9	6.9	0.7	5.8	3.8	12.2	0.4	0.8	3.6	5.0
5	0.2	2.5	0.1	2.0	1.1	5.2	0.1	0.2	1.1	1.6
6	0.0	0.9	0.0	0.7	0.3	2.1	0.0	0.0	0.3	0.5
7	0.0	0.3	0.0	0.2	0.1	0.8	0.0	0.0	0.1	0.1
8	0.0	0.1	0.0	0.1	0.0	0.3	0.0	0.0	0.0	0.0
9	0.0	0.0	0.0	0.0	0.0	0.1	0.0	0.0	0.0	0.0
10	0.0	0.0	0.0	0.0	0.0	0.0	0.0	0.0	0.0	0.0
11	0.0	0.0	0.0	0.0	0.0	0.0	0.0	0.0	0.0	0.0
12	0.0	0.0	0.0	0.0	0.0	0.0	0.0	0.0	0.0	0.0
13	0.0	0.0	0.0	0.0	0.0	0.0	0.0	0.0	0.0	0.0
14	0.0	0.0	0.0	0.0	0.0	0.0	0.0	0.0	0.0	0.0
15	0.0	0.0	0.0	0.0	0.0	0.0	0.0	0.0	0.0	0.0
16	0.0	0.0	0.0	0.0	0.0	0.0	0.0	0.0	0.0	0.0
17	0.0	0.0	0.0	0.0	0.0	0.0	0.0	0.0	0.0	0.0
18	0.0	0.0	0.0	0.0	0.0	0.0	0.0	0.0	0.0	0.0
19	0.0	0.0	0.0	0.0	0.0	0.0	0.0	0.0	0.0	0.0
20	0.0	0.0	0.0	0.0	0.0	0.0	0.0	0.0	0.0	0.0
21	0.0	0.0	0.0	0.0	0.0	0.0	0.0	0.0	0.0	0.0
22	0.0	0.0	0.0	0.0	0.0	0.0	0.0	0.0	0.0	0.0
23	0.0	0.0	0.0	0.0	0.0	0.0	0.0	0.0	0.0	0.0
Total Percentage	100	100	100	100	100	100	100	100	100	100
Layer ID from outdoors to indoors (See Table 18)	F01 F09 F04 I02 F04 G01 F02 0 0 0	F01 F09 F04 I02 F04 F04 G01 F02 0 0 0	F01 F08 F04 I02 F04 G01 F02 0 0 0	F01 F08 F04 I02 F04 F04 G01 F02 0 0 0	F01 F10 F04 I02 F04 I02 F02 0 0 0	F01 F10 F04 I02 F04 I02 G01 F02 0 0 0	F01 F08 G03 I04 G01 F02 0 0 0	F01 F08 G03 I04 I04 G01 F02 0 0 0	F01 F10 G03 I04 G01 F02 0 0 0	F01 F10 G03 I04 I04 G01 G01 F02 0 0 0

time-delayed portion of radiant heat gains for that hour and the previous 23 h. Table 14 contains recommendations for splitting each of the heat gain components into convective and radiant portions.

RTS converts the radiant portion of hourly heat gains to hourly cooling loads using radiant time factors, the coefficients of the radiant time series. Radiant time factors are used to calculate the cooling

load for the current hour on the basis of current and past heat gains. The radiant time series for a particular zone gives the time-dependent response of the zone to a single pulse of radiant energy. The series shows the portion of the radiant pulse that is convected to zone air for each hour. Thus, r_0 represents the fraction of the radiant pulse convected to the zone air in the current hour r_1 in the previous

Table 16 Wall Conduction Time Series (CTS) (Continued)

	Studwalls				EIFS					
	Wood Siding, Sheathing, R-1.9 Batt Insulation, 12.5 mm Wood	Wood Siding, Sheathing, R-3.9 Batt Insulation, 12.5 mm Wood	25 mm Stucco, Sheathing, R-1.9 Batt Insulation, Gyp. Board	25 mm Stucco, Sheathing, R-3.9 Batt Insulation, Gyp. Board	EIFS, R-0.9 Insulation Board, Sheathing, Gyp. Board	EIFS, R-1.8 Insulation Board, Sheathing, Gyp. Board	EIFS, R-0.9 Insulation Board, R-1.9 Batt Insulation, Gyp. Board	EIFS, R-0.9 Insulation Board, R-3.9 Batt Insulation, Gyp. Board	EIFS, R0.9 Insulation Board, 200 mm LW CMU, Gyp. Board	EIFS, R-1.8 Insulation Board, 200 mm LW CMU, Gyp. Board
Wall Number	11	12	13	14	15	16	17	18	19	20
U , W/(m ² ·K)	0.401	0.226	0.412	0.229	0.667	0.420	0.305	0.192	0.514	0.354
Total R	2.49	4.43	2.42	4.36	1.50	2.38	3.28	5.22	1.95	2.83
Hour	Conduction Time Factors, %				Conduction Time Factors, %					
0	5.1	2.7	8.4	4.6	11.5	5.4	3.7	1.7	1.1	1.4
1	33.5	27.4	44.0	38.1	48.6	39.5	28.5	20.8	1.8	1.7
2	31.1	32.5	30.8	34.9	26.6	32.3	30.5	29.2	5.1	4.0
3	16.5	19.3	11.6	15.0	9.0	13.8	18.2	20.5	8.1	6.7
4	7.7	9.6	3.7	5.1	2.9	5.5	9.5	12.2	9.0	8.0
5	3.4	4.6	1.1	1.6	0.9	2.1	4.8	6.9	8.7	8.0
6	1.5	2.1	0.3	0.5	0.3	0.8	2.4	3.9	8.1	7.6
7	0.7	1.0	0.1	0.1	0.1	0.3	1.2	2.1	7.3	7.1
8	0.3	0.4	0.0	0.0	0.0	0.1	0.6	1.2	6.5	6.5
9	0.1	0.2	0.0	0.0	0.0	0.1	0.3	0.7	5.8	5.9
10	0.1	0.1	0.0	0.0	0.0	0.0	0.1	0.4	5.2	5.4
11	0.0	0.0	0.0	0.0	0.0	0.0	0.1	0.2	4.7	4.9
12	0.0	0.0	0.0	0.0	0.0	0.0	0.0	0.1	4.1	4.4
13	0.0	0.0	0.0	0.0	0.0	0.0	0.0	0.1	3.7	4.0
14	0.0	0.0	0.0	0.0	0.0	0.0	0.0	0.0	3.3	3.6
15	0.0	0.0	0.0	0.0	0.0	0.0	0.0	0.0	2.9	3.3
16	0.0	0.0	0.0	0.0	0.0	0.0	0.0	0.0	2.6	3.0
17	0.0	0.0	0.0	0.0	0.0	0.0	0.0	0.0	2.3	2.7
18	0.0	0.0	0.0	0.0	0.0	0.0	0.0	0.0	2.1	2.5
19	0.0	0.0	0.0	0.0	0.0	0.0	0.0	0.0	1.9	2.2
20	0.0	0.0	0.0	0.0	0.0	0.0	0.0	0.0	1.7	2.0
21	0.0	0.0	0.0	0.0	0.0	0.0	0.0	0.0	1.5	1.9
22	0.0	0.0	0.0	0.0	0.0	0.0	0.0	0.0	1.3	1.7
23	0.0	0.0	0.0	0.0	0.0	0.0	0.0	0.0	1.2	1.5
Total Percentage	100	100	100	100	100	100	100	100	100	100
Layer ID from outdoors to indoors (See Table 18)	F01	F01	F01	F01	F01	F01	F01	F01	F01	F01
	F11	F11	F07	F07	F06	F06	F06	F06	F06	F06
	G02	G02	G03	G03	I01	I01	I01	I01	I01	I01
	I04	I04	I04	I04	G03	I01	G03	G03	G03	I01
	G01	I04	G01	I04	F04	G03	I04	I04	M03	G03
	F02	G01	F02	G01	G01	F04	G01	I04	F04	M03
	0	F02	0	F02	F02	G01	F02	G01	G01	F04
	0	0	0	0	0	F02	0	F02	F02	G01
	0	0	0	0	0	0	0	0	0	F02
	0	0	0	0	0	0	0	0	0	0

hour, and so on. The radiant time series thus generated is used to convert the radiant portion of hourly heat gains to hourly cooling loads according to the following equation:

$$Q_{r,\theta} = r_0 q_{r,\theta} + r_1 q_{r,\theta-1} + r_2 q_{r,\theta-2} + r_3 q_{r,\theta-3} + \dots + r_{23} q_{r,\theta-23} \quad (33)$$

where

$Q_{r,\theta}$ = radiant cooling load Q_r for current hour θ , W

$q_{r,\theta}$ = radiant heat gain for current hour, W

$q_{r,\theta-n}$ = radiant heat gain n hours ago, W

$r_0, r_1, \text{etc.}$ = radiant time factors

The radiant cooling load for the current hour, which is calculated using RTS and Equation (33), is added to the convective portion to determine the total cooling load for that component for that hour.

Radiant time factors are generated by a heat-balance-based procedure. A separate series of radiant time factors is theoretically

Table 16 Wall Conduction Time Series (CTS) (Continued)

	Brick Walls								
	Brick, R-0.9 Insulation Board, Sheathing, Gyp. Board	Brick, R-1.8 Insulation Board, Sheathing, Gyp. Board	Brick, Sheathing, R-1.9 Batt Insulation, Gyp. Board	Brick, Sheathing, R-3.9 Batt Insulation, Gyp. Board	Brick, R-0.9 Insulation Board, Sheathing, R-1.9 Batt Insulation, Gyp. Board	Brick, R-0.9 Insulation Board, Sheathing, R-3.9 Batt Insulation, Gyp. Board	Brick, R-0.9 Insulation Board, 200 mm LW CMU	Brick, R-1.8 Insulation Board, 200 mm LW CMU	Brick, 200 mm LW CMU, R-1.9 Batt Insulation, Gyp. Board
Wall Number	21	22	23	24	25	26	27	28	29
U , W/(m ² ·K)	0.571	0.380	0.376	0.218	0.283	0.157	0.568	0.378	0.343
Total R	1.75	2.63	2.66	4.59	3.54	6.36	1.76	2.64	2.92
Hour	Conduction Time Factors, %								
0	0.2	0.1	0.2	0.2	0.1	0.3	0.7	0.9	1.7
1	4.7	2.7	5.1	3.5	1.9	0.7	0.8	0.9	1.6
2	13.8	10.7	14.5	12.4	7.7	3.2	2.4	1.9	2.0
3	16.6	15.3	16.7	16.2	12.3	6.9	5.0	4.0	3.3
4	14.9	15.0	14.4	14.8	13.6	9.5	7.1	6.1	4.9
5	12.0	12.8	11.4	12.0	12.7	10.4	8.3	7.4	6.1
6	9.3	10.2	8.8	9.4	10.9	10.3	8.7	8.0	6.8
7	7.1	8.0	6.8	7.3	9.0	9.6	8.6	8.1	7.0
8	5.3	6.1	5.2	5.6	7.2	8.5	8.1	7.9	6.9
9	4.0	4.7	4.0	4.3	5.7	7.4	7.4	7.4	6.7
10	3.0	3.5	3.1	3.4	4.4	6.3	6.7	6.8	6.3
11	2.3	2.7	2.3	2.6	3.5	5.3	5.9	6.1	5.9
12	1.7	2.0	1.8	2.0	2.7	4.4	5.2	5.5	5.4
13	1.3	1.5	1.4	1.5	2.1	3.6	4.5	4.9	5.0
14	1.0	1.2	1.1	1.2	1.6	3.0	3.9	4.3	4.6
15	0.7	0.9	0.8	0.9	1.2	2.4	3.3	3.7	4.1
16	0.5	0.7	0.6	0.7	0.9	2.0	2.8	3.2	3.8
17	0.4	0.5	0.5	0.5	0.7	1.6	2.4	2.8	3.4
18	0.3	0.4	0.4	0.4	0.6	1.3	2.0	2.4	3.1
19	0.2	0.3	0.3	0.3	0.4	1.0	1.7	2.1	2.8
20	0.2	0.2	0.2	0.3	0.3	0.8	1.4	1.8	2.5
21	0.1	0.2	0.2	0.2	0.3	0.6	1.2	1.5	2.3
22	0.1	0.1	0.1	0.2	0.2	0.5	1.0	1.3	2.1
23	0.1	0.1	0.1	0.1	0.2	0.4	0.8	1.1	1.9
Total Percentage	100	100	100	100	100	100	100	100	100
Layer ID from outdoors to indoors (See Table 18)	F01	F01	F01	F01	F01	F01	F01	F01	F01
	M01	M01	M01	M01	M01	M01	M01	M01	M01
	F04	F04	F04	F04	F04	F04	F04	F04	F04
	I01	I01	G03	G03	I01	I01	I01	I01	M03
	G03	I01	I04	I04	G03	I01	M03	I01	I04
	F04	G03	G01	I04	I04	G03	F02	M03	G01
	G01	F04	F02	G01	G01	I04	0	F02	F02
	F02	G01	0	F02	F02	I04	0	0	0
	0	F02	0	0	0	G01	0	0	0
	0	0	0	0	0	F02	0	0	0

required for each unique zone and for each unique radiant energy distribution function assumption. For most common design applications, RTS variation depends primarily on the overall massiveness of the construction and the thermal responsiveness of the surfaces the radiant heat gains strike.

One goal in developing RTS was to provide a simplified method based directly on the HB method; thus, it was deemed desirable to generate RTS coefficients directly from a heat balance.

ance computer program was developed to do this: Hbfort, which is included as part of *Cooling and Heating Load Calculation Principles* (Pedersen et al. 1998). The RTS procedure is described by Spitler et al. (1997). The procedure for generating RTS coefficients may be thought of as analogous to the custom weighting factor generation procedure used by DOE 2.1 (Kerrisk et al. 1981; Sowell 1988a, 1988b). In both cases, a zone model is pulsed with a heat gain. With DOE 2.1, the resulting loads are used to estimate the

Table 16 Wall Conduction Time Series (CTS) (Continued)

	Brick Walls								
	Brick, 200 mm LW CMU, R-3.9 Batt Insulation, Gyp. Board	Brick, R-0.9 Insulation Board, 200 mm HW CMU, Gyp. Board	Brick, R-1.8 Insulation Board, 200 mm HW CMU, Gyp. Board	Brick, R-0.9 Insulation Board, Brick	Brick, R-1.8 Insulation Board, Brick	Brick, R-0.9 Insulation Board, 200 mm LW Concrete, Gyp. Board	Brick, R-1.8 Insulation Board, 200 mm LW Concrete, Gyp. Board	Brick, R-0.9 Insulation Board, 300 mm HW Concrete, Gyp. Board	Brick, R-1.8 Insulation Board, 300 mm HW Concrete, Gyp. Board
Wall Number	30	31	32	33	34	35	36	37	38
U , W/(m ² ·K)	0.206	0.627	0.404	0.701	0.433	0.514	0.353	0.545	0.351
Total R	4.86	1.59	2.48	1.43	2.31	1.95	2.83	1.83	2.85
Hour	Conduction Time Factors, %								
0	1.9	1.8	2.0	0.9	1.0	3.3	3.4	3.8	3.9
1	1.8	1.7	1.9	1.3	1.2	3.1	3.3	3.8	3.8
2	2.0	2.4	2.3	3.3	2.7	3.0	3.2	3.7	3.8
3	3.0	3.7	3.4	5.7	4.9	3.1	3.2	3.7	3.8
4	4.4	5.0	4.6	7.3	6.6	3.4	3.4	3.8	3.8
5	5.6	5.9	5.5	8.0	7.5	3.8	3.7	3.9	3.9
6	6.3	6.4	6.0	8.2	7.8	4.2	4.1	4.1	4.0
7	6.7	6.6	6.3	7.9	7.7	4.6	4.4	4.2	4.2
8	6.7	6.6	6.3	7.5	7.4	4.8	4.6	4.3	4.3
9	6.5	6.4	6.2	6.9	6.9	5.0	4.8	4.4	4.4
10	6.2	6.1	6.0	6.3	6.4	5.1	4.9	4.5	4.4
11	5.8	5.7	5.7	5.6	5.8	5.1	4.9	4.5	4.5
12	5.5	5.3	5.4	5.0	5.2	5.1	4.9	4.6	4.5
13	5.1	5.0	5.1	4.4	4.6	5.0	4.9	4.6	4.5
14	4.7	4.6	4.7	3.8	4.1	4.9	4.8	4.5	4.5
15	4.3	4.2	4.4	3.3	3.6	4.7	4.7	4.5	4.5
16	3.9	3.8	4.0	2.9	3.2	4.6	4.6	4.3	4.3
17	3.6	3.5	3.7	2.5	2.8	4.4	4.4	4.3	4.3
18	3.3	3.2	3.4	2.2	2.4	4.2	4.3	4.2	4.2
19	3.0	2.9	3.1	1.9	2.1	4.1	4.2	4.2	4.2
20	2.8	2.6	2.9	1.6	1.8	3.9	4.0	4.1	4.1
21	2.5	2.4	2.6	1.4	1.6	3.7	3.9	4.0	4.1
22	2.3	2.2	2.4	1.2	1.4	3.6	3.7	4.0	4.0
23	2.1	2.0	2.2	1.0	1.2	3.4	3.6	3.9	4.0
Total Percentage	100	100	100	100	100	100	100	100	100
Layer ID from outdoors to indoors (See Table 18)	F01	F01	F01	F01	F01	F01	F01	F01	F01
	M01	M01	M01	M01	M01	M01	M01	M01	M01
	F04	F04	F04	F04	F04	F04	F04	F04	F04
	M03	I01	I01	I01	I01	I01	I01	I01	I01
	I04	M05	I01	M01	I01	M13	I01	M16	I01
	I04	G01	M05	F02	M01	F04	M13	F04	M16
	G01	F02	G01	0	F02	G01	F04	G01	F04
	F02	0	F02	0	0	F02	G01	F02	G01
	0	0	0	0	0	0	F02	0	F02
	0	0	0	0	0	0	0	0	0

best values of the transfer function method weighting factors to most closely match the load profile. In the procedure described here, a unit periodic heat gain pulse is used to generate loads for a 24 h period. As long as the heat gain pulse is a unit pulse, the resulting loads are equivalent to the RTS coefficients.

Two different radiant time series are used: **solar**, for direct transmitted solar heat gain (radiant energy assumed to be distributed to the floor and furnishings only) and **nonsolar**, for all other types of

heat gains (radiant energy assumed to be uniformly distributed on all internal surfaces). Nonsolar RTS apply to radiant heat gains from people, lights, appliances, walls, roofs, and floors. Also, for diffuse solar heat gain and direct solar heat gain from fenestration with indoor shading (blinds, drapes, etc.), the nonsolar RTS should be used. Radiation from those sources is assumed to be more uniformly distributed onto all room surfaces. Effect of beam solar radiation distribution assumptions is addressed by Hittle (1999).

Table 16 Wall Conduction Time Series (CTS) (Continued)

	Brick Walls		Concrete Block Walls						
	Brick, 200 mm HW Concrete, R-1.9 Batt Insulation, Gyp. Board	Brick, 200 mm HW Concrete, R-3.9 Batt	200 mm LW CMU, R-1.9 Batt Insulation, Gyp. Board	200 mm LW CMU, R-3.9 Batt Insulation, Gyp. Board	200 mm LW CMU w/Fill Insulation, R-1.9 Batt Insulation, Gyp. Board	200 mm LW CMU w/Fill Insulation, R-3.9 Batt Insulation, Gyp. Board	25 mm Stucco, 200 mm HW CMU, R-1.9 Batt Insulation, Gyp. Board	25 mm Stucco, 200 mm HW CMU, R-3.9 Batt Insulation, Gyp. Board	200 mm LW CMU w/Fill Insulation
Wall Number	39	40	41	42	43	44	45	46	47
U , W/(m ² ·K)	0.383	0.218	0.377	0.218	0.332	0.202	0.413	0.229	1.027
Total R	2.61	4.60	2.65	4.59	3.01	4.95	2.42	4.36	0.97
Hour	Conduction Time Factors, %		Conduction Time Factors, %						
0	3.4	3.5	0.3	0.3	0.6	0.8	0.5	0.5	0.6
1	3.3	3.4	4.7	3.2	1.7	1.4	2.8	2.0	9.3
2	3.3	3.4	12.7	10.7	5.8	4.6	8.6	7.3	19.5
3	3.6	3.6	15.0	14.1	9.4	8.1	11.7	11.0	19.2
4	4.0	3.9	13.5	13.3	10.5	9.6	11.6	11.4	15.0
5	4.4	4.3	11.1	11.3	10.1	9.6	10.4	10.4	10.9
6	4.7	4.6	8.9	9.2	9.1	8.9	8.9	9.1	7.7
7	4.8	4.8	7.1	7.5	8.0	7.9	7.5	7.7	5.4
8	4.9	4.8	5.6	6.1	6.9	7.0	6.4	6.6	3.8
9	4.9	4.9	4.5	4.9	5.9	6.1	5.4	5.6	2.6
10	4.9	4.8	3.6	4.0	5.1	5.4	4.5	4.8	1.8
11	4.8	4.8	2.8	3.2	4.4	4.7	3.8	4.0	1.3
12	4.7	4.7	2.3	2.6	3.8	4.1	3.2	3.4	0.9
13	4.6	4.6	1.8	2.1	3.2	3.6	2.7	2.9	0.6
14	4.5	4.5	1.4	1.7	2.8	3.1	2.3	2.5	0.4
15	4.4	4.4	1.1	1.4	2.4	2.7	1.9	2.1	0.3
16	4.2	4.2	0.9	1.1	2.1	2.4	1.6	1.8	0.2
17	4.1	4.1	0.7	0.9	1.8	2.1	1.4	1.5	0.1
18	4.0	4.0	0.6	0.7	1.5	1.8	1.2	1.3	0.1
19	3.9	3.9	0.5	0.6	1.3	1.6	1.0	1.1	0.1
20	3.8	3.8	0.4	0.5	1.1	1.4	0.8	0.9	0.0
21	3.7	3.7	0.3	0.4	1.0	1.2	0.7	0.8	0.0
22	3.6	3.6	0.2	0.3	0.8	1.1	0.6	0.7	0.0
23	3.5	3.6	0.2	0.2	0.7	0.9	0.5	0.6	0.0
Total Percentage	100	100	100	100	100	100	100	100	100
Layer ID from outdoors to indoors (See Table 18)	F01	F01	F01	F01	F01	F01	F01	F01	F01
	M01	M01	M03	M03	M08	M08	F07	F07	M08
	F04	F04	I04	I04	I04	I04	M05	M05	F02
	M15	M15	G01	I04	G01	I04	I04	I04	0
	I04	I04	F02	G01	F02	G01	G01	I04	0
	G01	I04	0	F02	0	F02	F02	G01	0
	F02	G01	0	0	0	0	0	F02	0
	0	F02	0	0	0	0	0	0	0
	0	0	0	0	0	0	0	0	0
	0	0	0	0	0	0	0	0	0

Representative solar and nonsolar RTS data for light, medium, and heavyweight constructions are provided in Tables 19 and 20. Those were calculated using the Hbfort computer program (Pedersen et al. 1998) with zone characteristics listed in Table 21. Customized RTS values may be calculated using the HB method where the zone is not reasonably similar to these typical zones or where more precision is desired.

ASHRAE research project RP-942 compared HB and RTS results over a wide range of zone types and input variables (Rees et al. 2000; Spitler et al. 1998). In general, total cooling loads calculated using RTS closely agreed with or were slightly higher than those of the HB method with the same inputs. The project examined more than 5000 test cases of varying zone parameters. The dominating variable was overall thermal mass, and results were grouped into lightweight,

Table 16 Wall Conduction Time Series (CTS) (Continued)

	Concrete Block Walls		Precast and Cast-In-Place Block Walls							
	200 mm LW CMU w/Fill Insulation, Gyp. Board	300 mm LW CMU w/Fill Insulation, Gyp. Board	100 mm LW Concrete. R-0.9 Board Insulation, Gyp. Board	100 mm LW Concrete. R-1.8 Board Insulation, Gyp. Board	100 mm LW Concrete. R-1.9 Batt Insulation, Gyp. Board	100 mm LW Concrete. R-3.9 Batt Insulation, Gyp. Board	100 mm LW Concrete. R-1.8 Board Insulation, 100 mm LW Concrete	100 mm LW Concrete. R-3.5 Board Insulation, 100 mm LW Concrete	EIFS, R-0.9 Insulation Board, 200 mm LW Concrete, Gyp. Board	EIFS, R-1.8 Insulation Board, 200 mm LW Concrete, Gyp. Board
Wall Number	48	49	50	51	52	53	54	55	56	57
U , W/(m ² ·K)	0.815	0.695	0.672	0.422	0.418	0.231	0.433	0.246	0.650	0.413
Total R	1.23	1.44	1.49	2.37	2.39	4.33	2.31	4.07	1.54	2.42
Hour	Conduction Time Factors, %		Conduction Time Factors, %							
0	0.2	1.0	0.6	0.3	0.7	0.3	0.7	0.9	2.2	2.5
1	3.2	1.1	10.2	6.7	9.9	7.3	0.9	0.8	2.2	2.4
2	10.9	2.6	19.6	17.1	18.9	17.3	2.7	1.5	3.2	3.0
3	14.9	5.1	18.1	18.1	17.7	17.7	5.5	3.4	4.6	4.2
4	14.4	7.3	13.9	14.8	13.8	14.4	7.6	5.6	5.7	5.2
5	12.2	8.4	10.3	11.2	10.3	10.9	8.6	7.2	6.2	5.7
6	9.8	8.6	7.5	8.3	7.6	8.2	8.8	8.1	6.3	5.9
7	7.7	8.3	5.4	6.2	5.6	6.1	8.6	8.3	6.2	5.9
8	6.1	7.7	3.9	4.6	4.1	4.6	8.0	8.1	6.0	5.8
9	4.7	7.0	2.9	3.4	3.0	3.4	7.3	7.6	5.7	5.6
10	3.7	6.2	2.1	2.5	2.2	2.5	6.5	7.0	5.4	5.3
11	2.9	5.5	1.5	1.8	1.7	1.9	5.7	6.3	5.1	5.1
12	2.2	4.9	1.1	1.4	1.2	1.4	5.0	5.7	4.8	4.8
13	1.7	4.3	0.8	1.0	0.9	1.0	4.3	5.0	4.5	4.6
14	1.3	3.7	0.6	0.7	0.7	0.8	3.7	4.4	4.2	4.3
15	1.0	3.3	0.4	0.6	0.5	0.6	3.2	3.8	4.0	4.1
16	0.8	2.9	0.3	0.4	0.4	0.4	2.7	3.3	3.7	3.9
17	0.6	2.5	0.2	0.3	0.3	0.3	2.3	2.8	3.5	3.7
18	0.5	2.2	0.2	0.2	0.2	0.2	1.9	2.4	3.2	3.5
19	0.4	1.9	0.1	0.2	0.1	0.2	1.6	2.1	3.0	3.3
20	0.3	1.7	0.1	0.1	0.1	0.1	1.4	1.8	2.8	3.1
21	0.2	1.5	0.1	0.1	0.1	0.1	1.1	1.5	2.7	2.9
22	0.2	1.3	0.0	0.1	0.1	0.1	1.0	1.3	2.5	2.8
23	0.1	1.1	0.0	0.0	0.0	0.1	0.8	1.1	2.3	2.6
Total Percentage	100	100	100	100	100	100	100	100	100	100
Layer ID from outdoors to indoors (See Table 18)	F01 M08 F04 G01 F02 0 0 0 0 0	F01 M09 F04 G01 F02 0 0 0 0 0	F01 M11 I01 F04 G01 F02 0 0 0 0 0	F01 M11 I01 F04 F02 G01 0 0 0 0 0	F01 M11 I04 G01 F02 0 0 0 0 0	F01 M11 I04 I04 G01 F02 0 0 0 0 0	F01 M11 I02 M11 F02 0 0 0 0 0	F01 M11 I02 M11 F02 0 0 0 0 0	F01 F06 I01 M13 G01 F02 0 0 0 0 0	F01 F06 I01 I01 M13 G01 F02 0 0 0 0 0

U.S. medium-weight, U.K. medium-weight, and heavyweight construction. Best agreement between RTS and HB results was obtained for light- and medium-weight construction. Greater differences occurred in heavyweight cases, with RTS generally predicting slightly higher peak cooling loads than HB. Greater differences also were observed in zones with extremely high internal radiant loads

and large glazing areas or with a very lightweight exterior envelope. In this case, heat balance calculations predict that some of the internal radiant load will be transmitted to the outdoor environment and never becomes cooling load in the space. RTS does not account for energy transfer out of the space to the environment, and thus predicted higher cooling loads.

Table 16 Wall Conduction Time Series (CTS) (Concluded)

	Precast and Cast-In-Place Block Walls								
	200 mm LW Concrete, R-11 Batt Insulation, Gyp. Board	200 mm Concrete, R-22 Batt Insulation, Gyp. Board	EIFS Finish, R-1.8 Insulation Board, 200 mm HW Concrete, Gyp. Board	EIFS Finish, R-3.5 Insulation Board, 200 mm HW Concrete, Gyp. Board	200 mm HW Concrete, R-11 Batt Insulation, Gyp. Board	200 mm HW Concrete, R-22 Batt Insulation, Gyp. Board	300 mm HW Concrete, R-3.3 Batt Insulation, Gyp. Board	300 mm HW Concrete, R-6.7 Batt Insulation, Gyp. Board	300 mm HW Concrete
Wall Number	58	59	60	61	62	63	64	65	66
U , W/(m ² ·K)	0.387	0.221	0.465	0.255	0.434	0.236	0.265	0.140	3.120
Total R	2.58	4.52	2.15	3.92	2.31	4.24	3.77	7.12	0.32
Hour	Conduction Time Factors, %								
0	1.4	1.6	2.8	3.0	1.1	1.2	2.5	2.6	1.2
1	1.7	1.7	3.0	2.9	2.3	2.0	2.4	2.5	1.9
2	3.5	3.0	4.1	3.4	5.8	5.0	2.9	2.6	4.1
3	5.8	5.2	5.1	4.4	8.2	7.7	3.9	3.4	6.4
4	7.3	6.8	5.5	5.1	8.8	8.6	4.9	4.4	7.6
5	7.8	7.5	5.6	5.4	8.4	8.4	5.6	5.2	8.0
6	7.7	7.5	5.5	5.4	7.8	7.8	5.9	5.7	7.8
7	7.2	7.1	5.3	5.3	7.0	7.1	5.9	5.9	7.4
8	6.7	6.7	5.2	5.2	6.3	6.4	5.8	5.9	6.8
9	6.1	6.2	5.0	5.1	5.7	5.8	5.7	5.7	6.2
10	5.6	5.6	4.8	4.9	5.1	5.2	5.4	5.5	5.6
11	5.1	5.2	4.6	4.7	4.6	4.7	5.2	5.3	5.0
12	4.6	4.7	4.4	4.6	4.1	4.2	4.9	5.0	4.5
13	4.2	4.3	4.3	4.4	3.7	3.8	4.6	4.8	4.1
14	3.8	3.9	4.1	4.2	3.3	3.4	4.4	4.5	3.6
15	3.4	3.6	4.0	4.1	2.9	3.1	4.1	4.3	3.3
16	3.1	3.3	3.8	3.9	2.6	2.7	3.9	4.0	2.9
17	2.8	3.0	3.7	3.8	2.4	2.5	3.7	3.8	2.6
18	2.6	2.7	3.5	3.7	2.1	2.2	3.5	3.6	2.3
19	2.3	2.5	3.4	3.5	1.9	2.0	3.3	3.4	2.1
20	2.1	2.3	3.3	3.4	1.7	1.8	3.1	3.2	1.9
21	1.9	2.1	3.1	3.3	1.5	1.6	2.9	3.0	1.7
22	1.7	1.9	3.0	3.2	1.4	1.4	2.8	2.9	1.5
23	1.6	1.7	2.9	3.1	1.2	1.3	2.6	2.7	1.3
Total Percentage	100	100	100	100	100	100	100	100	100
Layer ID from outdoors to indoors (See Table 18)	F01	F01	F01	F01	F01	F01	F01	F01	F01
	M13	M13	F06	F06	M15	M15	M16	M16	M16
	I04	I04	I02	I02	I04	I04	I05	I05	F02
	G01	I04	M15	I02	G01	I04	G01	I05	0
	F02	G01	G01	M15	F02	G01	F02	G01	0
	0	F02	F02	G01	0	F02	0	F02	0
	0	0	0	F02	0	0	0	0	0
	0	0	0	0	0	0	0	0	0
	0	0	0	0	0	0	0	0	0

ASHRAE research project RP-1117 built two model rooms for which cooling loads were physically measured using extensive instrumentation. The results agreed with previous simulations (Chantrasrisalai et al. 2003; Eldridge et al. 2003; Ju et al. 2003). HB calculations closely approximated measured cooling loads when provided with detailed data for the test rooms. RTS overpre-

dicted measured cooling loads in tests with large, clear, single-glazed window areas with bare concrete floor and no furnishings or internal loads. Tests under more typical conditions (venetian blinds, carpeted floor, office-type furnishings, and normal internal loads) provided good agreement between HB, RTS, and measured loads.

Table 17 Roof Conduction Time Series (CTS)

	Sloped Frame Roofs								
	Metal Roof, R-3.3 Batt Insulation, Gyp. Board	Metal Roof, R-6.7 Batt Insulation, Gyp. Board	Metal Roof, R-3.3 Batt Insulation, Suspended Acoustical Ceiling	Metal Roof, R-6.7 Batt Insulation, Suspended Acoustical Ceiling	Metal Roof, R-3.3 Batt Insulation	Metal Roof, R-6.7 Batt Insulation	Asphalt Shingles, Wood Sheathing, R-3.3 Batt Insulation, Gyp. Board	Asphalt Shingles, Wood Sheathing, R-6.7 Batt Insulation, Gyp. Board	Slate or Tile, Wood Sheathing, R-3.3 Batt Insulation, Gyp. Board
Roof Number	1	2	3	4	5	6	7	8	9
U , W/(m ² ·K)	0.249	0.136	0.227	0.129	0.255	0.138	0.235	0.132	0.239
Total R	4.02	7.37	4.41	7.76	3.92	7.27	4.25	7.60	4.18
Hour	Conduction Time Factors, %								
0	15.4	4.2	25.6	7.0	52.6	19.7	2.8	0.6	2.4
1	53.6	39.1	62.7	51.9	46.0	61.5	25.8	13.5	26.8
2	22.6	35.9	10.8	31.8	1.4	16.3	31.1	28.8	34.2
3	6.1	14.2	0.8	7.5	0.0	2.2	19.8	24.7	20.3
4	1.6	4.6	0.0	1.5	0.0	0.3	10.5	15.4	9.5
5	0.4	1.4	0.0	0.3	0.0	0.0	5.2	8.4	4.1
6	0.1	0.4	0.0	0.1	0.0	0.0	2.5	4.4	1.6
7	0.0	0.1	0.0	0.0	0.0	0.0	1.2	2.2	0.6
8	0.0	0.0	0.0	0.0	0.0	0.0	0.6	1.1	0.2
9	0.0	0.0	0.0	0.0	0.0	0.0	0.3	0.5	0.1
10	0.0	0.0	0.0	0.0	0.0	0.0	0.1	0.3	0.0
11	0.0	0.0	0.0	0.0	0.0	0.0	0.1	0.1	0.0
12	0.0	0.0	0.0	0.0	0.0	0.0	0.0	0.1	0.0
13	0.0	0.0	0.0	0.0	0.0	0.0	0.0	0.0	0.0
14	0.0	0.0	0.0	0.0	0.0	0.0	0.0	0.0	0.0
15	0.0	0.0	0.0	0.0	0.0	0.0	0.0	0.0	0.0
16	0.0	0.0	0.0	0.0	0.0	0.0	0.0	0.0	0.0
17	0.0	0.0	0.0	0.0	0.0	0.0	0.0	0.0	0.0
18	0.0	0.0	0.0	0.0	0.0	0.0	0.0	0.0	0.0
19	0.0	0.0	0.0	0.0	0.0	0.0	0.0	0.0	0.0
20	0.0	0.0	0.0	0.0	0.0	0.0	0.0	0.0	0.0
21	0.0	0.0	0.0	0.0	0.0	0.0	0.0	0.0	0.0
22	0.0	0.0	0.0	0.0	0.0	0.0	0.0	0.0	0.0
23	0.0	0.0	0.0	0.0	0.0	0.0	0.0	0.0	0.0
Total Percentage	100	100	100	100	100	100	100	100	100
Layer ID from outdoors to indoors (See Table 18)	F01	F01	F01	F01	F01	F01	F01	F01	F01
	F08	F08	F08	F08	F08	F08	F12	F12	F14
	G03	G03	G03	G03	G03	G03	G05	G05	G05
	F05	F05	F05	F05	F05	F05	F05	F05	F05
	I05	I05	I05	I05	I05	I05	I05	I05	I05
	G01	I05	F05	I05	F03	I05	F05	I05	F05
	F03	G01	F16	F05	0	F03	G01	F05	G01
	0	F03	F03	F16	0	0	F03	G01	F03
	0	0	0	F03	0	0	0	F03	0
	0	0	0	0	0	0	0	0	0
	0	0	0	0	0	0	0	0	0
	0	0	0	0	0	0	0	0	0
	0	0	0	0	0	0	0	0	0
	0	0	0	0	0	0	0	0	0
	0	0	0	0	0	0	0	0	0

7. HEATING LOAD CALCULATIONS

Techniques for estimating design heating load for commercial,

institutional, and industrial applications are essentially the same as for those estimating design cooling loads for such uses, with the following exceptions:

Table 17 Roof Conduction Time Series (CTS) (Continued)

	Sloped Frame Roofs			Wood Deck				Metal Deck Roofs	
	Slate or Tile, Wood Sheathing, R-6.7 Batt Insulation, Gyp. Board	Wood Shingles, Wood Sheathing, R-3.3 Batt Insulation, Gyp. Board	Wood Shingles, Wood Sheathing, R-6.7 Batt Insulation, Gyp. Board	Membrane, Sheathing, R-1.8 Insulation Board, Wood Deck	Membrane, Sheathing, R-3.5 Insulation Board, Wood Deck	Membrane, Sheathing, R-1.8 Insulation Board, Wood Deck	Membrane, Sheathing, R-3.5 Insulation Board, Wood Deck	Membrane, Sheathing, R-1.8 Insulation Board, Metal Deck	Membrane, Sheathing, R-3.5 Insulation Board, Metal Deck
Roof Number	10	11	12	13	14	15	16	17	18
<i>U</i> , W/(m²·K)	0.133	0.231	0.130	0.393	0.232	0.329	0.208	0.452	0.251
Total <i>R</i>	7.53	4.34	7.68	2.55	4.31	3.04	4.80	2.21	3.98
Hour	Conduction Time Factors, %			Conduction Time Factors, %				Conduction Time Factors, %	
0	0.5	1.8	0.3	0.2	0.1	0.9	1.2	16.6	2.5
1	13.5	19.1	9.5	6.5	1.7	2.6	1.5	59.6	33.7
2	31.4	26.8	23.0	17.0	9.1	7.7	3.9	19.8	38.2
3	26.5	20.2	22.7	17.8	14.9	10.1	7.2	3.4	16.9
4	15.1	13.0	16.5	14.4	15.2	9.9	8.6	0.5	5.9
5	7.3	7.9	10.8	11.0	13.0	8.9	8.6	0.1	1.9
6	3.3	4.7	6.7	8.3	10.4	7.9	8.0	0.0	0.6
7	1.4	2.7	4.1	6.2	8.2	7.0	7.3	0.0	0.2
8	0.6	1.6	2.5	4.7	6.4	6.1	6.6	0.0	0.1
9	0.2	0.9	1.5	3.5	4.9	5.4	6.0	0.0	0.0
10	0.1	0.5	0.9	2.6	3.8	4.8	5.4	0.0	0.0
11	0.0	0.3	0.5	2.0	2.9	4.2	4.8	0.0	0.0
12	0.0	0.2	0.3	1.5	2.3	3.7	4.3	0.0	0.0
13	0.0	0.1	0.2	1.1	1.7	3.3	3.9	0.0	0.0
14	0.0	0.1	0.1	0.8	1.3	2.9	3.5	0.0	0.0
15	0.0	0.0	0.1	0.6	1.0	2.6	3.1	0.0	0.0
16	0.0	0.0	0.0	0.5	0.8	2.3	2.8	0.0	0.0
17	0.0	0.0	0.0	0.3	0.6	2.0	2.5	0.0	0.0
18	0.0	0.0	0.0	0.3	0.5	1.8	2.3	0.0	0.0
19	0.0	0.0	0.0	0.2	0.4	1.5	2.1	0.0	0.0
20	0.0	0.0	0.0	0.1	0.3	1.4	1.8	0.0	0.0
21	0.0	0.0	0.0	0.1	0.2	1.2	1.7	0.0	0.0
22	0.0	0.0	0.0	0.1	0.2	1.1	1.5	0.0	0.0
23	0.0	0.0	0.0	0.1	0.1	0.9	1.3	0.0	0.0
Total Percentage	100	100	100	100	100	100	100	100	100
Layer ID from outdoors to indoors (See Table 18)	F01	F01	F01	F01	F01	F01	F01	F01	F01
	F14	F15	F15	F13	F13	F13	F13	F13	F13
	G05	G05	G05	G03	G03	G03	G03	G03	G03
	F05	F05	F05	I02	I02	I02	I02	I02	I02
	I05	I05	I05	G06	I02	G06	I02	F08	I02
	I05	F05	I05	F03	G06	F05	G06	F03	F08
	F05	G01	F05	0	F03	F16	F05	0	F03
	G01	F03	G01	0	0	F03	F16	0	0
	F03	0	F03	0	0	0	F03	0	0
	0	0	0	0	0	0	0	0	0
	0	0	0	0	0	0	0	0	0
	0	0	0	0	0	0	0	0	0
	0	0	0	0	0	0	0	0	0
	0	0	0	0	0	0	0	0	0

Table 17 Roof Conduction Time Series (CTS) (Continued)

Roof Number	Metal Deck Roofs							Concrete Roofs	
	Membrane, Sheathing, R-1.8 Insulation Board, Metal Deck, Suspended Acoustical Ceiling	Membrane, Sheathing, R-3.5 Insulation Board, Metal Deck, Suspended Acoustical Ceiling	Membrane, Sheathing, R-2.6 Insulation Board, Metal Deck	Membrane, Sheathing, R-5.3 Insulation Board, Metal Deck	Membrane, Sheathing, R-4.4 Insulation Board, Metal Deck	50 mm Concrete Roof Ballast, Membrane, Sheathing, R-2.6 Insulation Board, Metal Deck	50 mm Concrete Roof Ballast, Membrane, Sheathing, R-5.3 Insulation Board, Metal Deck	Membrane, Sheathing, R-2.6 Insulation Board, 100 mm LW Concrete	Membrane, Sheathing, R-5.3 Insulation Board, 100 mm LW Concrete
Roof Number	19	20	21	22	23	24	25	26	27
$U, W/(m^2 \cdot K)$	0.370	0.224	0.323	0.174	0.249	0.297	0.166	0.304	0.169
Total R	2.71	4.47	3.10	5.74	4.02	3.37	6.01	3.29	5.93
Hour	Conduction Time Factors, %							Conduction Time Factors, %	
0	4.3	0.4	7.2	0.2	15.4	0.3	0.1	0.6	0.8
1	38.8	14.1	49.6	9.6	53.6	9.0	0.9	2.0	0.8
2	35.3	32.1	31.9	27.5	22.6	21.2	6.6	7.4	2.1
3	14.5	25.6	8.7	25.6	6.1	19.6	13.1	11.0	5.1
4	4.9	14.3	2.0	16.4	1.6	14.6	15.1	11.2	7.8
5	1.5	7.1	0.4	9.4	0.4	10.4	14.0	10.1	9.1
6	0.5	3.4	0.1	5.2	0.1	7.3	11.8	8.8	9.3
7	0.1	1.6	0.0	2.8	0.0	5.2	9.4	7.6	8.8
8	0.0	0.7	0.0	1.5	0.0	3.7	7.3	6.5	8.0
9	0.0	0.3	0.0	0.8	0.0	2.6	5.6	5.6	7.1
10	0.0	0.2	0.0	0.5	0.0	1.8	4.2	4.8	6.3
11	0.0	0.1	0.0	0.2	0.0	1.3	3.1	4.1	5.5
12	0.0	0.0	0.0	0.1	0.0	0.9	2.3	3.5	4.8
13	0.0	0.0	0.0	0.1	0.0	0.6	1.7	3.0	4.1
14	0.0	0.0	0.0	0.0	0.0	0.5	1.3	2.6	3.6
15	0.0	0.0	0.0	0.0	0.0	0.3	1.0	2.2	3.1
16	0.0	0.0	0.0	0.0	0.0	0.2	0.7	1.9	2.7
17	0.0	0.0	0.0	0.0	0.0	0.2	0.5	1.6	2.3
18	0.0	0.0	0.0	0.0	0.0	0.1	0.4	1.4	2.0
19	0.0	0.0	0.0	0.0	0.0	0.1	0.3	1.2	1.7
20	0.0	0.0	0.0	0.0	0.0	0.1	0.2	1.0	1.5
21	0.0	0.0	0.0	0.0	0.0	0.0	0.2	0.9	1.3
22	0.0	0.0	0.0	0.0	0.0	0.0	0.1	0.7	1.1
23	0.0	0.0	0.0	0.0	0.0	0.0	0.1	0.6	1.0
Total Percentage	100	100	100	100	100	100	100	100	100
Layer ID from outdoors to indoors (See Table 18)	F01	F01	F01	F01	F01	F01	F01	F01	F01
	F13	F13	F13	F13	F08	M17	M17	F13	F13
	G03	G03	G03	G03	G03	F13	F13	G03	G03
	I02	I02	I03	I03	F05	G03	G03	I03	I03
	F08	I02	F08	I03	I05	I03	I03	M11	I03
	F05	F08	F03	F08	G01	F08	I03	F03	M11
	F16	F05	0	F03	F03	F03	F08	0	F03
	F03	F16	0	0	0	0	F03	0	0
	0	F03	0	0	0	0	0	0	0
	0	0	0	0	0	0	0	0	0
	0	0	0	0	0	0	0	0	0
	0	0	0	0	0	0	0	0	0
	0	0	0	0	0	0	0	0	0
	0	0	0	0	0	0	0	0	0

Table 17 Roof Conduction Time Series (CTS) (Concluded)

	Concrete Roofs									
	Membrane, Sheathing, R- 2.6 Insulation Board, 150 mm LW Concrete	Membrane, Sheathing, R- 5.3 Insulation Board, 150 mm LW Concrete	Membrane, Sheathing, R- 2.6 Insulation Board, 200 mm LW Concrete	Membrane, Sheathing, R- 5.3 Insulation Board, 200 mm LW Concrete	Membrane, Sheathing, R- 2.6 Insulation Board, 150 mm HW Concrete	Membrane, Sheathing, R- 5.3 Insulation Board, 150 mm HW Concrete	Membrane, Sheathing, R- 2.6 Insulation Board, 200 mm HW Concrete	Membrane, Sheathing, R- 5.3 Insulation Board, 200 mm HW Concrete	Membrane, 150 mm HW Concrete, R-3.3 Batt Insulation, Suspended Acoustical Ceiling	Membrane, 150 mm HW Concrete, R-6.7 Batt Insulation, Suspended Acoustical Ceiling
Roof Number	28	29	30	31	32	33	34	35	36	37
<i>U</i> , W/(m ² ·K)	0.296	0.166	0.288	0.163	0.315	0.172	0.312	0.171	0.239	0.133
Total <i>R</i>	3.38	6.02	3.48	6.12	3.17	5.82	3.20	5.85	4.18	7.53
Hour	Conduction Time Factors, %									
0	1.5	1.9	2.4	2.8	2.0	2.4	2.6	2.9	1.4	1.5
1	1.6	1.8	2.3	2.6	2.4	2.2	2.6	2.8	3.2	2.1
2	3.2	1.9	2.6	2.5	4.4	2.6	3.4	2.8	6.9	5.1
3	5.7	2.9	3.6	2.7	6.2	3.7	4.7	3.3	8.3	7.5
4	7.3	4.4	4.8	3.3	6.9	5.0	5.5	4.1	8.1	8.1
5	7.8	5.8	5.6	4.1	6.8	5.8	5.8	4.8	7.5	7.7
6	7.6	6.6	6.1	4.9	6.4	6.2	5.8	5.3	6.9	7.2
7	7.1	6.9	6.1	5.4	6.1	6.2	5.7	5.5	6.3	6.6
8	6.6	6.8	6.0	5.7	5.7	6.1	5.5	5.5	5.8	6.1
9	6.0	6.6	5.8	5.7	5.3	5.8	5.3	5.5	5.3	5.5
10	5.5	6.2	5.6	5.7	5.0	5.5	5.0	5.3	4.8	5.1
11	5.0	5.8	5.3	5.5	4.7	5.2	4.8	5.1	4.4	4.6
12	4.6	5.4	5.0	5.3	4.4	4.9	4.6	4.9	4.0	4.3
13	4.2	4.9	4.7	5.1	4.1	4.6	4.4	4.7	3.7	3.9
14	3.8	4.6	4.4	4.9	3.9	4.4	4.2	4.5	3.4	3.6
15	3.5	4.2	4.2	4.6	3.6	4.1	4.0	4.3	3.1	3.3
16	3.2	3.8	3.9	4.4	3.4	3.9	3.8	4.2	2.8	3.0
17	2.9	3.5	3.7	4.1	3.2	3.6	3.6	4.0	2.6	2.7
18	2.7	3.2	3.5	3.9	3.0	3.4	3.5	3.8	2.4	2.5
19	2.4	3.0	3.3	3.7	2.8	3.2	3.3	3.6	2.2	2.3
20	2.2	2.7	3.1	3.5	2.6	3.0	3.2	3.5	2.0	2.1
21	2.0	2.5	2.9	3.3	2.5	2.8	3.0	3.3	1.8	1.9
22	1.8	2.3	2.7	3.1	2.3	2.7	2.9	3.2	1.6	1.8
23	1.7	2.1	2.5	2.9	2.2	2.5	2.8	3.0	1.5	1.6
Total Percentage	100	100	100	100	100	100	100	100	100	100
Layer ID from outdoors to indoors (See Table 18)	F01	F01	F01	F01	F01	F01	F01	F01	F01	F01
	F13	F13	F13	F13	F13	F13	F13	F13	F13	F13
	G03	G03	G03	G03	G03	G03	G03	G03	M14	M14
	I03	I03	I03	I03	I03	I03	I03	I03	F05	F05
	M12	I03	M13	I03	M14	I03	M15	I03	I05	I05
	F03	M12	F03	M13	F03	M14	F03	M15	F16	I05
	0	F03	0	F03	0	F03	0	F03	F03	F16
	0	0	0	0	0	0	0	0	0	F03
	0	0	0	0	0	0	0	0	0	0
	0	0	0	0	0	0	0	0	0	0
	0	0	0	0	0	0	0	0	0	0
	0	0	0	0	0	0	0	0	0	0
	0	0	0	0	0	0	0	0	0	0
	0	0	0	0	0	0	0	0	0	0

Table 18 Thermal Properties and Code Numbers of Layers Used in Wall and Roof Descriptions for Tables 16 and 17

Layer ID	Description	Thickness, mm	Conductivity, W/(m·K)	Density, kg/m ³	Specific Heat, kJ/(kg·K)	Resistance R, (m ² ·K)/W	R	Mass, kg/m ²	Thermal Capacity, kJ/(m ² ·K)	Notes
F01	Outdoor surface resistance	—	—	—	—	0.04	0.04	—	—	1
F02	Indoor vertical surface resistance	—	—	—	—	0.12	0.12	—	—	2
F03	Indoor horizontal surface resistance	—	—	—	—	0.16	0.16	—	—	3
F04	Wall air space resistance	—	—	—	—	0.15	0.15	—	—	4
F05	Ceiling air space resistance	—	—	—	—	0.18	0.18	—	—	5
F06	EIFS finish	9.5	0.72	1858	0.84	—	0.01	17.7	14.83	6
F07	25 mm stucco	25.4	0.72	1858	0.84	—	0.04	47.2	39.55	6
F08	Metal surface	0.8	45.35	7833	0.50	—	2×10 ⁻⁵	6.0	3.00	7
F09	Opaque spandrel glass	6.4	0.99	2531	0.88	—	0.01	16.1	14.14	8
F10	25 mm stone	25.4	3.17	2563	0.80	—	0.01	65.1	51.82	9
F11	Wood siding	12.7	0.09	593	1.63	—	0.14	7.5	12.30	10
F12	Asphalt shingles	3.2	0.04	1121	1.26	—	0.08	3.6	4.47	
F13	Built-up roofing	9.5	0.16	1121	1.47	—	0.06	10.7	15.66	
F14	Slate or tile	12.7	1.59	1922	1.26	—	0.01	24.4	30.68	
F15	Wood shingles	6.4	0.04	593	1.30	—	0.17	3.8	4.89	10
F16	Acoustic tile	19.1	0.06	368	0.59	—	0.32	7.0	4.12	11
F17	Carpet	9.5	0.08	320	1.38	—	0.12	3.1	4.22	12
F18	Terrazzo	25.4	1.80	2563	0.80	—	0.01	65.1	51.82	13
G01	16 mm gyp board	15.9	0.16	801	1.09	—	0.10	12.7	13.85	
G02	16 mm plywood	15.9	0.11	545	1.88	—	0.15	8.6	16.30	
G03	13 mm fiberboard sheathing	12.7	0.07	400	1.30	—	0.19	5.1	6.61	14
G04	13 mm wood	12.7	0.15	609	1.63	—	0.08	7.7	12.63	15
G05	25 mm wood	25.4	0.15	609	1.63	—	0.17	15.5	25.26	15
G06	50 mm wood	50.8	0.15	609	1.63	—	0.33	30.9	50.52	15
G07	100 mm wood	101.6	0.15	609	1.63	—	0.66	61.8	101.25	15
I01	25 mm insulation board	25.4	0.03	40	1.47	—	0.88	1.0	1.49	16
I02	50 mm insulation board	50.8	0.03	40	1.47	—	1.76	2.0	2.98	16
I03	75 mm insulation board	76.2	0.05	40	1.47	—	2.64	3.1	4.47	16
I04	89 mm batt insulation	89.4	0.05	8	0.84	—	1.94	0.7	0.59	17
I05	154 mm batt insulation	154.4	0.05	8	0.84	—	3.35	1.2	1.02	17
I06	244 mm batt insulation	243.8	0.05	8	0.84	—	5.28	1.9	1.60	17
M01	100 mm brick	101.6	0.89	1922	0.80	—	0.11	195.3	155.45	18
M02	150 mm LW concrete block	152.4	0.49	513	0.88	—	0.31	78.1	68.73	19
M03	200 mm LW concrete block	203.2	0.45	465	0.88	—	0.45	94.4	83.05	20
M04	300 mm LW concrete block	304.8	0.71	513	0.88	—	0.43	156.2	137.45	21
M05	200 mm concrete block	203.2	1.11	801	0.92	—	0.18	162.7	150.00	22
M06	300 mm concrete block	304.8	1.40	801	0.92	—	0.22	244.1	225.00	23
M07	150 mm LW concrete block (filled)	152.4	0.29	513	0.88	—	0.53	78.1	68.73	24
M08	200 mm LW concrete block (filled)	203.2	0.25	465	0.88	—	0.81	94.4	83.05	25
M09	300 mm LW concrete block (filled)	304.8	0.30	513	0.88	—	1.02	156.2	137.45	26
M10	200 mm concrete block (filled)	203.2	0.70	801	0.92	—	0.29	162.7	150.00	27
M11	100 mm lightweight concrete	101.6	0.53	1281	0.84	—	0.19	130.2	109.09	
M12	150 mm lightweight concrete	152.4	0.53	1281	0.84	—	0.29	195.3	163.64	
M13	200 mm lightweight concrete	203.2	0.53	1281	0.84	—	0.38	260.4	218.18	
M14	150 mm heavyweight concrete	152.4	1.95	2243	0.92	—	0.08	341.8	315.00	
M15	200 mm heavyweight concrete	203.2	1.95	2243	0.92	—	0.10	455.7	420.00	
M16	300 mm heavyweight concrete	304.8	1.95	2243	0.92	—	0.16	683.5	630.00	
M17	50 mm LW concrete roof ballast	50.8	0.19	641	0.84	—	0.27	32.5	27.27	28

Notes: The following notes give sources for the data in this table.

- Chapter 26, Table 10 for 3.4 m/s wind
- Chapter 26, Table 10 for still air, horizontal heat flow, 0.9 emittance
- Chapter 26, Table 10 for still air, downward heat flow, 0.2 emittance
- Chapter 26, Table 3 for 40 mm space, 32.2°C, horizontal heat flow, 0.82 emittance
- Chapter 26, Table 3 for 90 mm space, 32.2°C, downward heat flow, 0.82 emittance
- EIFS finish layers approximated by Chapter 26, Table 1 for cement plaster, sand aggregate
- Chapter 33, Table 3 for steel (mild)
- Chapter 26, Table 1 for architectural (soda-lime float) glass
- Chapter 26, Table 1 for calcitic, dolomitic, limestone, marble, and granite
- Chapter 26, Table 1, density assumed same as Southern pine
- Chapter 26, Table 1 for mineral fiberboard, wet molded, acoustical tile
- Chapter 26, Table 1 for carpet and rubber pad
- Chapter 26, Table 1, density assumed same as stone
- Chapter 26, Table 1 for nail-base sheathing
- Chapter 26, Table 1 for Southern pine
- Chapter 26, Table 1 for extruded polystyrene, smooth skin
- Chapter 26, Table 1 for glass fiber batt
- Chapter 26, Table 1 for clay fired brick
- Chapter 26, Table 1, lightweight aggregate, 6 in., 16 to 17 lb, 2 or 3 cores
- Chapter 26, Table 1, lightweight aggregate, 8 in., 19 to 22 lb
- Chapter 26, Table 1, lightweight aggregate, 32 to 36 lb, 2 or 3 cores
- Chapter 26, Table 1, normal weight aggregate, 8 in., 33 to 36 lb, 2 or 3 cores
- Chapter 26, Table 1, normal weight aggregate, 12 in., 50 lb, 2 cores
- Chapter 26, Table 1, same as note 19, plus vermiculite fill
- Chapter 26, Table 1, same as note 20, plus vermiculite fill
- Chapter 26, Table 1, same as note 21, plus vermiculite fill
- Chapter 26, Table 1, same as note 22, plus vermiculite fill
- Chapter 26, Table 1 for 640 kg/m³ lightweight or limestone concrete

Table 19 Representative Nonsolar RTS Values for Light to Heavy Construction

% Glass																			Interior Zones					
	Light						Medium						Heavy						Light		Medium		Heavy	
	With Carpet			No Carpet			With Carpet			No Carpet			With Carpet			No Carpet			With Carpet	No Carpet	With Carpet	No Carpet	With Carpet	No Carpet
	10%	50%	90%	10%	50%	90%	10%	50%	90%	10%	50%	90%	10%	50%	90%	10%	50%	90%	With Carpet	No Carpet	With Carpet	No Carpet	With Carpet	No Carpet
Hour	Radiant Time Factor, %																							
0	47	50	53	41	43	46	46	49	52	31	33	35	34	38	42	22	25	28	46	40	46	31	33	21
1	19	18	17	20	19	19	18	17	16	17	16	15	9	9	9	10	9	9	19	20	18	17	9	9
2	11	10	9	12	11	11	10	9	8	11	10	10	6	6	5	6	6	6	11	12	10	11	6	6
3	6	6	5	8	7	7	6	5	5	8	7	7	4	4	4	5	5	5	6	8	6	8	5	5
4	4	4	3	5	5	5	4	3	3	6	5	5	4	4	4	5	5	4	4	5	3	6	4	5
5	3	3	2	4	3	3	2	2	2	4	4	4	4	3	3	4	4	4	3	4	2	4	4	4
6	2	2	2	3	3	2	2	2	2	4	3	3	3	3	3	4	4	4	2	3	2	4	3	4
7	2	1	1	2	2	2	1	1	1	3	3	3	3	3	3	4	4	4	2	2	1	3	3	4
8	1	1	1	1	1	1	1	1	1	3	2	2	3	3	3	4	3	3	1	1	1	3	3	4
9	1	1	1	1	1	1	1	1	1	2	2	2	3	3	2	3	3	3	1	1	1	2	3	3
10	1	1	1	1	1	1	1	1	1	2	2	2	3	2	2	3	3	3	1	1	1	2	3	3
11	1	1	1	1	1	1	1	1	1	2	2	2	2	2	2	3	3	3	1	1	1	2	2	3
12	1	1	1	1	1	1	1	1	1	1	1	1	2	2	2	3	3	3	1	1	1	1	2	3
13	1	1	1	0	1	0	1	1	1	1	1	1	2	2	2	3	3	2	1	1	1	1	2	3
14	0	0	1	0	1	0	1	1	1	1	1	1	2	2	2	3	2	2	1	0	1	1	2	3
15	0	0	1	0	0	0	1	1	1	1	1	1	2	2	2	2	2	2	0	0	1	1	2	3
16	0	0	0	0	0	0	1	1	1	1	1	1	2	2	2	2	2	2	0	0	1	1	2	3
17	0	0	0	0	0	0	1	1	1	1	1	1	2	2	2	2	2	2	0	0	1	1	2	2
18	0	0	0	0	0	0	1	1	1	1	1	1	2	2	1	2	2	2	0	0	1	1	2	2
19	0	0	0	0	0	0	0	1	0	0	1	1	2	2	1	2	2	2	0	0	1	0	2	2
20	0	0	0	0	0	0	0	0	0	0	1	1	2	1	1	2	2	2	0	0	0	0	2	2
21	0	0	0	0	0	0	0	0	0	0	1	1	2	1	1	2	2	2	0	0	0	0	2	2
22	0	0	0	0	0	0	0	0	0	0	1	0	1	1	1	2	2	2	0	0	0	0	1	2
23	0	0	0	0	0	0	0	0	0	0	0	0	1	1	1	2	2	1	0	0	0	0	1	2
	100	100	100	100	100	100	100	100	100	100	100	100	100	100	100	100	100	100	100	100	100	100	100	100

Table 20 Representative Solar RTS Values for Light to Heavy Construction

% Glass	Light						Medium						Heavy					
	With Carpet			No Carpet			With Carpet			No Carpet			With Carpet			No Carpet		
	10%	50%	90%	10%	50%	90%	10%	50%	90%	10%	50%	90%	10%	50%	90%	10%	50%	90%
Hour	Radiant Time Factor, %																	
0	53	55	56	44	45	46	52	54	55	28	29	29	47	49	51	26	27	28
1	17	17	17	19	20	20	16	16	15	15	15	15	11	12	12	12	13	13
2	9	9	9	11	11	11	8	8	8	10	10	10	6	6	6	7	7	7
3	5	5	5	7	7	7	5	4	4	7	7	7	4	4	3	5	5	5
4	3	3	3	5	5	5	3	3	3	6	6	6	3	3	3	4	4	4
5	2	2	2	3	3	3	2	2	2	5	5	5	2	2	2	4	4	4
6	2	2	2	3	2	2	2	1	1	4	4	4	2	2	2	3	3	3
7	1	1	1	2	2	2	1	1	1	4	3	3	2	2	2	3	3	3
8	1	1	1	1	1	1	1	1	1	3	3	3	2	2	2	3	3	3
9	1	1	1	1	1	1	1	1	1	3	3	3	2	2	2	3	3	3
10	1	1	1	1	1	1	1	1	1	2	2	2	2	2	2	3	3	3
11	1	1	1	1	1	1	1	1	1	2	2	2	2	2	1	3	3	2
12	1	1	1	1	1	0	1	1	1	2	2	2	2	1	1	2	2	2
13	1	1	0	1	0	0	1	1	1	2	2	2	2	1	1	2	2	2
14	1	0	0	0	0	0	1	1	1	1	1	1	2	1	1	2	2	2
15	1	0	0	0	0	0	1	1	1	1	1	1	1	1	1	2	2	2
16	0	0	0	0	0	0	1	1	1	1	1	1	1	1	1	2	2	2
17	0	0	0	0	0	0	1	1	1	1	1	1	1	1	1	2	2	2
18	0	0	0	0	0	0	1	1	1	1	1	1	1	1	1	2	2	2
19	0	0	0	0	0	0	0	0	0	1	1	1	1	1	1	2	2	2
20	0	0	0	0	0	0	0	0	0	1	1	1	1	1	1	2	2	2
21	0	0	0	0	0	0	0	0	0	0	0	0	1	1	1	2	2	2
22	0	0	0	0	0	0	0	0	0	0	0	0	1	1	1	2	1	1
23	0	0	0	0	0	0	0	0	0	0	0	0	1	1	1	2	1	1
	100	100	100	100	100	100	100	100	100	100	100	100	100	100	100	100	100	100

Table 21 RTS Representative Zone Construction for Tables 19 and 20

Construction Class	Exterior Wall	Roof/Ceiling	Partitions	Floor	Furnishings
Light	Steel siding, 50 mm insulation, air space, 19 mm gyp.	100 mm LW concrete, ceiling air space, acoustic tile	19 mm gyp., air space, 19 mm gyp.	Acoustic tile, ceiling air space, 100 mm LW concrete	25 mm wood @ 50% of floor area
Medium	100 mm face brick, 50 mm insulation, air space, 19 mm gyp.	100 mm HW concrete, ceiling air space, acoustic tile	19 mm gyp., air space, 19 mm gyp.	Acoustic tile, ceiling air space, 100 mm HW concrete	25 mm wood @ 50% of floor area
Heavy	100 mm face brick, 200 mm HW concrete air space, 50 mm insulation, 19 mm gyp.	200 mm HW concrete, ceiling air space, acoustic tile	19 mm gyp., 200 mm HW concrete block, 19 mm gyp.	Acoustic tile, ceiling air space, 200 mm HW concrete	25 mm wood @ 50% of floor area

- Temperatures outdoor conditioned spaces are generally lower than maintained space temperatures.
- Credit for solar or internal heat gains is not included
- Thermal storage effect of building structure or content is ignored.

Thermal bridging effects on wall and roof conduction are greater for heating loads than for cooling loads, and greater care must be taken to account for bridging effects on U-factors used in heating load calculations.

Heat losses (negative heat gains) are thus considered to be instantaneous, heat transfer essentially conductive, and latent heat treated only as a function of replacing space humidity lost to the exterior environment.

This simplified approach is justified because it evaluates worst-case conditions that can reasonably occur during a heating season. Therefore, the near-worst-case load is based on the following:

- Design interior and exterior conditions
- Including infiltration and/or ventilation
- No solar effect (at night or on cloudy winter days)
- Before the periodic presence of people, lights, and appliances has an offsetting effect

Typical commercial and retail spaces have nighttime unoccupied periods at a setback temperature where little to no ventilation is required, building lights and equipment are off, and heat loss is primarily through conduction and infiltration. Before being occupied, buildings are warmed to the occupied temperature (see the following discussion). During occupied time, building lights, equipment, and people cooling loads can offset conduction heat loss, although some perimeter heat may be required, leaving infiltration and ventilation as the primary heating loads. Ventilation heat load may be offset with heat recovery equipment. These loads (conduction loss, warm-up load, and ventilation load) may not be additive when sizing building heating equipment, and it is prudent to analyze each load and their interactions to arrive at final equipment sizing for heating.

7.1 HEAT LOSS CALCULATIONS

The general procedure for calculation of design heat losses of a structure is as follows:

1. Select outdoor design conditions: temperature, humidity, and wind direction and speed.
2. Select indoor design conditions to be maintained.
3. Estimate temperature in any adjacent unheated spaces.
4. Select transmission coefficients and compute heat losses for walls, floors, ceilings, windows, doors, and foundation elements.
5. Compute heat load through infiltration and any other outdoor air introduced directly to the space.
6. Sum the losses caused by transmission and infiltration.

Outdoor Design Conditions

The ideal heating system provides enough heat to match the structure's heat loss. However, weather conditions vary considerably from year to year, and heating systems designed for the worst weather conditions on record would have a great excess of capacity

most of the time. A system's failure to maintain design conditions during brief periods of severe weather usually is not critical. However, close regulation of indoor temperature may be critical for some occupancies or industrial processes. Design temperature data and discussion of their application are given in Chapter 14. Generally, the 99% temperature values given in the tabulated weather data are used. However, caution is needed, and local conditions should always be investigated. In some locations, outdoor temperatures are commonly much lower and wind velocities higher than those given in the tabulated weather data.

Indoor Design Conditions

The main purpose of the heating system is to maintain indoor conditions that make most of the occupants comfortable. Keep in mind, however, that the purpose of heating load calculations is to obtain data for sizing the heating system components. In many cases, the system will rarely be called upon to operate at the design conditions. Therefore, the use and occupancy of the space are general considerations from the design temperature point of view. Later, when the building's energy requirements are computed, the actual conditions in the space and outdoor environment, including internal heat gains, must be considered.

The indoor design temperature should be selected at the lower end of the acceptable temperature range, so that the heating equipment will not be oversized. Even properly sized equipment operates under partial load, at reduced efficiency, most of the time; therefore, any oversizing aggravates this condition and lowers overall system efficiency. A maximum design dry-bulb temperature of 21°C is recommended for most occupancies. The indoor design value of relative humidity should be compatible with a healthful environment and the thermal and moisture integrity of the building envelope. A minimum relative humidity of 30% is recommended for most situations.

Calculation of Transmission Heat Losses

Exterior Surface Above Grade. All above-grade surfaces exposed to outdoor conditions (walls, doors, ceilings, fenestration, and raised floors) are treated identically, as follows:

$$q = A \times HF \quad (34)$$

$$HF = U \Delta t \quad (35)$$

where HF is the heating load factor in W/m².

Below-Grade Surfaces. An approximate method for estimating below-grade heat loss [based on the work of Latta and Boileau (1969)] assumes that the heat flow paths shown in Figure 12 can be used to find the steady-state heat loss to the ground surface, as follows:

$$HF = U_{avg} (t_{in} - t_{gr}) \quad (36)$$

where

U_{avg} = average U-factor for below-grade surface from Equation (38) or (39), W/(m²·K)

t_{in} = below-grade space air temperature, °C

t_{gr} = design ground surface temperature from Equation (37), °C

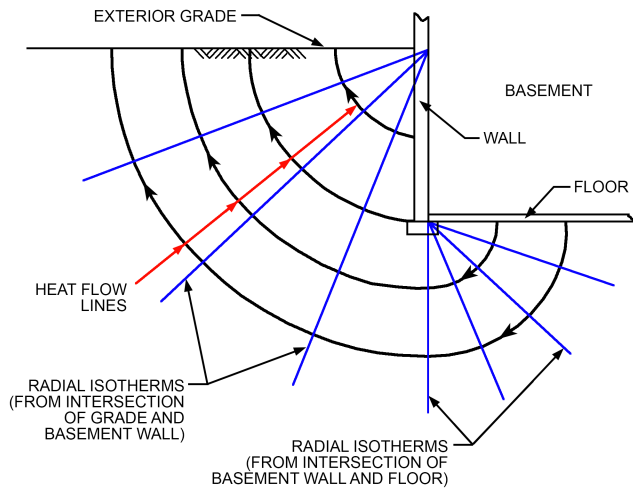


Fig. 12 Heat Flow from Below-Grade Surface

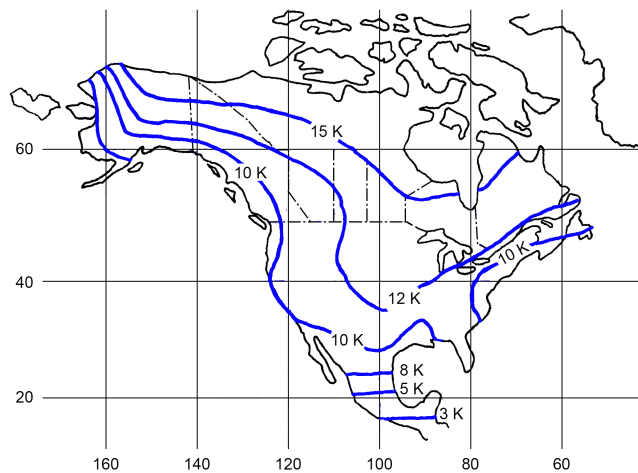


Fig. 13 Ground Temperature Amplitude

The effect of soil heat capacity means that none of the usual external design air temperatures are suitable values for t_{gr} . Ground surface temperature fluctuates about an annual mean value by amplitude A , which varies with geographic location and surface cover. The minimum ground surface temperature, suitable for heat loss estimates, is therefore

$$t_{gr} = \bar{t}_{gr} - A \quad (37)$$

where

\bar{t}_{gr} = mean ground temperature, °C, estimated from the annual average air temperature or from well-water temperatures, shown in Figure 18 of Chapter 34 in the 2019 ASHRAE Handbook—HVAC Applications

A = ground surface temperature amplitude, K, from Figure 13 for North America

Figure 14 shows depth parameters used in determining U_{avg} . For walls, the region defined by z_1 and z_2 may be the entire wall or any portion of it, allowing partially insulated configurations to be analyzed piecewise.

The below-grade wall average U-factor is given by

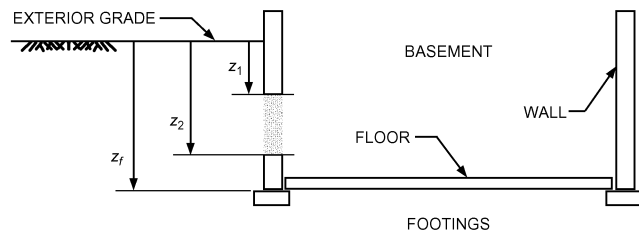


Fig. 14 Below-Grade Parameters

$$U_{avg,bw} = \frac{2k_{soil}}{\pi(z_2 - z_1)} \times \left[\ln\left(z_2 + \frac{2k_{soil}R_{other}}{\pi}\right) - \ln\left(z_1 + \frac{2k_{soil}R_{other}}{\pi}\right) \right] \quad (38)$$

where

$U_{avg,bw}$ = average U-factor for wall region defined by z_1 and z_2 , W/(m²·K)

k_{soil} = soil thermal conductivity, W/(m·K)

R_{other} = total resistance of wall, insulation, and indoor surface resistance, (m²·K)/W

z_1, z_2 = depths of top and bottom of wall segment under consideration, m (Figure 14)

The value of soil thermal conductivity k varies widely with soil type and moisture content. A typical value of 1.4 W/(m·K) has been used previously to tabulate U-factors, and R_{other} is approximately 0.259 (m²·K)/W for uninsulated concrete walls. For these parameters, representative values for $U_{avg,bw}$ are shown in Table 22.

The average below-grade floor U-factor (where the entire basement floor is uninsulated or has uniform insulation) is given by

$$U_{avg,bf} = \frac{2k_{soil}}{\pi w_b} \times \left[\ln\left(\frac{w_b}{2} + \frac{z_f}{2} + \frac{k_{soil}R_{other}}{\pi}\right) - \ln\left(\frac{z_f}{2} + \frac{k_{soil}R_{other}}{\pi}\right) \right] \quad (39)$$

where

w_b = basement width (shortest dimension), m

z_f = floor depth below grade, m (see Figure 14)

Representative values of $U_{avg,bf}$ for uninsulated basement floors are shown in Table 23.

At-Grade Surfaces. Concrete slab floors may be (1) unheated, relying for warmth on heat delivered above floor level by the heating system, or (2) heated, containing heated pipes or ducts that constitute a radiant slab or portion of it for complete or partial heating of the house.

The simplified approach that treats heat loss as proportional to slab perimeter allows slab heat loss to be estimated for both unheated and heated slab floors (Wang 1979):

$$q = p \times HF \quad (40)$$

$$HF = F_p \Delta t \quad (41)$$

where

q = heat loss through perimeter, W

F_p = heat loss coefficient per metre of perimeter, W/(m·K), Table 24

p = perimeter (exposed edge) of floor, m

Surfaces Adjacent to Buffer Space. Heat loss to adjacent unconditioned or semiconditioned spaces can be calculated using a heating factor based on the partition temperature difference:

$$HF = U(t_{in} - t_b) \quad (42)$$

Infiltration

Infiltration of outdoor air through openings into a structure is caused by thermal forces, wind pressure, and negative pressure (planned or unplanned) with respect to the outdoors created by mechanical systems. Typically, in building design, if the mechanical systems are designed to maintain positive building pressure, infiltration need not be considered except in ancillary spaces such as entryways and loading areas.

Infiltration is treated as a room load and has both sensible and latent components. During winter, this means heat and humidity loss because cold, dry air must be heated to design temperature and moisture must be added to increase the humidity to design condition. Typically, during winter, controlling indoor humidity is not a factor and infiltration is reduced to a simple sensible component. Under cooling conditions, both sensible and latent components are added to the space load to be treated by the air conditioning system. Procedures for estimating the infiltration rate are discussed in Chapter 16. The infiltration rate is reduced to a volumetric flow rate at a known dry bulb/wet bulb condition. Along with indoor air condition, the following equations define the infiltration sensible and latent loads.

$$q_s(\text{kW}) = [(m^3/s)/v]c_p(t_{in} - t_o) \quad (43)$$

where

m^3/s = volume flow rate of infiltrating air
 c_p = specific heat capacity of air, kJ/(kg·K)
 v = specific volume of infiltrating air, m³/kg

Assuming standard air conditions (15°C and sea-level conditions) for v and c_p , Equation (43) may be written as

$$q_s(\text{kW}) = 1.23(m^3/s)(t_{in} - t_o) \quad (44)$$

Table 22 Average U-Factor for Basement Walls with Uniform Insulation

Depth, m	$U_{avg,bw}$ from Grade to Depth, W/(m ² ·K)			
	Uninsulated	R-0.88	R-1.76	R-2.64
0.3	2.468	0.769	0.458	0.326
0.6	1.898	0.689	0.427	0.310
0.9	1.571	0.628	0.401	0.296
1.2	1.353	0.579	0.379	0.283
1.5	1.195	0.539	0.360	0.272
1.8	1.075	0.505	0.343	0.262
2.1	0.980	0.476	0.328	0.252
2.4	0.902	0.450	0.315	0.244

Soil conductivity = 1.4 W/(m·K); insulation is over entire depth. For other soil conductivities and partial insulation, use Equation (39).

Table 23 Average U-Factor for Basement Floors

z_f (Depth of Floor Below Grade), m	$U_{avg,bf}$, W/(m ² ·K)			
	w_b (Shortest Width of Basement), m			
	6	7	8	9
0.3	0.370	0.335	0.307	0.283
0.6	0.310	0.283	0.261	0.242
0.9	0.271	0.249	0.230	0.215
1.2	0.242	0.224	0.208	0.195
1.5	0.220	0.204	0.190	0.179
1.8	0.202	0.188	0.176	0.166
2.1	0.187	0.175	0.164	0.155

Soil conductivity is 1.4 W/(m·K); floor is uninsulated so that $R_{other} = 0.25$ (m²·K)/W. For other soil conductivities and insulation, use Equation (39).

The infiltrating air also introduces a latent heating load given by

$$q_l(\text{kW}) = [(m^3/s)/v](W_{in} - W_o)D_h \quad (45)$$

where

W_{in} = humidity ratio for indoor space air, kg_w/kg_a

W_o = humidity ratio for outdoor air, kg_w/kg_a

D_h = change in enthalpy to convert 1 kg water from vapor to liquid, kJ/kg

For standard air and nominal indoor comfort conditions, the latent load may be expressed as

$$q_l = 3010(m^3/s)(W_{in} - W_o) \quad (46)$$

The coefficients 1.23 in Equation (44) and 3010 in Equation (46) are given for standard conditions. They depend on temperature and altitude (and, consequently, pressure).

7.2 HEATING SAFETY FACTORS AND LOAD ALLOWANCES

Before mechanical cooling became common in the second half of the 1900s, and when energy was less expensive, buildings included much less insulation; large, operable windows; and generally more infiltration-prone assemblies than the energy-efficient and much tighter buildings typical of today. In the past, allowances of 10 to 20% of the net calculated heating load for piping losses to unheated spaces, and 10 to 20% more for a warm-up load, were common practice, along with other occasional safety factors reflecting the experience and/or concern of the individual designer. Today such safety allowances are more conservatively applied with modern construction practices. A combined warm-up/safety allowance of 20 to 25% is common but varies depending on the particular climate, building use, and type of construction. Engineering judgment must be applied for the particular project.

Table 24 Heat Loss Coefficient F_p of Slab Floor Construction

Construction	Insulation	F_p , W/(m·K)
200 mm block wall, brick facing	Uninsulated	1.17
	R-0.95 (m ² ·K)/W from edge to footer	0.86
100 mm block wall, brick facing	Uninsulated	1.45
	R-0.95 (m ² ·K)/W from edge to footer	0.85
Metal stud wall, stucco	Uninsulated	2.07
	R-0.95 (m ² ·K)/W from edge to footer	0.92
Poured concrete wall with duct near perimeter*	Uninsulated	3.67
	R-0.95 (m ² ·K)/W from edge to footer	1.24

Source: Wang (1979)

*Weighted average temperature of heating duct was assumed at 43°C during heating season (outdoor air temperature less than 18°C).

Table 25 Common Sizing Calculations in Other Chapters

Subject	Volume/Chapter	Equation(s)
Duct heat transfer	ASTM <i>Standard</i> C680	
Piping heat transfer	Fundamentals Ch. 4	Table 2
Pump power	Systems Ch. 44	(3), (4)
Moist-air sensible heating and cooling	Fundamentals Ch. 1	(43)
Moist-air cooling and dehumidification	Fundamentals Ch. 1	(45)
Air mixing	Fundamentals Ch. 1	(46)
Space heat absorption and moist-air moisture gains	Fundamentals Ch. 1	(48)
Adiabatic mixing of water injected into moist air	Fundamentals Ch. 1	(47)

Today's more efficient buildings have smaller overall heating loads at peak design conditions. The spare capacity in absolute terms needed for warm-up may not be any less in the highly efficient building than a more traditional building, assuming building mass is the same in both cases. Simply adding the same percentage factor to a lower peak load value may not result in enough spare capacity for timely warm up of the building. Transient models can be used to calculate both the quasi-steady state peak heating load and the spare capacity needed for building warm-up, but this level of analytical rigor may not be possible for a typical building design process. Experience and judgment must be applied, especially in cases where the base heating system capacity has been reduced through enhanced insulation and infiltration reduction.

7.3 OTHER HEATING CONSIDERATIONS

Calculation of design heating load estimates has essentially become a subset of the more involved and complex estimation of cooling loads for such spaces. Chapter 19 discusses using the heating load estimate to predict or analyze energy consumption over time. Special provisions to deal with particular applications are covered in the 2019 *ASHRAE Handbook—HVAC Applications* and the 2020 *ASHRAE Handbook—HVAC Systems and Equipment*.

8. SYSTEM HEATING AND COOLING LOAD EFFECTS

The heat balance (HB) or radiant time series (RTS) methods are used to determine cooling loads of rooms within a building, but they do not address the plant size necessary to reject the heat. Principal factors to consider in determining the plant size are ventilation, heat transport equipment, and air distribution systems. Some of these factors vary as a function of room load, ambient temperature, and control strategies, so it is often necessary to evaluate the factors and strategies dynamically and simultaneously with the heat loss or gain calculations.

Detailed analysis of system components and methods calculating their contribution to equipment sizing are beyond the scope of this chapter, which is general in nature. Table 25 lists the most frequently used calculations in other chapters and volumes.

8.1 ZONING

Organization of building rooms into zones as defined for load calculations and air-handling units has no effect on room cooling loads. However, specific grouping and ungrouping of rooms into zones may cause peak system loads to occur at different times during the day or year, and may significantly affect heat removal equipment sizes.

For example, if each room is cooled by a separate heat removal system, the total capacity of the heat transport systems equals the sum of peak room loads. Conditioning all rooms by a single heat transport system (e.g., a variable-volume air handler) requires less capacity (equal to the simultaneous peak of the combined rooms load, which includes some rooms at off-peak loads). This may significantly reduce equipment capacity, depending on the configuration of the building.

Grouping rooms together to reduce the number of HVAC systems or zones is called **thermal zoning**. Zoning choices can affect the HVAC system peak load as well as system energy performance. A detailed introduction to thermal zoning, including examples, is given in Rock (2018).

8.2 VENTILATION

Consult ASHRAE *Standard* 62.1 and building codes to determine the required quantity of ventilation air for an application, and

the various methods of achieving acceptable indoor air quality. The following discussion is confined to the effect of mechanical ventilation on sizing heat removal equipment. Where natural ventilation is used, through operable windows or other means, it is considered as infiltration and is part of the direct-to-room heat gain. Where ventilation air is conditioned and supplied through the mechanical system, its sensible and latent loads are applied directly to heat transport and central equipment, and do not affect room heating and cooling loads. If the mechanical ventilation rate sufficiently exceeds exhaust airflows, air pressure may be positive and infiltration from envelope openings and outdoor wind may not be included in the load calculations. Chapter 16 includes more information on ventilating commercial buildings.

Depending on ventilation requirements and local climate conditions, peak cooling coil loads may occur at peak dehumidification or enthalpy conditions instead of design dry-bulb conditions. Coil loads should be checked against all those peak conditions.

8.3 AIR HEAT TRANSPORT SYSTEMS

Heat transport equipment is usually selected to provide adequate heating or cooling for the peak load condition. However, selection must also consider maintaining desired indoor conditions during all occupied hours, which requires matching the rate of heat transport to room peak heating and cooling loads. Automatic control systems normally vary the heating and cooling system capacity during these off-peak hours of operation.

On/Off Control Systems

On/off control systems, common in residential and light commercial applications, cycle equipment on and off to match room load. They are adaptable to heating or cooling because they can cycle both heating and cooling equipment. In their purest form, their heat transport matches the combined room and ventilation load over a series of cycles.

Variable-Air-Volume Systems

Variable-air-volume (VAV) systems have airflow controls that adjust cooling airflow to match the room cooling load. Damper leakage or minimum airflow settings may cause overcooling, so most VAV systems are used in conjunction with separate heating systems. These may be duct-mounted heating coils, or separate radiant or convective heating systems.

The amount of heat added by the heating systems during cooling becomes part of the room cooling load. Calculations must determine the minimum airflow relative to off-peak cooling loads. The quantity of heat added to the cooling load can be determined for each terminal by Equation (8) using the minimum required supply airflow rate and the difference between supply air temperature and the room indoor heating design temperature.

Constant-Air-Volume Reheat Systems

In constant-air-volume (CAV) reheat systems, all supply air is cooled to remove moisture and then heated to avoid overcooling rooms. *Reheat* refers to the amount of heat added to cooling supply air to raise the supply air temperature to the temperature necessary for picking up the sensible load. The quantity of heat added can be determined by Equation (8).

With a constant-volume reheat system, heat transport system load does not vary with changes in room load, unless the cooling coil discharge temperature is allowed to vary. Where a minimum circulation rate requires a supply air temperature greater than the available design supply air temperature, reheat adds to the cooling load on the heat transport system. This makes the cooling load on the heat transport system larger than the room peak load.

Mixed Air Systems

Mixed air systems change the supply air temperature to match the cooling capacity by mixing airstreams of different temperatures; examples include multizone and dual-duct systems. Systems that cool the entire airstream to remove moisture and to reheat some of the air before mixing with the cooling airstream influence load on the heat transport system in the same way a reheat system does. Other systems separate the air paths so that mixing of hot- and cold-deck airstreams does not occur. For systems that mix hot and cold airstreams, the contribution to the heat transport system load is determined as follows.

1. Determine the ratio of cold-deck flow to hot-deck flow from

$$\frac{Q_h}{Q_c} = (T_c - T_r) / (T_r - T_h)$$

2. From Equation (9), the hot-deck contribution to room load during off-peak cooling is

$$q_{rh} = 1.23 Q_h (T_h - T_r)$$

where

- Q_h = heating airflow, L/s
- Q_c = cooling airflow, L/s
- T_c = cooling air temperature, °C
- T_h = heating air temperature, °C
- T_r = room or return air temperature, °C
- q_{rh} = heating airflow contribution to room load at off-peak hours, W

Heat Gain from Fans

Fans that circulate air through HVAC systems add energy to the system through the following processes:

- Increasing velocity and static pressure adds kinetic and potential energy
- Fan inefficiency in producing airflow and static pressure adds sensible heat (fan heat) to the airflow
- Inefficiency of motor and drive dissipates sensible heat

The power required to provide airflow and static pressure can be determined from the first law of thermodynamics with the following equation:

$$P_A = 0.009804 V p$$

where

- P_A = air power, kW
- V = flow rate, m³/s
- p = pressure, kPa

at standard air conditions with air density = 1.2 kg/m³ built into the multiplier 0.009804. The power necessary at the fan shaft must account for fan inefficiencies, which may vary from 50 to 70%. This may be determined from

$$P_F = P_A / \eta_F$$

where

- P_F = power required at fan shaft, kW
- η_F = fan efficiency, dimensionless

The power necessary at the input to the fan motor must account for fan motor inefficiencies and drive losses. Fan motor efficiencies generally vary from 80 to 95%, and drive losses for a belt drive are 3% of the fan power. This may be determined from

$$P_M = (1 + DL) P_F / E_M E_D$$

where

- P_M = power required at input to motor, kW
- E_D = belt drive efficiency, dimensionless
- E_M = fan motor efficiency, dimensionless
- P_F = power required at fan shaft, kW
- DL = drive loss, dimensionless

Almost all the energy required to generate airflow and static pressure is ultimately dissipated as heat in the building and HVAC system; a small portion is discharged with any exhaust air. Generally, it is assumed that all the heat is released at the fan rather than dispersed to the remainder of the system. The portion of fan heat released to the airstream depends on the location of the fan motor and drive: if they are within the airstream, all the energy input to the fan motor is released to the airstream. If the fan motor and drive are outdoor the airstream, the energy is split between the airstream and the room housing the motor and drive. Therefore, the following equations may be used to calculate heat generated by fans and motors:

If motor and drive are **outside** the airstream,

$$q_{fs} = P_F$$

$$q_{fr} = (P_M - P_F)$$

If motor and drive are **inside** the airstream,

$$q_{fs} = P_M$$

$$q_{fr} = 0.0$$

where

- P_F = power required at fan shaft, kW
- P_M = power required at input to motor, kW
- q_{fs} = heat release to airstream, kW
- q_{fr} = heat release to room housing motor and drive, kW

Supply airstream temperature rise may be determined from psychrometric formulas or Equation (8).

Variable- or adjustable-frequency drives (VFDs or AFDs) often drive fan motors in VAV air-handling units. These devices release heat to the surrounding space. Refer to manufacturers' data for heat released or efficiencies. The disposition of heat released is determined by the drive's location: in the conditioned space, in the return air path, or in a nonconditioned equipment room. These drives, and other electronic equipment such as building control, data processing, and communications devices, are temperature sensitive, so the rooms in which they are housed require cooling, frequently year round.

Duct Surface Heat Transfer

Heat transfer across the duct surface is one mechanism for energy transfer to or from air inside a duct. It involves conduction through the duct wall and insulation, convection at inner and outer surfaces, and radiation between the duct and its surroundings. Chapter 4 presents a rigorous analysis of duct heat loss and gain, and Chapter 23 addresses application of analysis to insulated duct systems.

The effect of duct heat loss or gain depends on the duct routing, duct insulation, and its surrounding environment. Consider the following conditions:

- For duct run within the area cooled or heated by air in the duct, heat transfer from the space to the duct has no effect on heating or cooling load, but beware of the potential for condensation on cold ducts.
- For duct run through unconditioned spaces or outdoors, heat transfer adds to the cooling or heating load for the air transport system but not for the conditioned space.

- For duct run through conditioned space not served by the duct, heat transfer affects the conditioned space as well as the air transport system serving the duct.
- For an extensive duct system, heat transfer reduces the effective supply air differential temperature, requiring adjustment through air balancing to increase airflow to extremities of the distribution system.

Duct Leakage

Air leakage from supply ducts can considerably affect HVAC system energy use. Leakage reduces cooling and/or dehumidifying capacity for the conditioned space, and must be offset by increased airflow (sometimes reduced supply air temperatures), unless leaked air enters the conditioned space directly. Supply air leakage into a ceiling return plenum or leakage from unconditioned spaces into return ducts also affects return air temperature and/or humidity.

Determining leakage from a duct system is complex because of the variables in paths, fabrication, and installation methods. Refer to Chapter 21 and publications from the Sheet Metal and Air Conditioning Contractors' National Association (SMACNA) for methods of determining leakage. In general, good-quality ducts and post-installation duct sealing provide highly cost-effective energy savings, with improved thermal comfort and delivery of ventilation air.

Ceiling Return Air Plenum Temperatures

The space above a ceiling, when used as a return air path, is a ceiling return air plenum, or simply a **return plenum**. Unlike a traditional ducted return, the plenum may have multiple heat sources in the air path. These heat sources may be radiant and convective loads from lighting and transformers; conduction loads from adjacent walls, roofs, or glazing; or duct and piping systems within the plenum.

As heat from these sources is picked up by the unducted return air, the temperature differential between the ceiling cavity and conditioned space is small. Most return plenum temperatures do not rise more than 0.6 to 1.7 K above space temperature, thus generating only a relatively small thermal gradient for heat transfer through plenum surfaces, except to the outdoors. This yields a relatively large-percentage reduction in space cooling load by shifting plenum loads to the system. Another reason plenum temperatures do not rise more is leakage into the plenum from supply air ducts, and, if exposed to the roof, increasing levels of insulation.

Where the ceiling space is used as a return air plenum, energy balance requires that heat picked up from the lights into the return air (1) become part of the cooling load to the return air (represented by a temperature rise of return air as it passes through the ceiling space), (2) be partially transferred back into the conditioned space through the ceiling material below, and/or (3) be partially lost from the space through floor surfaces above the plenum. If the plenum has one or more exterior surfaces, heat gains through them must be considered; if adjacent to spaces with different indoor temperatures, partition loads must be considered, too. In a multistory building, the conditioned space frequently gains heat through its floor from a similar plenum below, offsetting the floor loss. The radiant component of heat leaving the ceiling or floor surface of a plenum is normally so small, because of relatively small temperature differences, that all such heat transfer is considered convective for calculation purposes (Rock and Wolfe 1997).

Figure 15 shows a schematic of a typical return air plenum. The following equations, using the heat flow directions shown in Figure 15, represent the heat balance of a return air plenum design for a typical interior room in a multifloor building:

$$q_1 = U_c A_c (t_p - t_r) \quad (47)$$

$$q_2 = U_f A_f (t_p - t_{fa}) \quad (48)$$

$$q_3 = 1.1 Q (t_p - t_r) \quad (49)$$

$$q_{lp} - q_2 - q_1 - q_3 = 0 \quad (50)$$

$$Q = \frac{q_r + q_1}{1.23(t_r - t_s)} \quad (51)$$

where

q_1 = heat gain to space from plenum through ceiling, kW

q_2 = heat loss from plenum through floor above, kW

q_3 = heat gain "pickup" by return air, kW

Q = return airflow, L/s

q_{lp} = light heat gain to plenum via return air, kW

q_{lr} = light heat gain to space, kW

q_f = heat gain from plenum below, through floor, kW

q_w = heat gain from exterior wall, kW

q_r = space cooling load, including appropriate treatment of q_{lr} , q_f , and/or q_w , kW

t_p = plenum air temperature, °C

t_r = space air temperature, °C

t_{fa} = space air temperature of floor above, °C

t_s = supply air temperature, °C

By substituting Equations (47), (48), (49), and (51) into heat balance Equation (50), t_p can be found as the resultant return air temperature or plenum temperature. The results, although rigorous and best solved by computer, are important in determining the cooling load, which affects equipment size selection, future energy consumption, and other factors.

Equations (47) to (51) are simplified to illustrate the heat balance relationship. Heat gain into a return air plenum is not limited to heat from lights. Exterior walls directly exposed to the ceiling space can transfer heat directly to or from return air. For single-story buildings or the top floor of a multistory building, roof heat gain or loss enters or leaves the ceiling plenum rather than the conditioned space directly. The supply air quantity calculated by Equation (51) is only for the conditioned space under consideration, and is assumed to equal the return air quantity.

The amount of airflow through a return plenum above a conditioned space may not be limited to that supplied into the space; it will, however, have no noticeable effect on plenum temperature if the surplus comes from an adjacent plenum operating under similar conditions. Where special conditions exist, Equations (47) to (51) must be modified appropriately. Finally, although the building's thermal storage has some effect, the amount of heat entering the return air is small and may be considered as convective for calculation purposes.

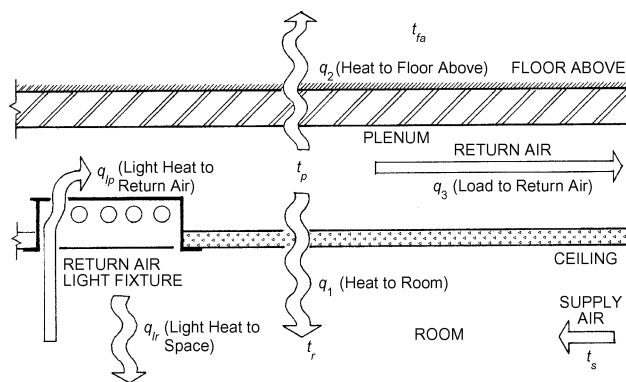


Fig. 15 Schematic Diagram of Typical Return Air Plenum

Ceiling Plenums with Ducted Returns

Compared to those in unducted plenum returns, temperatures in ceiling plenums that have well-sealed return or exhaust air ducts float considerably. In cooling mode, heat from lights and other equipment raises the ceiling plenum's temperature considerably. Solar heat gain through a poorly insulated roof can drive the ceiling plenum temperature to extreme levels, so much so that heat gains to uninsulated supply air ducts in the plenum can dramatically decrease available cooling capacity to the rooms below. In cold weather, much heat is lost from warm supply ducts. Thus, insulating supply air ducts and sealing them well to minimize air leaks are highly desirable, if not essential. Appropriately insulating roofs and plenums' exterior walls and minimizing infiltration are also key to lowering total building loads and improving HVAC system performance.

Underfloor Air Distribution Systems

Room cooling loads determined by methods in this chapter cannot model two distinguishing aspects of the thermal performance of underfloor air distribution (UFAD) systems under cooling operation:

- Room air stratification: UFAD systems supply cool air at the floor and extract warmer air at the ceiling, thus creating vertical thermal stratification. Cooling load models assume a well-mixed uniform space temperature.
- Underfloor air supply plenums: cool supply air flowing through the underfloor plenum is exposed to heat gain from both the concrete slab (conducted from the warm return air on the adjacent floor below in a multistory building) and the raised floor panels (conducted from the warmer room above).

Extensive simulation and experimental research led to the development of a whole-building energy simulation program capable of modeling energy performance and load calculations for UFAD systems (Bauman et al. 2007; Webster et al. 2008). Previously, it was thought that cooling loads for UFAD and overhead (OH) mixing systems were nearly identical. However, energy modeling studies show that the UFAD cooling load is generally higher than that calculated in the same building for a well-mixed system (Schiavon et al. 2010a). The difference is primarily caused by the thermal storage effect of the lower-mass raised-floor panels compared to the greater mass of a structural floor slab. Schiavon et al. (2010b) showed that the presence of the raised floor reduces the slab's ability to store heat, thereby producing higher peak cooling loads for a raised-floor system than for one without a raised floor. A second contributing factor is that the raised-floor surface above the underfloor plenum tends to be cooler (except when illuminated by the sun) than most other room surfaces, producing a room surface temperature distribution resembling a chilled radiant floor system, which has a different peak cooling load than an all-air system (Feng et al. 2012). The precise magnitude of difference in design cooling loads between OH and UFAD systems is still under investigation, but mainly depends on zone orientation and floor level, and possibly the effects of furniture. Methods for determining UFAD cooling loads will be updated as additional research results become available. For more information about simplified approaches to UFAD cooling load calculations, see the ASHRAE *Underfloor Air Distribution (UFAD) Design Guide* (ASHRAE 2013), Bauman et al. (2010), and Schiavon et al. (2010c).

Plenums in Load Calculations

Currently, most designers include ceiling and floor plenums within neighboring occupied spaces when thermally zoning a building. However, temperatures in these plenums, and the way that they behave, are significantly different from those of occupied spaces. Thus, they should be defined as a separate thermal zone. Most hand

and computer-based load calculation routines, though, currently do not allow floating air temperatures or humidities; assuming a constant air temperature in plenums, attics, and other unconditioned spaces is a poor, but often necessary, assumption. The heat balance method does allow floating space conditions, and when fully implemented in design load software, should allow more accurate modeling of plenums and other complex spaces.

8.4 CENTRAL PLANT

Piping

Losses must be considered for piping systems that transport heat. For water or hydronic piping systems, heat is transferred through the piping and insulation (see Chapter 23 for ways to determine this transfer). However, distribution of this transferred heat depends on the fluid in the pipe and the surrounding environment.

Consider a heating hot-water pipe. If the pipe serves a room heater and is routed through the heated space, any heat loss from the pipe adds heat to the room. Heat transfer to the heated space and heat loss from the piping system is null. If the piping is exposed to ambient conditions en route to the heater, the loss must be considered when selecting the heating equipment; if the pipe is routed through a space requiring cooling, heat loss from the piping also becomes a load on the cooling system.

In summary, the designer must evaluate both the magnitude of the pipe heat transfer and the routing of the piping.

Pumps

Calculating heat gain from pumps is addressed in the section on Electric Motors. For pumps serving hydronic systems, disposition of heat from the pumps depends on the service. For chilled-water systems, energy applied to the fluid to generate flow and pressure becomes a chiller load. For condenser water pumps, pumping energy must be rejected through the cooling tower. The magnitude of pumping energy relative to cooling load is generally small.

9. EXAMPLE COOLING AND HEATING LOAD CALCULATIONS

To illustrate the cooling and heating load calculation procedures discussed in this chapter, an example problem has been developed. The objectives of this example are to demonstrate (1) the component cooling load calculation procedures for a room using the radiant time series (RTS) method, (2) how orientation of opaque envelope and fenestration affects the magnitude and timing of peak room loads, (3) how a block load accounts for load diversity among rooms, and (4) the component heating load calculations for a room.

Table 26 summarizes RTS cooling load calculation procedures.

9.1 SINGLE-ROOM DETAILED COOLING LOAD EXAMPLE

The objective of this example is to calculate the cooling load for the office shown in Figure 16 for July 3:00 PM local standard time. This corner office is on the second floor of a two-story office building.

Room and Weather Characteristics

Opaque envelope: See Table 27 for surface areas, orientations and construction assembly details for floor, roof, and wall elements of the space.

Fenestration: See Table 27 for surface areas, orientations, window construction, and performance data.

Internal heat gain: See Table 28 for heat gain and schedule data.

Table 26 Summary of RTS Load Calculation Procedures

Equation	Equation No. in Chapter	Equation	Equation No. in Chapter
External Heat Gain		Partitions, Ceilings, Floors Transmission	
<i>Sol-Air Temperature</i>		$q = UA(t_b - t_i)$ (32)	
$t_e = t_o + \frac{\alpha E_t}{h_o} - \frac{\varepsilon \Delta R}{h_o}$ (29)		<i>where</i>	
<i>where</i>		q = heat transfer rate, W	
t_e = sol-air temperature, °C		U = coefficient of overall heat transfer between adjacent and conditioned space, W/(m ² ·K)	
t_o = outdoor air temperature, °C		A = area of separating section concerned, m ²	
a = absorptance of surface for solar radiation		t_b = average air temperature in adjacent space, °C	
E_t = total solar radiation incident on surface, W/m ²		t_i = air temperature in conditioned space, °C	
h_o = coefficient of heat transfer by long-wave radiation and convection at outer surface, W/(m ² ·K)		Internal Heat Gain	
ε = hemispherical emittance of surface		<i>Occupants</i>	
ΔR = difference between long-wave radiation incident on surface from sky and surroundings and radiation emitted by blackbody at outdoor air temperature, W/m ² ; 20 for horizontal surfaces; 0 for vertical surfaces		$q_s = q_{s,per} N$	
		$q_l = q_{l,per} N$	
		<i>where</i>	
		q_s = occupant sensible heat gain, W	
		q_l = occupant latent heat gain, W	
		$q_{l,per}$ = latent heat gain per person, W/person; see Table 1	
		N = number of occupants	
		Lighting	
<i>Wall and Roof Transmission</i>		$q_{el} = WF_{ul} F_{sa}$ (1)	
$q_0 = c_0 q_{i,0} + c_1 q_{i,0-1} + c_2 q_{i,0-2} + \dots + c_{23} q_{i,0-23}$ (31)		<i>where</i>	
$q_{i,0-n} = UA(t_{e,0-n} - t_{rc})$ (30)		q_{el} = heat gain, W	
<i>where</i>		W = total light wattage, W	
q_0 = hourly conductive heat gain for surface, W		F_{ul} = lighting use factor	
$q_{i,0}$ = heat input for current hour		F_{sa} = lighting special allowance factor	
$q_{i,0-n}$ = conductive heat input for surface n hours ago, W			
c_0, c_1, \dots = conduction time factors			
U = overall heat transfer coefficient for surface, W/(m ² ·K)			
A = surface area, m ²			
<i>Fenestration Transmission</i>		Electric Motors	
$q_c = UA(T_{out} - T_{in})$ (14)		$q_{em} = (P/E_M)F_{UM}F_{LM}$ (2)	
<i>where</i>		<i>where</i>	
q = fenestration transmission heat gain, W		q_{em} = heat equivalent of equipment operation, W	
U = overall U-factor, including frame and mounting orientation from Table 4 of Chapter 15, W/(m ² ·K)		P = motor power rating, W	
A = window area, m ²		E_M = motor efficiency, decimal fraction <1.0	
T_{in} = indoor temperature, °C		F_{UM} = motor use factor, 1.0 or decimal fraction <1.0	
T_{out} = outdoor temperature, °C		F_{LM} = motor load factor, 1.0 or decimal fraction <1.0	
<i>Fenestration Solar</i>		Hooded Cooking Appliances	
T_{out} = outdoor temperature, °C		$q_s = q_{input} F_U F_R$	
$q_b = AE_{t,b} SHGC(\theta) IAC(\theta, \Omega)$ (12)		<i>where</i>	
$q_d = A(E_{t,d} + E_{t,r})(SHGC)_D IAC_D$ (13)		q_s = sensible heat gain, W	
<i>where</i>		q_{input} = nameplate or rated energy input, W	
q_b = beam solar heat gain, W		F_U = usage factor; see Tables 5B, 5C, 5D	
q_d = diffuse solar heat gain, W		F_R = radiation factor; see Tables 5B, 5C, 5D	
A = window area, m ²		For other appliances and equipment, find q_s for	
$E_{t,b}, E_{t,d},$ and $E_{t,r}$ = beam, sky diffuse, and ground-reflected diffuse irradiance, calculated using equations in Chapter 14		Unhooded cooking appliances: Table 5A	
$SHGC(\theta)$ = beam solar heat gain coefficient as a function of incident angle θ ; may be interpolated between values in Table 10 of Chapter 15		Other kitchen equipment: Table 5E	
		Hospital and laboratory equipment: Tables 6 and 7	
		Computers, printers, scanners, etc.: Tables 8 and 9	
		Miscellaneous office equipment: Table 10	
$IAC(\theta, \Omega)$ = indoor solar attenuation coefficient for beam solar heat gain coefficient; = 1.0 if no indoor shading device. $IAC(\theta, \Omega)$ is a function of shade type and, depending on type, may also be a function of beam solar angle of incidence θ and shade geometry		Find q_l for	
		Unhooded cooking appliances: Table 5A	
		Other kitchen equipment: Table 5E	
IAC_D = indoor solar attenuation coefficient for diffuse solar heat gain coefficient; = 1.0 if not indoor shading device. IAC_D is a function of shade type and, depending on type, may also be a function of shade geometry		Ventilation and Infiltration Air Heat Gain	
		$q_s = 1230 Q_s \Delta t$ (9)	
		$q_l = 1.20 \times 2500 Q_s \Delta W = 3000 Q_s \Delta W$ (10)	
		<i>where</i>	
		q_s = sensible heat gain due to infiltration, W	

Table 26 Summary of RTS Load Calculation Procedures (Concluded)

Equation	Equation No. in Chapter	Equation	Equation No. in Chapter
q_l = latent heat gain due to infiltration, W		$q_{r,\theta} = q_{i,s} F_r$	
Q_s = infiltration airflow at standard air conditions, L/s		<i>where</i>	
t_o = outdoor air temperature, °C		$q_{i,s}$ = sensible heat gain from heat gain element i , W	
t_i = indoor air temperature, °C		F_r = fraction of heat gain that is radiant.	
W_o = outdoor air humidity ratio, kg/kg		Data Sources:	
W_i = indoor air humidity ratio, kg/kg		Wall transmission: see Table 14	
1230 = air sensible heat factor at standard air conditions, (W·s)/(m ² ·K)		Roof transmission: see Table 14	
3000 = air latent heat factor at standard air conditions, (W·s)/(m ² ·K)		Floor transmission: see Table 14	
Instantaneous Room Cooling Load		Fenestration transmission: see Table 14	
$Q_s = \sum Q_{i,r} + \sum Q_{i,c}$		Fenestration solar heat gain: see Table 14, Chapter 18 and Tables 14A to 14G, Chapter 15	
$Q_l = \sum q_{i,l}$		Lighting: see Table 3	
<i>where</i>		Occupants: see Tables 1 and 14	
Q_s = room sensible cooling load, W		Hooded cooking appliances: see Tables 5B, 5C, and 5D	
$Q_{i,r}$ = radiant portion of sensible cooling load for current hour, resulting from heat gain element i , W		Unhooded cooking appliances: see Table 5A	
$Q_{i,c}$ = convective portion of sensible cooling load, resulting from heat gain element i , W		Other appliances and equipment: see Tables 5E, 8, 9, 10, and 14	
Q_l = room latent cooling load, W		Infiltration: see Table 14	
$q_{i,l}$ = latent heat gain for heat gain element i , W		Lighting: see Table 3	
Radiant Portion of Sensible Cooling Load		Convective Portion of Sensible Cooling Load	
$Q_{i,r} = Q_{r,\theta}$		$Q_{i,c} = q_{i,c}$	
$Q_{r,\theta} = r_0 q_{r,\theta} + r_1 q_{r,\theta-1} + r_2 q_{r,\theta-2} + r_3 q_{r,\theta-3} + \cdots + r_{23} q_{r,\theta-23}$ (33)		<i>where</i> $q_{i,c}$ is convective portion of heat gain from heat gain element i , W.	
<i>where</i>		$q_{i,c} = q_{i,s}(1 - F_r)$	
$Q_{r,\theta}$ = radiant cooling load Q_r for current hour θ , W		<i>where</i>	
$q_{r,\theta}$ = radiant heat gain for current hour, W		$q_{i,s}$ = sensible heat gain from heat gain element i , W	
$q_{r,\theta-n}$ = radiant heat gain n hours ago, W		fraction of heat gain that is radiant; see row for radiant portion	
r_0, r_1 , etc. = radiant time factors; see Table 19 for radiant time factors for nonsolar heat gains: wall, roof, partition, ceiling, floor, fenestration transmission heat gains, and occupant, lighting, motor, appliance heat gain. Also used for fenestration diffuse solar heat gain; see Table 20 for radiant time factors for fenestration beam solar heat gain.		F_r = for sources of radiant fraction data for individual heat gain elements	

Infiltration: For purposes of this example, assume the building is maintained under positive pressure during peak cooling conditions and therefore has no infiltration. Assume that infiltration during peak heating conditions is equivalent to one air change per hour.

Indoor design conditions: 23.9°C with 50% rh for cooling; 22.2°C for heating

Weather data: This example uses the Example City weather data found in Chapter 14, Table 1: Latitude = 33.64° North, Longitude = 84.43° West, elevation = 313 m above sea level. For heating load calculation, the heating design dry-bulb temperature is -5.6°C. For cooling load calculations the 5% monthly design dry-bulb and coincident wet-bulb temperature data from Chapter 14 Table 1 is used. This is statistically equivalent to a 2% annual cooling design condition. See Table 29 for the 24 h temperature profiles calculated per Chapter 14.

Cooling Loads Using RTS Method

Traditionally, simplified cooling load calculation methods such as the radiant time series (RTS) Method have estimated the total cooling load at a particular design condition by independently calculating each component load (wall, windows, occupants, lighting, etc.) and then summing the component loads. Although the actual heat transfer processes for each component do affect each other, this

simplification, known as the **principle of superposition**, is appropriate for design load calculations and useful to the designer in understanding the relative contribution of each component to the total cooling load.

On the following pages RTS procedures will be demonstrated for calculating (1) load due to internal heat gain, (2) exterior wall load, (3) load for windows with no shading, (4) load for windows with internal shading, (5) load for windows with internal and external shading, and (6) the total room load. All loads will be calculated for July 3:00 PM local standard time. Equations used in these calculations are summarized in Table 26.

Part 1. Cooling load due to internal heat gain.

Objective: Calculate the cooling load due to overhead lighting heat gain at 3:00 PM local standard time.

Solution: Calculation of the lighting load involves the following steps: (a) calculate the 24 h heat gain profile, (b) split those heat gains into convective and radiant components, (c) determine the radiant portion of the load by applying appropriate RTS factors, and (d) sum the convective and radiant load components to determine the total lighting load.

The heat gain profile is calculated using Equation (1) for each hour of the day. Calculations are shown in columns *b* through *e* in

Table 30. Each heat gain is designated as q_i . For example, for 3:00 PM (hour 15):

$$\{q_{15} = (110 \text{ W})(1.00)(100\%) = 110 \text{ W}$$

Next, the lighting heat gain is divided into convective and radiant portions. Table 3 shows that a “Non-in-ceiling fluorescent luminaire” has a radiant factor between 0.5 and 0.57. We will use the higher value of 0.57 or 57%. Therefore 57% of the heat gain is radiant and the remaining 43% is convective. Columns f and g in Table 30 show the results of this calculation: convective heat gain is 47 W while radiant heat gain is 63 W.

The convective portion of the heat gain immediately becomes a cooling load. The radiant portion undergoes a conversion process from heat gain to cooling load which is modeled using the appropriate RTS factors. Those factors are obtained from Table 19 using the data for medium weight construction, carpeted floor, and 50% glass. The factors are reproduced in Table 31 in the “non-solar RTS factors, zone type 8” column. The radiant load is calculated using Equation (33). Results are shown in column i of Table 30. For 3:00 PM, for example, the calculation is

$$\begin{aligned} Q_{r,15} &= r_0 q_{r,15} + r_1 q_{r,14} + r_2 q_{r,13} + r_3 q_{r,12} + \dots + r_{23} q_{r,16} \\ &= (0.49)(63) + (0.17)(63) \\ &\quad + (0.09)(63) + (0.05)(63) + (0.03)(63) \\ &\quad + (0.02)(63) + (0.02)(63) + (0.01)(63) \\ &\quad + (0.01)(63) + (0.01)(0) + (0.01)(0) \\ &\quad + (0.01)(0) + (0.01)(0) + (0.01)(0) \\ &\quad + (0.01)(0) + (0.01)(0) + (0.01)(0) \\ &\quad + (0.01)(0) + (0.01)(0) + (0.01)(0) \\ &\quad + (0.00)(0) + (0.00)(63) + (0.00)(63) \\ &\quad + (0.00)(63) = 56 \text{ W} \end{aligned}$$

Finally, the total lighting cooling load at the designated hour is the sum of convective and radiant portions. Table 30 shows the results in column j . For 3:00 PM the calculation is as follows:

$$Q_{\text{light}} = Q_{c,15} + Q_{r,15} = 47 + 56 = 103 \text{ W}$$

Part 2. Wall cooling load.

Objective: Calculate the cooling load for the spandrel wall section facing 60° west of south for July 3:00 PM local standard time.

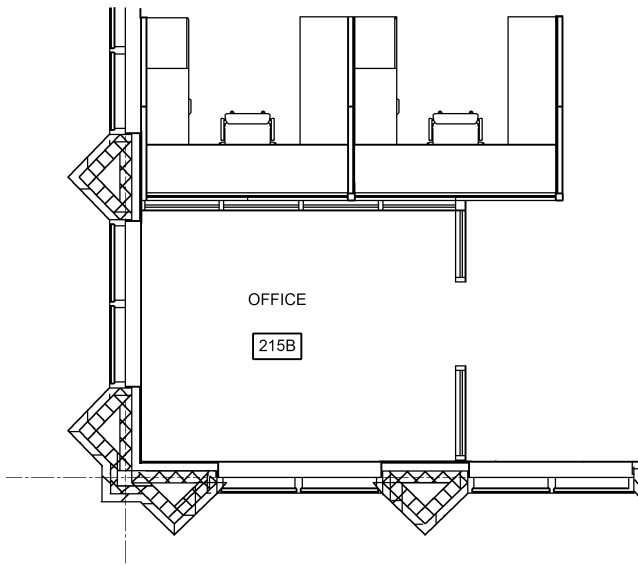


Fig. 16 Single-Room Example Office

Solution: Determining the wall cooling load requires calculation of: (a) the sol-air temperature at the exterior surface (b) the heat input at the exterior surface based on sol-air temperature, (c) the delayed heat gain through the mass of the wall to the interior surface using conduction time series factors, (d) convective and radiant portions of the heat gain, (e) the delayed space cooling load from interior surface radiant heat gain using radiant time series factors, and (f) the total wall load as the sum of convective and radiant load components.

First, calculate the sol-air temperature at 3:00 PM local standard time (LST) on July 21 for a vertical, spandrel glass wall assembly, facing 60° west of south. Key input data for the calculation is shown in Table 32.

Sol-air temperature is calculated using Equation (29). For the dark-colored wall, $\alpha/h_o = 0.053$, and for vertical surfaces, $\varepsilon\Delta R/h_o = 0$. The solar irradiance E_t on the wall must be determined using the equations in Chapter 14:

Solar Angles:

$$\psi = \text{surface azimuth} = +60^\circ$$

$$\Sigma = \text{surface tilt from horizontal (where horizontal} = 0^\circ) = 90^\circ \text{ for vertical wall surface}$$

$$3:00 \text{ PM LST} = \text{hour 15}$$

Calculate solar altitude, solar azimuth, surface solar azimuth, and incident angle as follows:

From Table 2 in Chapter 14, solar position data and constants for July 21 are

$$ET = -6.3536 \text{ min}$$

$$\delta = 20.44^\circ$$

$$E_o = 1324 \text{ W/m}^2$$

$$\text{Local standard meridian (LSM) for Eastern Time Zone} = -75^\circ$$

Apparent solar time AST

$$\begin{aligned} \text{AST} &= \text{LST} + ET/60 + (\text{LSM} - \text{LON})/15 \\ &= 15 + (-6.3536/60) + [(-75 - (-84.43))/15] \\ &= 14.2388 \end{aligned}$$

Hour angle H , degrees

$$\begin{aligned} H &= 15(\text{AST} - 12) \\ &= 15(14.2388 - 12) \\ &= 33.58^\circ \end{aligned}$$

Solar altitude β

$$\begin{aligned} \sin \beta &= \cos L \cos \delta \cos H + \sin L \sin \delta \\ &= \cos (33.64) \cos (20.44) \cos (33.58) + \sin (33.64) \sin (20.44) \\ &= 0.8434 \\ \beta &= \sin^{-1}(0.8434) = 57.5^\circ \end{aligned}$$

Solar azimuth ϕ

$$\begin{aligned} \cos \phi &= (\sin \beta \sin L - \sin \delta) / (\cos \beta \cos L) \\ &= [(\sin (57.5) \sin (33.64) - \sin (20.44)) / (\cos (57.5) \cos (33.64))] \\ &= 0.2637 \\ \phi &= \cos^{-1}(0.2637) = 74.71^\circ \end{aligned}$$

Surface-solar azimuth γ

$$\begin{aligned} \gamma &= \phi - \psi \\ &= 74.71 - 60 \\ &= 14.71^\circ \end{aligned}$$

Incident angle θ

$$\begin{aligned} \cos \theta &= \cos \beta \cos \gamma \sin \Sigma + \sin \beta \cos \Sigma \\ &= \cos (57.5) \cos (14.71) \sin (90) + \sin (57.5) \cos (90) \\ &= 0.5197 \\ \theta &= \cos^{-1}(0.5197) = 58.69^\circ \end{aligned}$$

Beam normal irradiance E_b

$$E_b = E_o \exp(-\tau_b m^{ab})$$

Table 27 Room Characteristics – Opaque Envelope and Fenestration

Element	Net Surface Area, m ²	Surface Orientation	Assembly Details	Performance / Other Details
Floor	12.1	Horizontal	(top to bottom) Carpet 127 mm concrete slab on metal deck (above conditioned space)	—
Roof	12.1	Horizontal	(top to bottom) Light-colored membrane roofing Rigid closed-cell polyisocyanurate foam core insulation (RSI-5.3) Flat metal deck Ceiling space Acoustic tile	U = 0.165 W/(m ² ·K) Ceiling used as a return plenum. Assume 30% of roof cooling load directly absorbed by return air stream without becoming room load.
Spandrel Wall	5.6	30° east of true south	(outside to inside) Spandrel bronze-tinted glass, opaque, backed with air space Rigid mineral fiber insulation (RSI=0.9) Mineral fiber batt insulation (RSI=2.3) 16 mm gypsum wall board	U = 0.278 W/(m ² ·K)
Spandrel Wall	5.6	60° west of true south	Same as above	Same as above
Brick Wall	5.6	30° east of true south	(outside to inside) 102 mm light brown colored face brick 152 mm low-mass concrete block Rigid continuous insulation (RSI = 0.9) Mineral fiber batt insulation (RSI = 2.3) 16 mm gypsum board	U = 0.261 W/(m ² ·K)
Brick Wall	3.7	60° west of true south	Same as above	Same as above
Window	3.7	30° east of true south	(outside to inside) 6 mm bronze-tinted outdoor pane 13 mm air space 6 mm clear indoor pane Light-colored mini blinds	Window dimensions: 1.91 m W × 1.95 m H. Normal incidence solar heat gain coefficient (SHGC) = 0.49 Window non-operable mounted in aluminum frame with thermal breaks. Overall U-value = 3.18 W/(m ² ·K) (Reference: Chapter 15, Tables 4 and 10, glazing type 5d) Indoor attenuation coefficients (IAC): IAC(0) = 0.74 IAC(60) = 0.65 IAC(diff) = 0.79 Radiant Fraction = 0.54 (Reference: Chapter 15, Table 14B, glazing type 5d, louver location = inside, louver reflectance = 0.8, louvers positioned at 45° angle.)
Window	3.7	60° west of true south	Same as above	Same as above

Table 28 Room Characteristics – Internal Heat Gains

Heat Gain Source	Heat Gain	Schedule	Details
Overhead Lighting	110 W total	7:00 AM to 7:00 PM	One 4-lamp pendant fluorescent 2.4 m type fixture Fixture has four 32 W T-8 lamps plus electronic ballasts with special allowance factor = 0.85 per manufacturer's data. Assume all cooling load from lighting is directly absorbed in the room, per Table 3.
Equipment	130 W total	8:00 AM to 5:00 PM	One computer and one personal printer for total 10.8 W/m ² heat gain.
Occupants	73 W sensible 59 W latent	8:00 AM to 5:00 PM	1 occupant Activity level: Moderately active office work. Heat gains per Table 1

m = relative air mass

$$= 1/[\sin\beta + 0.50572(6.07995 + \beta)^{-1.6364}], \beta \text{ expressed in degrees}$$

$$= 1.1849$$

ab = beam air mass exponent

$$= 1.454 - 0.406\tau_b - 0.268\tau_d + 0.021\tau_b\tau_d$$

$$= 0.71357$$

$$E_b = 1325 \exp[-0.515(1.1849^{0.71357})]$$

$$= 741 \text{ W/m}^2$$

Surface beam irradiance $E_{t,b}$

$$E_{t,b} = E_b \cos\theta$$

$$= (741) \cos(58.69)^\circ$$

$$= 385.1 \text{ W/m}^2$$

Diffuse irradiance E_d – Horizontal surfaces

Table 29 Monthly/Hourly 5% Design Temperatures for Example City, °C

Hour	January		February		March		April		May		June		July		August		September		October		November		December	
	db	wb	db	wb	db	wb	db	wb	db	wb	db	wb	db	wb	db	wb	db	wb	db	wb	db	wb	db	wb
1	7.7	7.3	8.6	7.3	12.1	9.7	15.4	12.8	19.4	16.8	22.3	19.3	23.2	20.5	23.2	20.5	20.9	18.2	15.7	13.8	11.1	10.2	8.6	8.6
2	7.3	7.1	8.2	7.1	11.6	9.4	15.0	12.6	18.9	16.6	21.8	19.1	22.8	20.4	22.8	20.4	20.4	18.0	15.2	13.6	10.6	9.9	8.2	8.2
3	6.9	6.8	7.8	6.8	11.2	9.3	14.6	12.4	18.6	16.5	21.5	19.0	22.4	20.3	22.4	20.3	20.2	17.9	14.9	13.4	10.2	9.7	7.8	7.8
4	6.6	6.6	7.4	6.6	10.8	9.1	14.2	12.3	18.3	16.4	21.2	18.9	22.1	20.2	22.1	20.2	19.8	17.8	14.6	13.3	9.9	9.5	7.5	7.5
5	6.4	6.4	7.2	6.4	10.6	8.9	14.0	12.2	18.1	16.3	20.9	18.8	21.9	20.1	21.9	20.1	19.6	17.7	14.3	13.2	9.7	9.4	7.3	7.3
6	6.6	6.6	7.4	6.6	10.8	9.1	14.2	12.3	18.3	16.4	21.2	18.9	22.1	20.2	22.1	20.2	19.8	17.8	14.6	13.3	9.9	9.5	7.5	7.5
7	7.4	7.1	8.3	7.1	11.7	9.5	15.1	12.7	19.1	16.7	21.9	19.2	22.9	20.4	22.9	20.4	20.6	18.1	15.3	13.7	10.7	10.0	8.3	8.3
8	9.2	8.4	10.2	8.4	13.8	10.6	17.2	13.6	20.9	17.4	23.8	19.8	24.8	21.0	24.7	21.0	22.4	18.7	17.3	14.5	12.7	11.1	10.1	9.6
9	11.3	9.8	12.4	9.8	16.2	11.7	19.5	14.6	23.1	18.2	25.9	20.5	26.9	21.6	26.8	21.6	24.4	19.4	19.4	15.4	14.9	12.3	12.2	10.9
10	13.1	11.1	14.4	11.0	18.3	12.7	21.6	15.4	25.0	18.9	27.9	21.1	28.8	22.2	28.6	22.2	26.2	20.1	21.3	16.3	16.9	13.4	14.0	12.2
11	14.7	12.3	16.2	12.1	20.2	13.7	23.4	16.2	26.7	19.5	29.6	21.7	30.6	22.7	30.2	22.7	27.8	20.6	23.1	17.1	18.6	14.4	15.6	13.3
12	15.8	13.0	17.3	12.9	21.4	14.3	24.6	16.8	27.8	19.9	30.7	22.0	31.7	23.1	31.3	23.0	28.8	21.0	24.2	17.5	19.8	15.1	16.7	14.1
13	16.7	13.6	18.3	13.4	22.4	14.8	25.6	17.2	28.7	20.2	31.6	22.3	32.6	23.3	32.2	23.3	29.7	21.3	25.1	17.9	20.7	15.6	17.6	14.6
14	17.2	14.0	18.8	13.8	23.1	15.1	26.2	17.4	29.2	20.4	32.1	22.5	33.1	23.5	32.7	23.4	30.2	21.5	25.7	18.2	21.3	15.9	18.1	15.0
15	17.2	14.0	18.8	13.8	23.1	15.1	26.2	17.4	29.2	20.4	32.1	22.5	33.1	23.5	32.7	23.4	30.2	21.5	25.7	18.2	21.3	15.9	18.1	15.0
16	16.6	13.6	18.1	13.4	22.3	14.7	25.5	17.1	28.6	20.2	31.4	22.3	32.4	23.3	32.1	23.2	29.6	21.3	25.0	17.9	20.6	15.5	17.4	14.6
17	15.7	12.9	17.2	12.8	21.3	14.2	24.5	16.7	27.7	19.9	30.6	22.0	31.6	23.0	31.2	23.0	28.7	20.9	24.1	17.5	19.7	15.0	16.6	14.0
18	14.6	12.2	16.1	12.1	20.1	13.6	23.3	16.2	26.6	19.4	29.4	21.6	30.4	22.7	30.1	22.7	27.7	20.6	22.9	17.0	18.5	14.3	15.5	13.2
19	13.0	11.1	14.3	10.9	18.2	12.7	21.4	15.4	24.9	18.8	27.8	21.1	28.7	22.2	28.5	22.2	26.1	20.0	21.2	16.2	16.7	13.3	13.9	12.2
20	11.8	10.2	13.1	10.2	16.8	12.0	20.1	14.8	23.7	18.4	26.6	20.7	27.5	21.8	27.3	21.8	24.9	19.6	20.0	15.7	15.5	12.7	12.7	11.3
21	10.8	9.6	12.0	9.5	15.7	11.4	19.0	14.3	22.6	18.0	25.5	20.3	26.5	21.5	26.3	21.5	23.9	19.3	19.0	15.2	14.4	12.1	11.7	10.7
22	9.8	8.9	10.9	8.8	14.6	10.9	17.9	13.8	21.6	17.6	24.5	20.0	25.5	21.2	25.3	21.2	23.0	18.9	17.9	14.8	13.4	11.4	10.7	10.0
23	9.1	8.3	10.1	8.3	13.7	10.5	17.1	13.5	20.8	17.3	23.7	19.8	24.7	20.9	24.6	20.9	22.3	18.7	17.2	14.4	12.6	11.0	10.0	9.5
24	8.3	7.8	9.3	7.8	12.8	10.1	16.2	13.1	20.1	17.1	22.9	19.5	23.9	20.7	23.8	20.7	21.5	18.4	16.4	14.1	11.8	10.6	9.2	9.0

Table 30 Lighting Load

Hour	Lighting Wattage	Conversion Factor	Usage Factor, %	Lighting Heat Gain, Btu/h	Heat Gain, W		Cooling Load, W		
					Convective 43%	Radiant 57%	Convective	Radiant	Total
<i>a</i>	<i>b</i>	<i>c</i>	<i>d</i>	<i>e</i>	<i>f</i>	<i>g</i>	<i>h</i>	<i>i</i>	<i>j</i>
1	110	1.00	0	0	0	0	0	8	8
2	110	1.00	0	0	0	0	0	7	7
3	110	1.00	0	0	0	0	0	6	6
4	110	1.00	0	0	0	0	0	6	6
5	110	1.00	0	0	0	0	0	5	5
6	110	1.00	0	0	0	0	0	4	4
7	110	1.00	100	110	47	63	47	38	85
8	110	1.00	100	110	47	63	47	47	94
9	110	1.00	100	110	47	63	47	51	99
10	110	1.00	100	110	47	63	47	53	101
11	110	1.00	100	110	47	63	47	55	102
12	110	1.00	100	110	47	63	47	55	102
13	110	1.00	100	110	47	63	47	55	102
14	110	1.00	100	110	47	63	47	56	103
15	110	1.00	100	110	47	63	47	56	103
16	110	1.00	100	110	47	63	47	57	104
17	110	1.00	100	110	47	63	47	58	105
18	110	1.00	100	110	47	63	47	58	106
19	110	1.00	0	0	0	0	0	25	25
20	110	1.00	0	0	0	0	0	16	16
21	110	1.00	0	0	0	0	0	11	11
22	110	1.00	0	0	0	0	0	9	9
23	110	1.00	0	0	0	0	0	8	8
24	110	1.00	0	0	0	0	0	7	7
Totals:	—	—	—	1,320	568	752	568	751	1319

$$E_d = E_o \exp(-\tau_d m^{ad})$$

ad = diffuse air mass exponent

$$= 0.507 + 0.205\tau_b - 0.080\tau_d - 0.190\tau_b\tau_d$$

$$= 0.24514$$

$$E_d = E_o \exp(-\tau_d m^{ad})$$

$$= 1325 \exp(-2.066(1.1849^{0.24514}))$$

$$= 154 \text{ W/m}^2$$

Table 31 Radiant Time Series and Conduction Time Series Factors for Example Problem

Hour	Non-Solar RTS Factors, Zone Type 8, %	Solar RTS Factors, Zone Type 8, %	Conduction Time Series (CTS) Factors, Wall Type 2, %
0	49	54	2.5
1	17	16	31.6
2	9	8	37.1
3	5	4	18.1
4	3	3	6.9
5	2	2	2.5
6	2	1	0.9
7	1	1	0.3
8	1	1	0.1
9	1	1	0.0
10	1	1	0.0
11	1	1	0.0
12	1	1	0.0
13	1	1	0.0
14	1	1	0.0
15	1	1	0.0
16	1	1	0.0
17	1	1	0.0
18	1	1	0.0
19	1	0	0.0
20	0	0	0.0
21	0	0	0.0
22	0	0	0.0
23	0	0	0.0

Table 32 Input Data for Calculation of Sol-Air Temperature

Item	Value	Notes
Local Standard Time	3:00 PM	
Month and Day	July 21	
Orientation	60° west of true south	
Latitude	33.64° N	
Longitude	84.43° W	
τ_b	0.515	Chapter 14, Table 1, July. τ_b = solar clear sky optical depth for beam irradiance
τ_d	2.066	Chapter 14, Table 1, July. τ_d = solar clear sky optical depth for diffuse irradiance.
Outdoor air dry-bulb temperature	33.1°C	Table 29, July 3:00 PM
Ground reflectivity, ρ_g	0.2	Assumed

Diffuse irradiance E_d — Vertical surface with surface azimuth +60°

AI = anisotropy index

$$= E_b / E_o$$

$$= 741 / 1325$$

$$= 0.5592$$

$$R_b = \cos \theta / \sin \beta$$

$$= \cos(58.69^\circ) / \sin(57.5^\circ)$$

$$= 0.6162$$

$$E_{i,d} = E_d [AI R_b + (1 - AI)(1 + \cos \Sigma)/2]$$

$$= 154 [(0.5592)(0.6162) + (1 - 0.5592)(1 - \cos(90^\circ))/2]$$

$$= 154 [0.5683]$$

$$= 86.9 \text{ W/m}^2$$

Ground reflected irradiance $E_{t,r}$

$$E_{t,r} = (E_b \sin \beta + E_d) \rho_g (1 - \cos \Sigma) / 2$$

$$= [741 \sin(57.5^\circ) + 154](0.2)[1 - \cos(90^\circ)] / 2$$

$$= 77.9 \text{ W/m}^2$$

Total surface irradiance E_t

$$E_t = E_{t,b} + E_{t,d} + E_{t,r}$$

$$= 385.1 + 86.9 + 77.9$$

$$= 549.8 \text{ W/m}^2$$

Sol-air temperature [from Equation (29)]:

$$T_e = t_o + \alpha E_t / h_o - \varepsilon \Delta R / h_o$$

$$= 33.1 + (0.053)(549.8) - 0$$

$$= 62.2^\circ\text{C}$$

This procedure is used to calculate the sol-air temperatures for each hour. Because of the tedious solar angle and intensity calculations, using a simple computer spreadsheet or other computer software can reduce the effort involved. A spreadsheet was used to calculate a 24 h sol-air temperature profile for the data of this example. See Table 33A for the solar angle and intensity calculations and Table 33B for the sol-air temperatures for this wall surface and orientation.

Next, use the sol-air temperature to calculate the heat input at the exterior surface of the wall using Equation (30). Table 33B shows the results of this calculation in column *f*. The calculation for 3:00 PM is

$$\begin{aligned} q_{i,0} &= UA (t_{e,0} - t_{rc}) \\ &= 0.278(62.2 - 23.9) \\ &= 59 \text{ W} \end{aligned}$$

With the heat input at the exterior surface known, the conduction heat gain at the interior surface of the wall can be calculated using Equation (31). This involves applying the conduction time series to calculate the delay as heat flows through the wall. In Table 16, the most similar wall construction is wall number 2. This is a spandrel glass wall that has similar mass and thermal resistance. Conduction time series factors for this wall are also shown in Table 31. Results of this calculation are shown in Table 33B in column *g*. For example, the calculation for 3:00 PM is

$$\begin{aligned} q_{15} &= c_0 q_{i,15} + c_1 q_{i,14} + c_2 q_{i,13} + c_3 q_{i,12} + \dots + c_{23} q_{i,16} \\ &= (0.025)(59) + (0.316)(50) + (0.371)(36) + (0.181)(22) \\ &\quad + (0.069)(20) + (0.025)(16) + (0.009)(12) + (0.003)(7) \\ &\quad + (0.001)(2) + (0.000)(-2) + (0.000)(-3) + (0.000)(-3) \\ &\quad + (0.000)(-2) + (0.000)(-2) + (0.000)(-1) + (0.000)(0) \\ &\quad + (0.000)(1) + (0.000)(3) + (0.000)(4) + (0.000)(6) \\ &\quad + (0.000)(22) + (0.000)(45) + (0.000)(58) + (0.000)(62) \\ &= 36 \text{ W} \end{aligned}$$

Next, split the conduction heat gain into convective and radiant portions. Table 14 shows that for conduction heat gain through walls and floors the convective fraction is 54% and the radiant fraction is 46%. Table 33B shows the division of the total heat gain into convective and radiant portions for all hours of the July design day in columns *h* and *i*. For 3:00 PM the calculation is

$$Q_c = (36)(0.54) = 20 \text{ W}$$

The convective heat gain will immediately become a cooling load. The radiant portion of the heat gain will undergo a conversion process to cooling load that is modeled using the RTS factors for the room. The same RTS factors used in Part 1 for lighting load calculation will be applied to the wall calculation since the room conditions are the same. Table 31 lists these factors in the “non-solar RTS factors, zone type 8” column. Table 33B shows the result of this calculation in column *k*. The calculation for 3:00 PM is as follows:

$$Q_{r,15} = r_0 q_{ir,15} + r_1 q_{ir,14} + r_2 q_{ir,13} + r_3 q_{ir,12} + \dots + r_{23} q_{ir,16}$$

Table 33A Wall Component of Solar Irradiance for July

Local Standard Hour	Apparent Solar Time	Hour Angle H	Solar Altitude β	Solar Azimuth ϕ	Solar Air Mass m	Beam Solar Irradiance			Diffuse Solar Irradiance				Total Surface Irradiance E_p , W/m ²
						Beam Normal $E_{b,n}$, W/m ²	Surface Incident Angle θ	Surface Direct Beam $E_{t,b}$, W/m ²	Diffuse Horizontal $E_{d,h}$, W/m ²	Sky Diffuse $E_{t,d}$, W/m ²	Ground Diffuse $E_{t,r}$, W/m ²	Diffuse Subtotal, W/m ²	
a	b	c	d	e	f	g	h	i	j	k	l	m	n
1	0.24	-176	-36	-176	—	0.0	—	0.0	0.0	0.0	0.0	0.0	0.0
2	1.24	-161	-33	-159	—	0.0	—	0.0	0.0	0.0	0.0	0.0	0.0
3	2.24	-146	-27	-144	—	0.0	—	0.0	0.0	0.0	0.0	0.0	0.0
4	3.24	-131	-19	-132	—	0.0	—	0.0	0.0	0.0	0.0	0.0	0.0
5	4.24	-116	-9	-122	—	0.0	—	0.0	0.0	0.0	0.0	0.0	0.0
6	5.24	-101	2	-113	18.23816	22.2	172.8	0.0	19.7	9.7	2.1	11.7	11.7
7	6.24	-86	14	-105	4.06606	326.4	159.9	0.0	71.9	27.1	15.1	42.2	42.2
8	7.24	-71	26	-98	2.25339	528.3	146.3	0.0	106.5	32.0	34.0	66.0	66.0
9	8.24	-56	39	-90	1.59750	645.4	132.7	0.0	130.6	33.5	53.4	86.9	86.9
10	9.24	-41	51	-81	1.28345	716.1	119.2	0.0	147.4	33.9	70.5	104.3	104.3
11	10.24	-26	63	-67	1.12031	758.0	105.9	0.0	158.4	33.9	83.5	117.3	117.3
12	11.24	-11	73	-40	1.04326	779.3	93.0	0.0	164.3	33.8	91.1	124.9	124.9
13	12.24	4	76	14	1.02835	783.6	80.5	128.8	165.5	50.4	92.7	143.1	271.9
14	13.24	19	69	56	1.07141	771.4	68.9	277.1	162.1	70.2	88.2	158.4	435.5
15	14.2388	33.58	57.5	74.71	1.18490	741.0	58.69	385.1	153.8	86.9	77.9	164.7	549.8
16	15.24	49	45	86	1.40773	686.7	50.6	435.9	140.1	98.7	62.7	161.5	597.4
17	16.24	64	33	94	1.84558	596.9	45.8	415.9	120.1	102.7	44.3	147.0	563.0
18	17.24	79	20	102	2.85472	446.1	45.5	312.9	91.6	92.6	24.7	117.2	430.2
19	18.24	94	8	109	6.61488	182.4	49.6	118.3	49.7	52.1	7.6	59.7	178.0
20	19.24	109	-3	117	—	0.0	—	0.0	0.0	0.0	0.0	0.0	0.0
21	20.24	124	-14	127	—	0.0	—	0.0	0.0	0.0	0.0	0.0	0.0
22	21.24	139	-23	138	—	0.0	—	0.0	0.0	0.0	0.0	0.0	0.0
23	22.24	154	-30	151	—	0.0	—	0.0	0.0	0.0	0.0	0.0	0.0
24	23.24	169	-35	167	—	0.0	—	0.0	0.0	0.0	0.0	0.0	0.0

$$\begin{aligned}
&= (0.49)(36) + (0.17)(26) + (0.09)(19) + (0.05)(16) \\
&+ (0.03)(11) + (0.02)(7) + (0.02)(3) + (0.01)(-1) \\
&+ (0.01)(-2) + (0.01)(-3) + (0.01)(-2) + (0.01)(-2) \\
&+ (0.01)(-1) + (0.01)(0) + (0.01)(2) + (0.01)(4) \\
&+ (0.01)(7) + (0.01)(13) + (0.01)(25) + (0.01)(41) \\
&+ (0.00)(53) + (0.00)(58) + (0.00)(55) + (0.00)(48) \\
&= 12 \text{ W}
\end{aligned}$$

Finally, the total wall cooling load is the sum of the convective and radiant loads. Table 33B shows these results in column l . For July 3:00 PM the calculation is as follows:

$$Q_{\text{wall}} = Q_{c15} + Q_{r15} = 20 + 12 = 32 \text{ W}$$

Part 3. Window cooling load without internal or external shading

Objective: Calculate the cooling load for the 3.72 m² window facing 60° west of south for July 3:00 PM local standard time, without considering internal or external shading. Internal and external shading will be considered in Parts 4 and 5, respectively.

Solution: Determining the window cooling load requires calculation of: (a) the 24 h window heat gain profile, (b) the convective and radiant portions of the heat gain, (c) the conversion of the radiant heat gain into cooling load using RTS factors, and (d) the total window load as the sum of convective and radiant loads.

First calculate the window heat gain profile using Equations (12) to (15). Respectively, these equations calculate the direct beam solar heat gain q_b , the diffuse solar heat gain q_d , the conduction heat gain q_c , and the total fenestration heat gain. The calculation uses solar irradiance and solar angle values calculated in Part 2. The solar irradiance and solar angle values along with the window heat gain results are shown in Table 34 in columns b through d and h through k . For July 3:00 PM (hour 15), for example, Part 2 calculated:

$$E_{t,b} = 385.1 \text{ W/m}^2$$

$$E_{t,d} = 86.9 \text{ W/m}^2$$

$$E_r = 77.9 \text{ W/m}^2$$

$$\theta = 58.7^\circ$$

From Chapter 15, Table 10, for glass type 5d, $q_{b15} = AE_{t,b}$

$$\text{SHGC}(\theta)(\text{IAC}) = (3.72)(385.2)(0.400)(1.00) = 573 \text{ W}$$

$$q_{d15} = A(E_{t,d} + E_r)(\text{SHGC})_D(\text{IAC})_D = (3.72)(86.9 + 77.9)(0.41)(1.00) = 251 \text{ W}$$

$$q_{c15} = UA(t_{\text{out}} - t_{\text{in}}) = (3.18)(3.72)(33.1 - 23.9) = 109 \text{ W}$$

$$Q_{15} = q_{b15} + q_{d15} + q_{c15} = 573 + 251 + 109 = 933 \text{ W}$$

$$\text{SHGC}(\theta) = \text{SHGC}(58.7) = 0.400 \text{ (interpolated)}$$

$$(\text{SHGC})_D = 0.41$$

The indoor attenuation coefficient (IAC) is 1.0 because internal shades are not considered in this calculation.

Then, applying Equations (12) to (15) for July 3:00 PM:

$$q_{b15} = AE_{t,b} \text{SHGC}(\theta)(\text{IAC}) = (3.72)(385.2)(0.400)(1.00) = 573 \text{ W}$$

$$q_{d15} = A(E_{t,d} + E_r)(\text{SHGC})_D(\text{IAC})_D = (3.72)(86.9 + 77.9)(0.41)(1.00) = 251 \text{ W}$$

$$q_{c15} = UA(t_{\text{out}} - t_{\text{in}}) = (3.18)(3.72)(33.1 - 23.9) = 109 \text{ W}$$

$$Q_{15} = q_{b15} + q_{d15} + q_{c15} = 573 + 251 + 109 = 933 \text{ W}$$

Next, divide the window heat gain into convective and radiant components. Because loads for windows without internal shading (blinds, drapes, etc.) are being calculated, the direct beam solar gain must be treated separately from the diffuse and conduction heat gains. The direct beam heat gain is treated as 100% radiant, and the conversion from heat gain to load uses special solar RTS factors dif-

Table 33B Wall Sol-Air Temperatures, Heat Input, Heat Gain, and Cooling Load for July

Local Standard Hour	Total Surface Irradiance E_t W/m ²	Outdoor Dry-Bulb, °C	Sol-Air Temp., °C	Indoor Dry-Bulb, °C	Heat Input W	Heat Gain, W			Cooling Load, W		
						Total	Convective (54%)	Radiant (46%)	Convective	Radiant	Total
<i>a</i>	<i>b</i>	<i>c</i>	<i>d</i>	<i>e</i>	<i>f</i>	<i>g</i>	<i>h</i>	<i>i</i>	<i>j</i>	<i>k</i>	<i>l</i>
1	0.0	23.2	23.2	23.9	-1	2	1	1	1	3	4
2	0.0	22.8	22.8	23.9	-2	0	0	0	0	3	3
3	0.0	22.4	22.4	23.9	-2	-1	0	0	0	2	2
4	0.0	22.1	22.1	23.9	-3	-2	-1	-1	-1	2	1
5	0.0	21.9	21.9	23.9	-3	-2	-1	-1	-1	1	0
6	11.7	22.1	22.7	23.9	-2	-3	-1	-1	-1	1	0
7	42.2	22.9	25.1	23.9	2	-2	-1	-1	-1	1	0
8	66.0	24.8	28.3	23.9	7	-1	0	0	0	1	1
9	86.9	26.9	31.5	23.9	12	3	1	1	1	2	3
10	104.3	28.8	34.3	23.9	16	7	4	3	4	3	7
11	117.3	30.6	36.8	23.9	20	11	6	5	6	4	11
12	124.9	31.7	38.3	23.9	22	16	8	7	8	6	14
13	271.9	32.6	46.9	23.9	36	19	10	9	10	7	18
14	435.5	33.1	56.1	23.9	50	26	14	12	14	9	23
15	549.8	33.1	62.2	23.9	59	36	20	17	20	12	32
16	597.4	32.4	64.0	23.9	62	48	26	22	26	16	42
17	563.0	31.6	61.3	23.9	58	55	30	26	30	20	50
18	430.2	30.4	53.2	23.9	45	58	31	27	31	22	53
19	178.0	28.7	38.1	23.9	22	53	29	25	29	21	50
20	0.0	27.5	27.5	23.9	6	41	22	19	22	19	41
21	0.0	26.5	26.5	23.9	4	25	13	11	13	14	27
22	0.0	25.5	25.5	23.9	3	13	7	6	7	10	16
23	0.0	24.7	24.7	23.9	1	7	4	3	4	7	10
24	0.0	23.9	23.9	23.9	0	4	2	2	2	5	7

ferent from those used to convert other types of radiant heat gain to load. Therefore, the total window heat gain must be divided into three parts: (1) the direct beam heat gain, (2) the radiant part of the conduction plus diffuse solar heat gain, and (3) the convective part of the conduction plus diffuse solar heat gain. In Table 35, columns *b* to *d* show the direct beam component of heat gain. For conduction and diffuse solar heat gains, Table 14 shows that for conduction heat gains through windows where the SHGC is less than 0.5, the convective fraction of the heat gain is 54% and the radiative fraction is 46%. Columns *f* to *j* in Table 35 show how the sum of diffuse solar and conduction heat gain is split into convective and radiant portions.

With the heat gains split into three categories, the conversion of heat gain to cooling load can be calculated for each radiant gain. First, for the load due to the direct beam solar heat gain is calculated using Equation (33). The solar RTS factors from Table 20 for medium weight construction, carpeted floor, and 50% window area will be used. These factors are also shown in Table 31 in the column titled “Solar RTS Factors, Room Type 8.” Cooling load results appear in column *e* of Table 35. For July 3:00 PM the calculation is as follows:

$$\begin{aligned}
 Q_{b,15} &= r_{0q_{b,15}} + r_{1q_{b,14}} + r_{2q_{b,13}} + r_{3q_{b,12}} + \dots + r_{23q_{b,14}} \\
 &= (0.54)(573) + (0.16)(329) + (0.08)(81) + (0.04)(0) \\
 &\quad + (0.03)(0) + (0.02)(0) + (0.01)(0) + (0.01)(0) \\
 &\quad + (0.01)(0) + (0.01)(0) + (0.01)(0) + (0.01)(0) \\
 &\quad + (0.01)(0) + (0.01)(0) + (0.01)(0) + (0.01)(0) \\
 &\quad + (0.01)(0) + (0.01)(0) + (0.01)(0) + (0.00)(0) \\
 &\quad + (0.00)(193) + (0.00)(524) + (0.00)(695) + (0.00)(707) \\
 &= 369 \text{ W}
 \end{aligned}$$

The cooling load due to the radiant portion of the diffuse solar and conduction window heat gain is also calculated with Equation (33). This time the non-solar RTS factors are used. These are the same factors used for conversion of lighting and wall conduction heat gains to load in Parts 1 and 2. The non-solar RTS factors are shown in Table 31 in the column titled “Non-Solar RTS Factors, Room Type 8.” Results appear in column *l* of Table 35.

The convective portion of the diffuse solar and conduction window heat gains immediately converts to load and is shown Table 35 column *k*. The total diffuse solar and conduction load is the sum of radiant and convective components and is shown in column *m*.

Finally, the total window load is the sum of the direct beam solar load, and the diffuse solar plus convective load. These loads are shown in Table 35 column *n*. For July 3:00 PM the calculation is

$$Q_{\text{window}} = Q_b + Q_{\text{diff} + \text{cond}} = 369 + 334 = 703 \text{ W}$$

Part 4. Window cooling load with internal shading

Objective: Building on the window load calculation in Part 3, calculate the window load considering internal shading due to light-colored mini-blinds. Consider the same 3.72 m² window facing 60° west of south for July 3:00 PM local standard time.

Solution: Calculation of the window cooling load requires the same four steps used in Part 3, but with different application data. Calculate: (a) the 24 h window heat gain profile, (b) the convective and radiant portions of the heat gain, (c) the conversion of the radiant heat gain into cooling load using RTS factors, and (d) the total window load as the sum of convective and radiant loads.

Calculation of the 24 h heat gain profiles requires consideration of the effect of the mini-blinds. This effect is calculated with indoor

Table 34 Window Heat Gain for July (No Blinds or Overhang)

Beam Solar Heat Gain							Diffuse Solar Heat Gain						Conduction Heat Gain		
Local Std Hour	Beam Normal E_b , W/m ²	Surface Incident Angle θ	Surface Direct Beam $E_{t,b}$, W/m ²	Beam SHGC	Adjusted Beam IAC	Beam Solar Heat Gain, q_b , W	Diffuse Hor. E_d , W/m ²	Sky Diffuse $E_{t,d}$, W/m ²	Ground Diffuse $E_{t,r}$, W/m ²	Subtotal Diffuse, W/m ²	Hemis. SHGC	Diffuse Solar Heat Gain q_d , W	Outdoor Dry-Bulb, °C	Conduction Heat Gain, q_c , W	Total Window Heat Gain Q , W
<i>a</i>	<i>b</i>	<i>c</i>	<i>d</i>	<i>e</i>	<i>f</i>	<i>g</i>	<i>h</i>	<i>i</i>	<i>j</i>	<i>k</i>	<i>l</i>	<i>m</i>	<i>n</i>	<i>o</i>	<i>p</i>
1	0.0	—	0.0	—	—	0	0.0	0.0	0.0	0.0	—	0	23.2	−8	−8
2	0.0	—	0.0	—	—	0	0.0	0.0	0.0	0.0	—	0	22.8	−13	−13
3	0.0	—	0.0	—	—	0	0.0	0.0	0.0	0.0	—	0	22.4	−17	−17
4	0.0	—	0.0	—	—	0	0.0	0.0	0.0	0.0	—	0	22.1	−21	−21
5	0.0	—	0.0	—	—	0	0.0	0.0	0.0	0.0	—	0	21.9	−24	−24
6	22.2	172.8	0.0	—	—	0	19.7	9.7	2.1	11.7	0.410	18	22.1	−21	−3
7	326.4	159.9	0.0	—	—	0	71.9	27.1	15.1	42.2	0.410	64	22.9	−12	52
8	528.3	146.3	0.0	—	—	0	106.5	32.0	34.0	66.0	0.410	101	24.8	11	112
9	645.4	132.7	0.0	—	—	0	130.6	33.5	53.4	86.9	0.410	132	26.9	36	169
10	716.1	119.2	0.0	—	—	0	147.4	33.9	70.5	104.3	0.410	159	28.8	58	218
11	758.0	105.9	0.0	—	—	0	158.4	33.9	83.5	117.3	0.410	179	30.6	79	258
12	779.3	93.0	0.0	—	—	0	164.3	33.8	91.1	124.9	0.410	190	31.7	92	282
13	783.6	80.5	128.8	0.170	1.000	81	165.5	50.4	92.7	143.1	0.410	218	32.6	102	402
14	771.4	68.9	277.1	0.320	1.000	329	162.1	70.2	88.2	158.4	0.410	241	33.1	109	680
15	741.0	58.69	385.1	0.400	1.000	573	153.8	86.9	77.9	164.7	0.410	251	33.1	109	933
16	686.7	50.6	435.9	0.436	1.000	707	140.1	98.7	62.7	161.5	0.410	246	32.4	101	1054
17	596.9	45.8	415.9	0.450	1.000	695	120.1	102.7	44.3	147.0	0.410	224	31.6	91	1010
18	446.1	45.5	312.9	0.451	1.000	524	91.6	92.5	24.7	117.2	0.410	179	30.4	78	780
19	182.4	49.6	118.3	0.439	1.000	193	49.7	52.1	7.6	59.7	0.410	91	28.7	57	341
20	0.0	—	0.0	—	—	0	0.0	0.0	0.0	0.0	—	0	27.5	43	43
21	0.0	—	0.0	—	—	0	0.0	0.0	0.0	0.0	—	0	26.5	31	31
22	0.0	—	0.0	—	—	0	0.0	0.0	0.0	0.0	—	0	25.5	19	19
23	0.0	—	0.0	—	—	0	0.0	0.0	0.0	0.0	—	0	24.7	10	10
24	0.0	—	0.0	—	—	0	0.0	0.0	0.0	0.0	—	0	23.9	0	0

attenuation coefficients (IAC), and different radiant and convective fractions than an unshaded window.

IAC values depend on several factors: (1) type of shading device, (2) position of shading device relative to window, (3) reflectivity of shading device, (4) angular adjustment of shading device, as well as (5) solar position relative to the shading device. These factors are discussed in detail in Chapter 15. For this example with mini-blinds, the IAC for beam radiation is treated separately from the IAC for diffuse solar gain. The direct beam IAC must be adjusted based on the profile angle of the sun.

The mini-blinds are assumed to be light colored with louver reflectance = 0.8 and louvers positioned at a 45° angle on double-glazed heat absorbing windows. Chapter 15 Table 14B lists IAC factors for window type 5d plus this shading type as IAC(0) = 0.74, IAC(60) = 0.65, IAC(diff) = 0.79, and radiant fraction = 0.54.

At 3:00 PM in July, the profile angle of the sun relative to the window surface is 58.4°. Using interpolation, the beam IAC is 0.652. The diffuse IAC is 0.79. As calculated in Part 3, SHGC(0) = 0.400 and $\langle\text{SHGC}\rangle_D = 0.41$. Thus, the window heat gains at 3:00 PM are

$$q_{b15} = A E_{t,b} \text{SHGC}(\theta) \text{IAC} = (3.72)(385.2)(0.400)(0.653) = 374 \text{ W}$$

$$q_{d15} = A(E_{t,d} + E_{t,r})\langle\text{SHGC}\rangle_D \text{IAC}_D = (3.72)(86.8 + 77.9)(0.41)(0.79) = 198 \text{ W}$$

$$q_{c15} = UA(t_{\text{out}} - t_{\text{in}}) = (3.18)(3.72)(33.1 - 23.9) = 109 \text{ W}$$

Calculation of beam solar heat gain is shown in Table 36 columns *b* through *e*. Calculation of the diffuse solar heat gain is shown in columns *f* through *i*. The conduction heat gain is found in column *j*.

Because internal shades are used, the direct beam solar heat gain is assumed to be absorbed by the shading device, and a portion immediately becomes a cooling load by convection. The remaining solar heat absorbed by the blind is assumed to be radiated to all surfaces of the room just as the diffuse and conduction heat gains are. As a result, the beam direct solar heat gain is combined with diffuse and conduction heat gains to obtain the total heat gain shown in column *k* of Table 36.

Next, the total heat gain is divided into convective and radiant portions. For window type 5d with mini-blinds, Chapter 15 Table 14B lists a radiant fraction as 0.54. Thus 54% of the heat gain is radiant and 46% is convective. These convective and radiant heat gains are shown in columns *l* and *m* in Table 36.

The radiant portion of the heat gain is converted to cooling load using Equation (33). In this equation the “Non-Solar RTS Factors, Zone Type 8” factors from Table 31 are used. Results appear in Table 36 in column *o*. The convective part of the heat gain immediately becomes a load and is shown in column *n*.

The total window load is then calculated combining the radiant and convective loads. Results are shown in Table 36 column *p*. For July 3:00 PM the calculation is

Table 35 Window Cooling Loads for July (No Blinds or Overhang)

Local Standard Hour	Unshaded Direct Beam Solar Cooling Load				Diffuse Solar + Conduction Cooling Load								
	Beam Solar Heat Gain W	Con- vective Heat Gain 0%, W	Radiant Heat Gain 100%, W	Radiant Cooling Load, W	Diffuse Solar Heat Gain, W	Conduc- tion Heat Gain, W	Total Heat Gain, W	Con- vective Heat Gain 54%, W	Radiant Heat Gain 46%, W	Convective Load W	Radiant, Cooling Load W	Total Cooling Load, W	Window Cooling Load, W
<i>a</i>	<i>b</i>	<i>c</i>	<i>d</i>	<i>e</i>	<i>f</i>	<i>g</i>	<i>h</i>	<i>i</i>	<i>j</i>	<i>k</i>	<i>l</i>	<i>m</i>	<i>n</i>
1	0	0	0	31	0	-8	-8	-4	-4	-4	14	10	41
2	0	0	0	31	0	-13	-13	-7	-6	-7	12	4	35
3	0	0	0	31	0	-17	-17	-9	-8	-9	9	0	31
4	0	0	0	31	0	-21	-21	-11	-10	-11	7	-5	26
5	0	0	0	31	0	-24	-24	-13	-11	-13	4	-9	22
6	0	0	0	31	18	-21	-3	-2	-1	-2	8	6	37
7	0	0	0	31	64	-12	52	28	24	28	21	50	81
8	0	0	0	30	101	11	112	60	51	60	39	100	130
9	0	0	0	27	132	36	169	91	78	91	58	149	176
10	0	0	0	21	159	58	218	117	100	117	76	194	215
11	0	0	0	14	179	79	258	139	119	139	92	232	246
12	0	0	0	7	190	92	282	153	130	153	104	257	264
13	81	0	81	46	218	102	321	173	147	173	118	291	337
14	329	0	329	191	241	109	350	189	161	189	131	320	511
15	573	0	573	369	251	109	360	195	166	195	139	334	703
16	707	0	707	503	246	101	347	188	160	188	140	328	831
17	695	0	695	550	224	91	315	170	145	170	134	304	854
18	524	0	524	485	179	78	256	138	118	138	119	257	742
19	193	0	193	297	91	57	148	80	68	80	88	168	465
20	0	0	0	137	0	43	43	23	20	23	53	76	213
21	0	0	0	81	0	31	31	17	14	17	38	55	136
22	0	0	0	54	0	19	19	10	9	10	29	39	93
23	0	0	0	40	0	10	10	5	5	5	23	28	68
24	0	0	0	33	0	0	0	0	0	0	17	17	50

$$Q_{\text{window}} = Q_{\text{radiant}} + Q_{\text{convective}} = 269 + 313 = 583 \text{ W}$$

$$\Omega = 58.4^\circ$$

Part 5. Window cooling load with internal and external shading

Objective: Calculate the cooling load for the window in Part 4 with the addition of a 1.5 m overhang shading the window.

Solution: As in Parts 3 and 4, determining the window cooling load requires calculation of (a) the 24 h window heat gain profile, (b) the convective and radiant portions of the heat gain, (c) the conversion of the radiant heat gain into cooling load using RTS factors, and (d) the total window load as the sum of convective and radiant loads.

The diffuse solar and conduction heat gain profiles are the same as in Part 4 and are shown in columns *h* and *i* of Table 37. The direct beam solar heat gain profile must be recalculated accounting for the shading effect of the overhang. In Chapter 15, methods are described and examples provided for calculating the area of a window shaded by attached vertical or horizontal projections. For July 3:00 PM, the solar position calculated in previous parts of this example is

$$\text{Solar altitude } \beta = 57.5^\circ$$

$$\text{Solar azimuth } \phi = 74.7^\circ$$

$$\text{Surface-solar azimuth } \gamma = 14.7^\circ$$

From Chapter 15, Equation (33), profile angle Ω is calculated by

$$\tan \Omega = \tan \beta / \cos \gamma = \tan(57.5) / \cos(14.7) = 1.6228$$

From Chapter 15, Equation (35), shadow height S_H is

$$S_H = P_H \tan \Omega = 1.5(1.6228) = 2.4 \text{ m}$$

Because the window is 1.95 m tall, at July 3:00 PM the window is completely shaded by the 1.5 m deep overhang. Thus, the shaded window heat gain includes only diffuse solar and conduction gains for this hour. When the shadow height is less than 1.95 m then part of the window is exposed to direct beam solar. The sunlit area is calculated as $A = 1.91(1.95 - S_H)$ where 1.91 is the window width in metres. The direct beam heat gain is then Sunlit Area $\times E_{t,b}$. Table 37 shows the profile angle, shadow height, sunlit area and direct beam heat gain in columns *d* through *g*. Note that the overhang shades the window completely for all hours except hours 16 through 19 when the solar altitude angle is low enough that part of the window is sunlit.

As in Part 4, due to the use of internal shading, direct beam solar heat gain is combined with diffuse solar and conduction heat gains to obtain the total heat gain shown in Table 37, column *j*. The total heat gain is divided using the 46% convective fraction and 54% radiative fraction used in Part 4 for a window with internal shades. These heat gain components are shown in Table 37, columns *k* and *l*.

The radiant heat gain is converted to cooling load using the “Non-Solar RTS Factors, Zone Type 8” from Table 31 as before. The radiant cooling load is shown in Table 37, column *n*. Combin-

Table 36 Window Cooling Loads for July (Blinds and no Overhang)

Local Standard Time	Surface Beam Irradiance $E_{t,b}$, Btu/h-ft ²	Beam SHGC	Beam IAC	Beam Solar Heat Gain, W	Total Diffuse Irradiance W/m ²	Diffuse SHGC	Diffuse IAC	Diffuse Solar Heat Gain, W	Conduc- tion Heat Gain, W	Total Heat Gain, W	Conv. Heat Gain (46%), W	Radiant Heat Gain (54%), W	Conv. Cooling Load, W	Radiant Cooling Load, W	Total Window Cooling Load, W
<i>a</i>	<i>b</i>	<i>c</i>	<i>d</i>	<i>e</i>	<i>f</i>	<i>g</i>	<i>h</i>	<i>i</i>	<i>j</i>	<i>k</i>	<i>l</i>	<i>m</i>	<i>n</i>	<i>o</i>	<i>p</i>
1	0.0	—	—	0	0	—	—	0	−8	−8	−4	−4	−4	25	22
2	0.0	—	—	0	0	—	—	0	−13	−13	−6	−7	−6	22	16
3	0.0	—	—	0	0	—	—	0	−17	−17	−8	−9	−8	20	12
4	0.0	—	—	0	0	—	—	0	−21	−21	−10	−11	−10	17	7
5	0.0	—	—	0	0	—	—	0	−24	−24	−11	−13	−11	14	3
6	0.0	—	—	0	12	0.41	0.79	14	−21	−7	−3	−4	−3	17	14
7	0.0	—	—	0	42	0.41	0.79	51	−12	39	18	21	18	30	48
8	0.0	—	—	0	66	0.41	0.79	79	11	91	42	49	42	48	90
9	0.0	—	—	0	87	0.41	0.79	105	36	141	65	76	65	67	131
10	0.0	—	—	0	104	0.41	0.79	126	58	184	85	99	85	83	168
11	0.0	—	—	0	117	0.41	0.79	141	79	220	101	119	101	97	199
12	0.0	—	—	0	125	0.41	0.79	150	92	242	112	131	112	107	219
13	128.8	0.170	0.650	53	143	0.41	0.79	172	102	328	151	177	151	135	286
14	277.1	0.320	0.650	214	158	0.41	0.79	191	109	514	236	278	236	199	435
15	385.0	0.400	0.652	374	165	0.41	0.79	198	109	681	313	368	313	269	583
16	435.9	0.436	0.668	472	161	0.41	0.79	194	101	768	353	415	353	320	674
17	415.9	0.450	0.683	475	147	0.41	0.79	177	91	743	342	401	342	335	676
18	312.9	0.451	0.700	367	117	0.41	0.79	141	78	586	269	316	269	299	569
19	118.3	0.439	0.721	139	60	0.41	0.79	72	57	268	123	145	123	200	324
20	0.0	—	—	0	0	—	—	0	43	43	20	23	20	106	125
21	0.0	—	—	0	0	—	—	0	31	31	14	17	14	70	84
22	0.0	—	—	0	0	—	—	0	19	19	9	10	9	50	59
23	0.0	—	—	0	0	—	—	0	10	10	5	5	5	39	43
24	0.0	—	—	0	0	—	—	0	0	0	0	0	0	30	30

ing with the convective load yields the total cooling load listed in Table 37, column *o*. For July 3:00 PM the total window cooling load is 281 W.

Part 6. Total room sensible cooling load.

Objective: Calculate the total sensible cooling load for the example office for July 3:00 PM local standard time.

Solution: To calculate the total sensible cooling load for the office, cooling loads for all ten heat gain components must be calculated and then summed.

Part 1 demonstrated the calculation of the lighting load. The same general procedure can be applied to calculating the occupant and equipment cooling loads using those component heat gains.

Part 2 demonstrated the calculation of the cooling load for the spandrel glass wall facing 60° west of true south. The same procedures can be used to calculate wall cooling loads for the other spandrel wall section and the two sections of brick wall. In addition, the same procedures can be used to calculate the roof load. Note that because the ceiling space is used as a return air plenum, we are assuming 30% of the roof load is directly absorbed by the return air and only the remaining 70% reaches the room.

Part 5 demonstrated the calculation of the cooling load for the window facing west of true south, with internal shading and external overhang shading. The same procedures can be used for the window facing east of true south.

Finally the 10 load components are summed to obtain the total sensible load for the room. Table 38 shows the 24 h component and total room load profiles for July. The total room load is in column *l*. The 3:00 PM load is 926 W.

9.2 THE EFFECT OF ORIENTATION ON PEAK COOLING LOAD MAGNITUDE AND TIME

A room cooling load is the combination of multiple load components, each driven by separate, independently varying heat gains. The peak room load occurs when the sum of all component loads is largest. This is often at a time when many of the individual component loads are not at their largest value. Among the heat gains driving loads in a room,

- There are multiple different internal sources of heat gain whose intensity varies with time.
- Opaque envelope heat gains are a function of the thermal properties of the assembly, surface area, outdoor and indoor dry-bulb temperature, and the orientation of the surface. Orientation affects when the surface is exposed to solar irradiance of varying intensities.
- Fenestration heat gains are a function of the thermal and optical performance of the fenestration assembly, surface area, outdoor and indoor dry-bulb temperature, and orientation of the surface. Like opaque envelope components, orientation affects when the fenestration is exposed to solar irradiance of different intensities.

Orientation can significantly affect the peak time of individual opaque envelope and fenestration component loads. For example, driven by solar irradiance, an east-facing room will have peak opaque envelope and fenestration loads earlier in the day than a west-facing room. Orientation can also affect the time of year when peak loads occur. In the northern hemisphere, a south-facing window will experience a peak load during a fall month due to the solar altitude angle being lower so solar irradiance on the window is more intense than during summer months. Because of the effect of orien-

Table 37 Window Cooling Loads for July (with Blinds and Overhang)

Overhang and Fins Shading Calculations						Shaded Direct Beam + Diffuse + Conduction Cooling Load								
Local Standard Hour	Surface Solar Irradiance, W/m ²	Surface Incident Angle θ	Profile Angle Ω	Shadow Height, m	Direct Sunlit Area, m ²	Beam Solar Heat Gain, W	Diffuse Heat Gain, W	Conduction Heat Gain, W	Total Heat Gain, W	Conv. Heat Gain 46%, W	Radiant Heat Gain 54%, W	Conv. Cooling Load, W	Radiant Cooling Load, W	Total Cooling Load, W
<i>a</i>	<i>b</i>	<i>c</i>	<i>d</i>	<i>e</i>	<i>f</i>	<i>g</i>	<i>h</i>	<i>i</i>	<i>j</i>	<i>k</i>	<i>l</i>	<i>m</i>	<i>n</i>	<i>o</i>
1	0.0	—	—	—	—	0	0	-8	-8	-4	-4	-4	17	14
2	0.0	—	—	—	—	0	0	-13	-13	-6	-7	-6	14	8
3	0.0	—	—	—	—	0	0	-17	-17	-8	-9	-8	11	4
4	0.0	—	—	—	—	0	0	-21	-21	-10	-11	-10	9	-1
5	0.0	—	—	—	—	0	0	-24	-24	-11	-13	-11	6	-5
6	0.0	172.8	—	—	—	0	14	-21	-7	-3	-4	-3	9	6
7	0.0	159.9	—	—	—	0	51	-12	39	18	21	18	22	40
8	0.0	146.3	—	—	—	0	79	11	91	42	49	42	40	82
9	0.0	132.7	—	—	—	0	105	36	141	65	76	65	60	125
10	0.0	119.2	—	—	—	0	126	58	184	85	99	85	79	163
11	0.0	105.9	—	—	—	0	141	79	220	101	119	101	95	196
12	0.0	93.0	—	—	—	0	150	92	242	112	131	112	106	218
13	128.8	80.5	80.4	9.02	0.0	0	172	102	275	126	148	126	119	246
14	277.1	68.9	68.9	4.00	0.0	0	191	109	300	138	162	138	132	270
15	385.1	58.69	58.4	2.45	0.0	0	198	109	307	141	166	141	140	281
16	435.9	50.6	48.2	1.70	0.6	60	194	101	355	164	192	164	158	321
17	415.9	45.8	37.8	1.18	1.8	187	177	91	455	209	246	209	193	403
18	312.9	45.5	26.4	0.76	2.8	225	141	78	444	204	240	204	203	407
19	118.3	49.6	12.6	0.34	3.8	115	72	57	244	112	132	112	151	263
20	0.0	—	—	—	—	0	0	43	43	20	23	20	79	99
21	0.0	—	—	—	—	0	0	31	31	14	17	14	53	67
22	0.0	—	—	—	—	0	0	19	9	10	9	39	48	0
23	0.0	—	—	—	—	0	0	10	5	5	5	29	34	0
24	0.0	—	—	—	—	0	0	0	0	0	0	21	21	0

Table 38 Example Office Cooling Loads, July Design Day

Sensible Cooling Load, W												Room Total
Local Standard Hour	Spandrel Wall $\psi = -30^\circ$	Spandrel Wall $\psi = +60^\circ$	Brick Wall $\psi = -30^\circ$	Brick Wall $\psi = +60^\circ$	Window $\psi = -30^\circ$	Window $\psi = +60^\circ$	Roof (70% to Room)	Overhead Lighting	Equipment	Occupants		
<i>a</i>	<i>b</i>	<i>c</i>	<i>d</i>	<i>e</i>	<i>f</i>	<i>g</i>	<i>h</i>	<i>i</i>	<i>j</i>	<i>k</i>		<i>l</i>
1	3	4	16	16	10	14	3	8	4	4		82
2	2	3	14	15	4	8	1	7	4	4		62
3	1	2	13	13	-1	4	-1	6	4	4		45
4	0	1	12	12	-6	-1	-2	6	3	4		28
5	0	0	10	10	-10	-5	-3	5	3	3		14
6	-1	0	9	9	2	6	-4	4	2	3		30
7	-1	0	8	8	59	40	-5	85	2	2		198
8	2	1	7	7	109	82	-5	94	114	55		466
9	10	3	6	6	160	125	-4	99	119	61		586
10	19	7	6	5	202	163	0	101	122	65		689
11	28	11	6	5	233	196	5	102	123	66		775
12	35	14	8	5	249	218	11	102	124	67		833
13	38	18	10	5	253	246	17	102	125	68		882
14	37	23	13	6	243	270	23	103	125	68		911
15	33	32	16	6	232	281	28	104	126	68		926
16	28	42	18	8	212	321	31	104	126	69		959
17	25	50	19	9	185	403	33	105	126	69		1024
18	22	53	20	11	152	407	32	106	15	17		834
19	19	50	21	14	108	263	29	25	9	10		549
20	16	41	21	16	65	99	25	16	6	7		310
21	12	27	20	18	49	67	19	11	5	6		235
22	9	16	20	18	37	48	14	9	4	5		179
23	7	10	19	18	27	34	9	8	4	4		140
24	5	7	16	17	16	21	5	7	4	4		101

Table 39 Example Office Cooling Loads, September Design Day

Local Standard Hour	Sensible Cooling Load, W										Room Total
	Spandrel Wall $\psi = -30^\circ$	Spandrel Wall $\psi = +60^\circ$	Brick Wall $\psi = -30^\circ$	Brick Wall $\psi = +60^\circ$	Window $\psi = -30^\circ$	Window $\psi = +60^\circ$	Roof (70% to room)	Overhead Lighting	Equip- ment	Occupants	
<i>a</i>	<i>b</i>	<i>c</i>	<i>d</i>	<i>e</i>	<i>f</i>	<i>g</i>	<i>h</i>	<i>i</i>	<i>j</i>	<i>k</i>	<i>l</i>
1	0	0	16	15	-15	-13	-2	8	4	4	17
2	-1	-1	14	13	-21	-18	-4	7	4	4	-2
3	-2	-2	12	11	-27	-22	-5	6	4	4	-20
4	-3	-3	11	10	-33	-26	-6	6	3	4	-38
5	-3	-3	9	8	-38	-30	-7	5	3	3	-53
6	-4	-4	8	7	-38	-29	-8	4	2	3	-59
7	-4	-4	6	6	84	-8	-8	85	2	2	160
8	-1	-3	5	5	272	32	-9	94	114	55	564
9	10	-1	4	4	337	75	-8	99	119	61	700
10	25	2	4	3	324	112	-6	101	122	65	751
11	39	5	5	3	262	142	-1	102	123	66	745
12	48	9	7	2	237	173	4	102	124	67	775
13	52	15	11	3	231	205	11	102	125	68	822
14	51	26	15	3	215	228	16	103	125	68	850
15	46	38	19	4	187	388	21	104	126	68	1001
16	37	50	22	6	155	535	24	104	126	69	1128
17	27	58	25	8	123	582	25	105	126	69	1148
18	20	58	26	11	86	379	23	106	15	17	740
19	15	49	26	14	48	107	20	25	9	10	323
20	10	32	25	16	32	62	15	16	6	7	222
21	7	18	23	18	19	35	10	11	5	6	151
22	5	10	22	18	9	17	6	9	4	5	104
23	3	5	20	17	0	4	3	8	4	4	69
24	1	2	17	16	-11	-6	0	7	4	4	34

Table 40 Room Peak Cooling Loads for Different Room Orientations

Case	Surface Azimuth, Exposure 1	Surface Azimuth, Exposure 2	Time of True Peak Load	True Peak Room Load, W	Room Load at July 3:00 PM, W
1 (SE,SW)	-30°	+60°	Sept 5:00 PM	1148	926
2 (SW,NW)	+60°	+150°	Sept 5:00 PM	1138	916
3 (NW, NE)	+150°	-120°	July 3:00 PM	872	872
4 (NE,SE)	-120°	-30°	July 1:00 PM	905	883
Total	—	—	—	4063	—

tation, the time of peak load for individual envelope load components and for the room itself can be difficult to predict from intuition or experience for a specific building project. As a result the common practice is to calculate loads for a range of times of day and times of year, and then examine the results to identify the true peak load and time of load for individual rooms. Room load calculations are tedious by hand, but a multiple-hour calculation is feasible using a spreadsheet or software application for load calculation. When software is used, this typically involves calculating room loads for 24 h design cooling days corresponding to the 21st of each month. This section will demonstrate the importance of calculating loads for a wide range of times of day and times of year to determine the true peak load for rooms. If the range of times is too constrained, the engineer risks missing the true peak load and therefore under sizing airflow and thermal cooling capacity for the room.

In section 9.1, a detailed cooling load calculation was presented for the example office for July 3:00 PM. This time was chosen because it is the time of peak outdoor air dry-bulb temperature in design-day weather profiles and historically has been assumed to be the time of peak room load. However, July 3:00 PM is not the time of true peak load for this room. It is not the largest load in July, and in fact, the true peak load occurs at September 5:00 PM. Tables 38 and 39 show the detailed load profiles for July and September, respectively. Comparing Tables 38 and 39, the July peak is at 5:00 PM and is 1029 W while the September peak in Table 39 is 1151 W at 5:00 PM (hour 17). The true peak is 12% larger than the July peak, and

24% larger than the July 3:00 PM load. Note that the internal load components are the same in July and September. The wall loads are smaller due to the cooler design-day outdoor temperatures in September and in spite of the higher solar irradiance on the walls. The roof load is also lower, due both to the cooler outdoor temperatures and lower intensity of solar irradiance on the horizontal roof surface. But the window loads are much larger due to the more intense solar irradiance, and this overcomes the reduction in wall and roof loads to result in a higher total room load than in July.

To illustrate the effect of orientation further, examine four copies of the example office, each rotated 90 from the other, as shown in Table 40. In the four cases, all room characteristics are the same except orientation. As the table shows the peak load times vary.

- Case 1: As noted, the peak time of September 5:00 PM is driven by the window loads due to more intense solar irradiance in fall months. This peak load is 24% larger than the July 3:00 PM load.
- Case 2: This office also has a peak time of September 5:00 PM, driven by the same factors as Case 1. While the northwest-facing window will be less strongly affected by fall solar irradiance, the effect for the southwest-facing window is strong enough to drive the room peak to September. In this case the peak load is also 24% larger than the July 3:00 PM load for this room.
- Case 3: Walls and windows face northerly directions and as a result window loads and wall loads are smaller. This reduces the

Table 41 Peak Heating Load Calculation

Opaque Envelope Component	U-factor, W/(m ² ·K)		Area, m ²		(Indoor DB – Outdoor DB), K		Heating Load, W
Windows	3.180	×	(3.72 + 3.72)	×	(22.2 – (-5.6))	=	658
Spandrel Walls	0.278	×	(5.57 + 5.57)	×	(22.2 – (-5.6))	=	86
Brick Walls	0.261	×	(5.57 + 3.72)	×	(22.2 – (-5.6))	=	67
Roof	0.165	×	12.08	×	(22.2 – (-5.6))	=	55
Infiltration Component	Infiltration C _s , J/°K		Infiltration Flow Rate Q _s , L/s		(Indoor DB – Outdoor DB), K		Heating Load, W
Infiltration	1.206	×	9.2	×	(22.2 – (-5.6))	=	308
Total							Heating Load, W
Total Room Load	—		—		—		1174

effect of orientation and the peak time occurs at July 3:00 PM when outdoor dry-bulb is at its maximum value.

- Case 4: Walls and windows face north-easterly and south-easterly. The southeasterly facing window has higher load during the fall months, but the northeasterly facing window does not. As a result this case behaves like Case 3, peaking in a summer month. Note the time of peak load is at 1:00 PM, earlier in the day than the other cases because its exterior surfaces face eastward. In this case the true peak is 2% larger than the July 3:00 PM load.

Finally, note that three of the four rooms do not peak at July 3:00 PM. If loads were only calculated for July 3:00 PM due to intuition about when peak loads were likely to occur, much larger loads for two of the cases would be missed and supply airflow and thermal cooling capacity would be significantly undersized for these rooms.

9.3 EFFECT OF COOLING LOAD DIVERSITY ON PEAK BLOCK LOAD

Previous sections of this example focused on calculation of peak cooling loads for individual rooms. Room loads are important for sizing supply airflow rates for individual rooms and cooling capacity when using room by room equipment such as water source heat pumps or fan coil units. However, the calculation of the peak “block load” also has relevance for building projects. The peak block load is the largest simultaneous load among all rooms in a building, or in a portion of a building such as a floor. The peak block load can be used for a preliminary assessment of airflow capacity or thermal capacity for the project. For example, a central VAV AHU only needs sufficient airflow capacity to meet the simultaneous peak of rooms it serves, rather than the sum of individual room peak airflow rates. A central chiller plant only needs enough capacity to meet the simultaneous peak load of AHUs or fan-coil units it serves rather than the sum of individual AHU or fan-coil peak loads.

When determining the block load it is important not to sum the individual peak room loads. Rather, room loads should be calculated for a wide range of times of day and times of year. Then for each hour, sum the room loads to obtain an hourly block load. Review the resulting hourly block loads across all hours calculated to identify the peak value. This section will illustrate the concept of calculating the peak block load.

Instead of calculating the peak block load for a full-scale building, this example will consider a simplified case where a building contains only the four corner offices described in section 9.2. First, loads for the four offices were calculated for a 24 h design day for the 21st of each month. For each hour the resulting loads were summed to obtain an hourly block load. Then the largest block load was identified. The peak block load is 3752 W at July 5:00 PM.

In this example, the peak block load was at a different time than all four individual room peaks shown in Table 40. Further the peak block load is 8% less than the sum of individual room peak loads

shown at the bottom of Table 40. This difference between the peak block load and the “sum of the peaks” load is known as **load diversity**. Although the diversity of 8% is relatively small in this simple example, it can be much larger in a full scale building. The ultimate effect of load diversity is that central HVAC equipment serving multiple rooms can be sized for a peak load that is often considerably less than the sum of the individual peaks of those rooms.

9.4 SINGLE-ROOM DETAILED HEATING LOAD EXAMPLE

Although the physics of heat transfer that creates heating loads is identical to that for cooling loads, a number of traditionally used simplifying assumptions facilitate a much simpler procedure for peak heating load calculation. As described in the section 7.1, Heat Loss Calculations, design heating load calculations typically assume a single outdoor temperature with no heat gain from solar or internal sources, under steady-state conditions. Thus, space heating load is determined by computing the instantaneous heat transfer rate through building envelope elements ($UA \Delta T$) plus heat required because of outdoor air infiltration.

Room heating load.

Objective: Calculate the peak heating load for the example office.

Solution: Calculation of the individual component heating loads and the total room heating load is shown in Table 41.

For the opaque envelope components, the calculation is $UA \Delta T$. For the Example City location the 99.6% heating design dry-bulb is -5.6°C . The indoor design temperature is 22.2°C . Because solar heat gain is not considered in calculating peak heating loads, similar envelope elements can be combined without regard to orientation. For example the two spandrel wall sections can be combined in a single component load calculation. For this example the U-factors used for cooling calculations were also used for the heating load calculation. In some climates, higher prevalent winds in winter should be considered in calculating U-factors. Chapter 25 provides information on calculating U-factors and surface heat transfer coefficients appropriate for local wind conditions.

For heating conditions an infiltration rate of 1 air change per hour was assumed. The room volume with a 2.74 m floor to ceiling height is $2.74 \times 12.1 = 33.2 \text{ m}^3 = 33 \text{ 200 L}$. Therefore, the infiltration flow rate at one air change per hour is $(33 \text{ 200 L/h})/(3600 \text{ s/h}) = 9.2 \text{ L/s}$. With these airflows, infiltration load can be computed using Equation (9) as shown in Table 41.

The total heating load, shown in the last row of Table 41, is 1174 W.

9.5 CONCLUSION

The example problem illustrates key issues that should be understood and accounted for in calculating peak room cooling and heating loads:

- Room peak cooling and heating loads result from many independently varying sources of heat gain or loss.
- For cooling loads, the sensible heat gain profile must be determined first and then divided into convective and radiant components. The load due to the radiant component of heat gain is calculated considering the dynamic conversion of radiant heat gain to load using RTS factors. Finally, the sensible room load is computed as convective load plus radiant load.
- Peak room cooling loads occur at different times of day and times of year depending on the orientation of exterior walls and fenestration. Calculating loads for a single point in time may miss the true peak load and therefore risks under sizing supply airflow and thermal cooling capacity for the room. Instead, peak room loads should be calculated for a range of times of day and times of year to identify the true peak cooling load.
- The relative importance of each cooling and heating load component varies, depending on the portion of the building being considered. Characteristics of a particular window may have little effect on the entire building load, but could have a significant effect on the supply airflow to the room where the window is located and thus on the comfort of the occupants of that space.
- The peak block load is valuable for preliminary assessments of airflow or thermal capacity for an entire building or a portion of the building such as a floor. To accurately identify the peak block load, room loads must first be computed over a range of times of day and times of year and then summed for each hour to obtain the block load for each hour. The peak block load is identified from the profile of hourly block loads.

10. PREVIOUS COOLING LOAD CALCULATION METHODS

Procedures described in this chapter are the most current and scientifically derived means for estimating cooling load for a defined building space, but methods in earlier editions of the ASHRAE Handbook are valid for many applications. These earlier procedures are simplifications of the heat balance principles, and their use requires experience to deal with atypical or unusual circumstances. In fact, any cooling or heating load estimate is no better than the assumptions used to define conditions and parameters such as physical makeup of the various envelope surfaces, conditions of occupancy and use, and ambient weather conditions. Experience of the practitioner can never be ignored.

The primary difference between the HB and RTS methods and the older methods is the newer methods' direct approach, compared to the simplifications necessitated by the limited computer capability available previously.

The **transfer function method (TFM)**, for example, required many calculation steps. It was originally designed for energy analysis with emphasis on daily, monthly, and annual energy use, and thus was more oriented to average hourly cooling loads than peak design loads.

The **total equivalent temperature differential method with time averaging (TETD/TA)** has been a highly reliable (if subjective) method of load estimating since its initial presentation in the 1967 *Handbook of Fundamentals*. Originally intended as a manual method of calculation, it proved suitable only as a computer application because of the need to calculate an extended profile of hourly heat gain values, from which radiant components had to be averaged over a time representative of the general mass of the building

involved. Because perception of thermal storage characteristics of a given building is almost entirely subjective, with little specific information for the user to judge variations, the TETD/TA method's primary usefulness has always been to the experienced engineer.

The **cooling load temperature differential method with solar cooling load factors (CLTD/CLF)** attempted to simplify the two-step TFM and TETD/TA methods into a single-step technique that proceeded directly from raw data to cooling load without intermediate conversion of radiant heat gain to cooling load. A series of factors were taken from cooling load calculation results (produced by more sophisticated methods) as "cooling load temperature differences" and "cooling load factors" for use in traditional conduction ($q = UA\Delta t$) equations. The results are approximate cooling load values rather than simple heat gain values. The simplifications and assumptions used in the original work to derive those factors limit this method's applicability to those building types and conditions for which the CLTD/CLF factors were derived; the method should not be used beyond the range of applicability.

Although the TFM, TETD/TA, and CLTD/CLF procedures are not republished in this chapter, those methods are not invalidated or discredited. Experienced engineers have successfully used them in millions of buildings around the world. The accuracy of cooling load calculations in practice depends primarily on the availability of accurate information and the design engineer's judgment in the assumptions made in interpreting the available data. Those factors have much greater influence on a project's success than does the choice of a particular cooling load calculation method.

The primary benefit of HB and RTS calculations is their somewhat reduced dependency on purely subjective input (e.g., determining a proper time-averaging period for TETD/TA; ascertaining appropriate safety factors to add to the rounded-off TFM results; determining whether CLTD/CLF factors are applicable to a specific unique application). However, using the most up-to-date techniques in real-world design still requires judgment on the part of the design engineer and care in choosing appropriate assumptions, just as in applying older calculation methods.

REFERENCES

- ASHRAE members can access *ASHRAE Journal* articles and ASHRAE research project final reports at technologyportal.ashrae.org. Articles and reports are also available for purchase by nonmembers in the online ASHRAE Bookstore at www.ashrae.org/bookstore.
- Abushakra, B., J.S. Haberl, and D.E. Claridge. 2004. Overview of literature on diversity factors and schedules for energy and cooling load calculations (1093-RP). *ASHRAE Transactions* 110(1):164-176.
- ASHRAE. 2013. Thermal environmental conditions for human occupancy. ANSI/ASHRAE *Standard* 55-2013.
- ASHRAE. 2019. Ventilation for acceptable indoor air quality. ANSI/ASHRAE *Standard* 62.1-2016.
- ASHRAE. 2019. Energy standard for building except low-rise residential buildings. ANSI/ASHRAE/IES *Standard* 90.1-2016.
- ASHRAE. 2012. Updating the climatic design conditions in the *ASHRAE Handbook—Fundamentals* (RP-1613). ASHRAE Research Project, *Final Report*.
- ASHRAE. 2013. *Underfloor air distribution (UFAD) design guide*, 2nd ed.
- ASTM. 2008. Practice for estimate of the heat gain or loss and the surface temperatures of insulated flat, cylindrical, and spherical systems by use of computer programs. *Standard* C680-08. American Society for Testing and Materials, West Conshohocken, PA.
- Bach, C., and O. Sarfraz. 2018. Update to measurements of office heat gain data. ASHRAE Research Project RP-1742, *Final Project Report*.
- Bauman, F., T. Webster, P. Linden, and F. Buhl. 2007. Energy performance of UFAD systems. CEC-500-2007-050, *Final Report* to CEC PIER Buildings Program. Center for the Built Environment, University of California, Berkeley. www.energy.ca.gov/2007publications/CEC-500-2007-050/CEC-500-2007-050.PDF.

- Bauman, F., S. Schiavon, T. Webster, and K.H. Lee. 2010. Cooling load design tool for UFAD systems. *ASHRAE Journal* (September):62-71. escholarship.org/uc/item/9d8430v3.
- Bliss, R.J.V. 1961. Atmospheric radiation near the surface of the ground. *Solar Energy* 5(3):103.
- CFR. Annual. Energy efficiency program for certain commercial and industrial equipment. *Code of Federal Regulations* 10 CFR 431. U.S. Government Publishing Office, Washington, D.C. www.ecfr.gov.
- Chantrasrisalai, C., D.E. Fisher, I. Iu, and D. Eldridge. 2003. Experimental validation of design cooling load procedures: The heat balance method. *ASHRAE Transactions* 109(2):160-173.
- Claridge, D.E., B. Abushakra, J.S. Haberl, and A. Sreshthaputra. 2004. Electricity diversity profiles for energy simulation of office buildings (RP-1093). *ASHRAE Transactions* 110(1):365-377.
- Eldridge, D., D.E. Fisher, I. Iu, and C. Chantrasrisalai. 2003. Experimental validation of design cooling load procedures: Facility design (RP-1117). *ASHRAE Transactions* 109(2):151-159.
- Feng, J., S. Schiavon, and F. Bauman. 2012. Comparison of zone cooling load for radiant and air conditioning systems. Proceedings of the International Conference on Building Energy and Environment. Boulder, CO. escholarship.org/uc/item/9g24f38j.
- Fisher, D.R. 1998. New recommended heat gains for commercial cooking equipment. *ASHRAE Transactions* 104(2):953-960.
- Fisher, D.E., and C. Chantrasrisalai. 2006. Lighting heat gain distribution in buildings (RP-1282). ASHRAE Research Project, *Final Report*.
- Fisher, D.E., and C.O. Pedersen. 1997. Convective heat transfer in building energy and thermal load calculations. *ASHRAE Transactions* 103(2):137-148.
- Gordon, E.B., D.J. Horton, and F.A. Parvin. 1994. Development and application of a standard test method for the performance of exhaust hoods with commercial cooking appliances. *ASHRAE Transactions* 100(2).
- Hittle, D.C. 1999. The effect of beam solar radiation on peak cooling loads. *ASHRAE Transactions* 105(2):510-513.
- Hittle, D.C., and C.O. Pedersen. 1981. Calculating building heating loads using the frequency of multi-layered slabs. *ASHRAE Transactions* 87(2):545-568.
- Hosni, M.H., and B.T. Beck. 2008. Update to measurements of office equipment heat gain data (RP-1482). ASHRAE Research Project 1482, *Progress Report*.
- Hosni, M.H., B.W. Jones, J.M. Sipes, and Y. Xu. 1998. Total heat gain and the split between radiant and convective heat gain from office and laboratory equipment in buildings. *ASHRAE Transactions* 104(1A):356-365.
- Hosni, M.H., B.W. Jones, and H. Xu. 1999. Experimental results for heat gain and radiant/convective split from equipment in buildings. *ASHRAE Transactions* 105(2):527-539.
- Incropera, F.P., and D.P. DeWitt. 1990. *Fundamentals of heat and mass transfer*, 3rd ed. Wiley, New York.
- Iu, I., and D.E. Fisher. 2004. Application of conduction transfer functions and periodic response factors in cooling load calculation procedures. *ASHRAE Transactions* 110(2):829-841.
- Iu, I., C. Chantrasrisalai, D.S. Eldridge, and D.E. Fisher. 2003. Experimental validation of design cooling load procedures: The radiant time series method (RP-1117). *ASHRAE Transactions* 109(2):139-150.
- Jones, B.W., M.H. Hosni, and J.M. Sipes. 1998. Measurement of radiant heat gain from office equipment using a scanning radiometer. *ASHRAE Transactions* 104(1B):1775-1783.
- Karambakkam, B.K., B. Nigusse, and J.D. Spitler. 2005. A one-dimensional approximation for transient multi-dimensional conduction heat transfer in building envelopes. *Proceedings of the 7th Symposium on Building Physics in the Nordic Countries*, The Icelandic Building Research Institute, Reykjavik, vol. 1, pp. 340-347.
- Kerrisk, J.F., N.M. Schnurr, J.E. Moore, and B.D. Hunn. 1981. The custom weighting-factor method for thermal load calculations in the DOE-2 computer program. *ASHRAE Transactions* 87(2):569-584.
- Komor, P. 1997. Space cooling demands from office plug loads. *ASHRAE Journal* 39(12):41-44.
- Kong, M., and J. Zhang. 2016. Life-cycle cost and benefit analysis of utilizing hoods for light-duty cooking appliances in commercial kitchens (RP-1631, part 2). *Science and Technology for the Built Environment* 22(6):866-882.
- Kong, M., J. Zhang, B. Guo, and K. Han. 2016. Measurements of grease emission and heat generation rates of electric countertop appliances (RP-1631, part 1). *Science and Technology for the Built Environment* 22(6):845-865.
- Kusuda, T. 1967. *NBSLD, the computer program for heating and cooling loads for buildings*. BSS 69 and NBSIR 74-574. National Bureau of Standards.
- Latta, J.K., and G.G. Boileau. 1969. Heat losses from house basements. *Canadian Building* 19(10):39.
- LBNL. 2019. *WINDOW 7.7.10: Window 7 User Manual*, LBNL-48255. Windows and Daylighting Group. Lawrence Berkeley National Laboratory, Berkeley, CA.
- Liesen, R.J., and C.O. Pedersen. 1997. An evaluation of inside surface heat balance models for cooling load calculations. *ASHRAE Transactions* 103(2):485-502.
- Livchak, D., and R. Swierczyna. 2020. Heat and moisture load from commercial dishroom appliances and equipment. ASHRAE Research Project RP-1778, *Final Report*.
- Marn, W.L. 1962. Commercial gas kitchen ventilation studies. *Research Bulletin* 90(March). Gas Association Laboratories, Cleveland, OH.
- McClellan, T.M., and C.O. Pedersen. 1997. Investigation of outdoor heat balance models for use in a heat balance cooling load calculation procedure. *ASHRAE Transactions* 103(2):469-484.
- McQuiston, F.C., and J.D. Spitler. 1992. *Cooling and heating load calculation manual*, 2nd ed. ASHRAE.
- Miller, A. 1971. *Meteorology*, 2nd ed. Charles E. Merrill, Columbus.
- Moftakhari, A., S. Bourne, and A. Novoselac. 2020. Experimental verification of cooling load calculations for spaces with non-uniform temperature radiant surfaces. ASHRAE Research Project RP-172, *Final Report*.
- Nigusse, B.A. 2007. *Improvements to the radiant time series method cooling load calculation procedure*. Ph.D. dissertation, Oklahoma State University.
- Parker, D.S., J.E.R. McIlvaine, S.F. Barkaszi, D.J. Beal, and M.T. Anello. 2000. *Laboratory testing of the reflectance properties of roofing material*. FSEC-CR670-00. Florida Solar Energy Center, Cocoa.
- Pedersen, C.O., D.E. Fisher, and R.J. Liesen. 1997. Development of a heat balance procedure for calculating cooling loads. *ASHRAE Transactions* 103(2):459-468.
- Pedersen, C.O., D.E. Fisher, J.D. Spitler, and R.J. Liesen. 1998. *Cooling and heating load calculation principles*. ASHRAE.
- PG&E. 2010-2016. *Dishwashing machine performance reports: Application of ASTM F2474, standard test method for heat gain to space performance of commercial kitchen ventilation/appliance systems*. PG&E Food Service Technology Center, San Ramon, CA. www.fish-nick.com/publications/appliancereports/dishmachines/.
- Rees, S.J., J.D. Spitler, M.G. Davies, and P. Haves. 2000. Qualitative comparison of North American and U.K. cooling load calculation methods. *International Journal of Heating, Ventilating, Air-Conditioning and Refrigerating Research* 6(1):75-99.
- Rock, B.A. 2005. A user-friendly model and coefficients for slab-on-grade load and energy calculation. *ASHRAE Transactions* 111(2):122-136.
- Rock, B.A. 2018. Thermal zoning for HVAC design: Art or science? *ASHRAE Journal* 60(12):20-30.
- Rock, B.A., and D.J. Wolfe. 1997. A sensitivity study of floor and ceiling plenum energy model parameters. *ASHRAE Transactions* 103(1):16-30.
- Schiavon, S., F. Bauman, K.H. Lee, and T. Webster. 2010a. Simplified calculation method for design cooling loads in underfloor air distribution (UFAD) systems. *Energy and Buildings* 43(1-2):517-528. escholarship.org/uc/item/5w53c7kr.
- Schiavon, S., K.H. Lee, F. Bauman, and T. Webster. 2010b. Influence of raised floor on zone design cooling load in commercial buildings. *Energy and Buildings* 42(5):1182-1191. escholarship.org/uc/item/2bv61ldt.
- Schiavon, S., F. Bauman, K.H. Lee, and T. Webster. 2010c. Development of a simplified cooling load design tool for underfloor air distribution systems. *Final Report to CEC PIER Program*, July. escholarship.org/uc/item/6278m12z.
- Smith, V.A., R.T. Swierczyna, and C.N. Claar. 1995. Application and enhancement of the standard test method for the performance of commercial kitchen ventilation systems. *ASHRAE Transactions* 101(2).
- Sowell, E.F. 1988a. Cross-check and modification of the DOE-2 program for calculation of zone weighting factors. *ASHRAE Transactions* 94(2).
- Sowell, E.F. 1988b. Load calculations for 200,640 zones. *ASHRAE Transactions* 94(2):716-736.

- Spitler, J.D., and D.E. Fisher. 1999a. Development of periodic response factors for use with the radiant time series method. *ASHRAE Transactions* 105(2):491-509.
- Spitler, J.D., and D.E. Fisher. 1999b. On the relationship between the radiant time series and transfer function methods for design cooling load calculations. *International Journal of Heating, Ventilating, Air-Conditioning and Refrigerating Research* (now *Science and Technology for the Built Environment*) 5(2):125-138.
- Spitler, J.D., D.E. Fisher, and C.O. Pedersen. 1997. The radiant time series cooling load calculation procedure. *ASHRAE Transactions* 103(2).
- Spitler, J.D., S.J. Rees, and P. Haves. 1998. Quantitative comparison of North American and U.K. cooling load calculation procedures—Part I: Methodology, Part II: Results. *ASHRAE Transactions* 104(2):36-46, 47-61.
- Sun, T.-Y. 1968. Shadow area equations for window overhangs and side-fins and their application in computer calculation. *ASHRAE Transactions* 74(1):I-1.1 to I-1.9.
- Swierczyna, R., P. Sobiski, and D. Fisher. 2008. Revised heat gain and capture and containment exhaust rates from typical commercial cooking appliances (RP-1362). ASHRAE Research Project, *Final Report*.
- Swierczyna, R., P.A. Sobiski, and D.R. Fisher. 2009. Revised heat gain rates from typical commercial cooking appliances from RP-1362. *ASHRAE Transactions* 115(2):138-160.
- Talbert, S.G., L.J. Canigan, and J.A. Eibling. 1973. An experimental study of ventilation requirements of commercial electric kitchens. *ASHRAE Transactions* 79(1):34.
- Walton, G. 1983. *Thermal analysis research program reference manual*. National Bureau of Standards.
- Wang, F.S. 1979. Mathematical modeling and computer simulation of insulation systems in below grade applications. *Proceedings of the ASHRAE/DOE Thermal Performance of Exterior Envelopes of Buildings Conference*, pp. 456-470. ASHRAE.
- Webster, T., F. Bauman, F. Buhl, and A. Daly. 2008. Modeling of underfloor air distribution (UFAD) systems. SimBuild 2008, University of California, Berkeley.
- Wilkins, C.K., and M.R. Cook. 1999. Cooling loads in laboratories. *ASHRAE Transactions* 105(1):744-749.
- Wilkins, C.K., and M.H. Hosni. 2000. Heat gain from office equipment. *ASHRAE Journal* 42(6):33-44.
- Wilkins, C.K., and M. Hosni. 2011. Plug load design factors. *ASHRAE Journal* 53(5):30-34.
- Wilkins, C.K., and N. McGaffin. 1994. Measuring computer equipment loads in office buildings. *ASHRAE Journal* 36(8):21-24.
- Wilkins, C.K., R. Kosonen, and T. Laine. 1991. An analysis of office equipment load factors. *ASHRAE Journal* 33(9):38-44.
- Zhou, X., S.J. Lochhead, Z. Zhong, and C.V. Huynh. 2016. Low energy LED lighting heat distribution in buildings. ASHRAE Research Project RP-1681, *Final Report*.

BIBLIOGRAPHY

- Alereza, T., and J.P. Breen, III. 1984. Estimates of recommended heat gain due to commercial appliances and equipment. *ASHRAE Transactions* 90(2A):25-58.
- ASHRAE. 1975. *Procedure for determining heating and cooling loads for computerized energy calculations, algorithms for building heat transfer subroutines*.
- ASHRAE. 1979. *Cooling and heating load calculation manual*.
- BLAST Support Office. 1991. *BLAST user reference*. University of Illinois, Urbana-Champaign.
- Buffington, D.E. 1975. Heat gain by conduction through exterior walls and roofs—Transmission matrix method. *ASHRAE Transactions* 81(2):89.
- Burch, D.M., B.A. Peavy, and F.J. Powell. 1974. Experimental validation of the NBS load and indoor temperature prediction model. *ASHRAE Transactions* 80(2):291.
- Burch, D.M., J.E. Seem, G.N. Walton, and B.A. Licitra. 1992. Dynamic evaluation of thermal bridges in a typical office building. *ASHRAE Transactions* 98:291-304.
- Butler, R. 1984. The computation of heat flows through multi-layer slabs. *Building and Environment* 19(3):197-206.
- Ceylan, H.T., and G.E. Myers. 1985. Application of response-coefficient method to heat-conduction transients. *ASHRAE Transactions* 91:30-39.
- Chiles, D.C., and E.F. Sowell. 1984. A counter-intuitive effect of mass on zone cooling load response. *ASHRAE Transactions* 91(2A):201-208.
- Chorpene, B.T. 1997. The sensitivity of cooling load calculations to window solar transmission models. *ASHRAE Transactions* 103(1).
- Clarke, J.A. 1985. *Energy simulation in building design*. Adam Hilger Ltd., Boston.
- Davies, M.G. 1996. A time-domain estimation of wall conduction transfer function coefficients. *ASHRAE Transactions* 102(1):328-208.
- Falconer, D.R., E.F. Sowell, J.D. Spitler, and B.B. Todorovich. 1993. Electronic tables for the ASHRAE load calculation manual. *ASHRAE Transactions* 99(1):193-200.
- Harris, S.M., and F.C. McQuiston. 1988. A study to categorize walls and roofs on the basis of thermal response. *ASHRAE Transactions* 94(2):688-714.
- Hittle, D.C. 1981. *Calculating building heating and cooling loads using the frequency response of multilayered slabs*, Ph.D. dissertation, Department of Mechanical and Industrial Engineering, University of Illinois, Urbana-Champaign.
- Hittle, D.C., and R. Bishop. 1983. An improved root-finding procedure for use in calculating transient heat flow through multilayered slabs. *International Journal of Heat and Mass Transfer* 26:1685-1693.
- Kimura and Stephenson. 1968. Theoretical study of cooling loads caused by lights. *ASHRAE Transactions* 74(2):189-197.
- Kusuda, T. 1969. Thermal response factors for multilayer structures of various heat conduction systems. *ASHRAE Transactions* 75(1):246.
- Mast, W.D. 1972. Comparison between measured and calculated hour heating and cooling loads for an instrumented building. *ASHRAE Symposium Bulletin* 72(2).
- McBridge, M.F., C.D. Jones, W.D. Mast, and C.F. Sepsey. 1975. Field validation test of the hourly load program developed from the ASHRAE algorithms. *ASHRAE Transactions* 1(1):291.
- Mitalas, G.P. 1968. Calculations of transient heat flow through walls and roofs. *ASHRAE Transactions* 74(2):182-188.
- Mitalas, G.P. 1969. An experimental check on the weighting factor method of calculating room cooling load. *ASHRAE Transactions* 75(2):22.
- Mitalas, G.P. 1972. Transfer function method of calculating cooling loads, heat extraction rate, and space temperature. *ASHRAE Journal* 14(12):52.
- Mitalas, G.P. 1973. Calculating cooling load caused by lights. *ASHRAE Transactions* 75(6):7.
- Mitalas, G.P. 1978. Comments on the Z-transfer function method for calculating heat transfer in buildings. *ASHRAE Transactions* 84(1):667-674.
- Mitalas, G.P., and J.G. Arsenault. 1970. Fortran IV program to calculate Z-transfer functions for the calculation of transient heat transfer through walls and roofs. *Use of Computers for Environmental Engineering Related to Buildings*, pp. 633-668. National Bureau of Standards, Gaithersburg, MD.
- Mitalas, G.P., and K. Kimura. 1971. A calorimeter to determine cooling load caused by lights. *ASHRAE Transactions* 77(2):65.
- Mitalas, G.P., and D.G. Stephenson. 1967. Room thermal response factors. *ASHRAE Transactions* 73(2):III.2.1.
- Nevins, R.G., H.E. Straub, and H.D. Ball. 1971. Thermal analysis of heat removal troffers. *ASHRAE Transactions* 77(2):58-72.
- NFPA. 2012. Health care facilities code. *Standard 99-2012*. National Fire Protection Association, Quincy, MA.
- Ouyang, K., and F. Haghighat. 1991. A procedure for calculating thermal response factors of multi-layer walls—State space method. *Building and Environment* 26(2):173-177.
- Peavy, B.A. 1978. A note on response factors and conduction transfer functions. *ASHRAE Transactions* 84(1):688-690.
- Peavy, B.A., F.J. Powell, and D.M. Burch. 1975. Dynamic thermal performance of an experimental masonry building. *NBS Building Science Series* 45 (July).
- Romine, T.B., Jr. 1992. Cooling load calculation: Art or science? *ASHRAE Journal*, 34(1):14.
- Rudoy, W. 1979. Don't turn the tables. *ASHRAE Journal* 21(7):62.
- Rudoy, W., and F. Duran. 1975. Development of an improved cooling load calculation method. *ASHRAE Transactions* 81(2):19-69.
- Seem, J.E., S.A. Klein, W.A. Beckman, and J.W. Mitchell. 1989. Transfer functions for efficient calculation of multidimensional transient heat transfer. *Journal of Heat Transfer* 111:5-12.
- Sowell, E.F., and D.C. Chiles. 1984a. Characterization of zone dynamic response for CLF/CLTD tables. *ASHRAE Transactions* 91(2A):162-178.
- Sowell, E.F., and D.C. Chiles. 1984b. Zone descriptions and response characterization for CLF/CLTD calculations. *ASHRAE Transactions* 91(2A):179-200.

- Spitler, J.D. 1996. *Annotated guide to load calculation models and algorithms*. ASHRAE.
- Spitler, J.D., F.C. McQuiston, and K.L. Lindsey. 1993. The CLTD/SCL/CLF cooling load calculation method. *ASHRAE Transactions* 99(1): 183-192.
- Spitler, J.D., and F.C. McQuiston. 1993. Development of a revised cooling and heating calculation manual. *ASHRAE Transactions* 99(1):175-182.
- Stephenson, D.G. 1962. Method of determining non-steady-state heat flow through walls and roofs at buildings. *Journal of the Institution of Heating and Ventilating Engineers* 30:5.
- Stephenson, D.G., and G.P. Mitalas. 1967. Cooling load calculation by thermal response factor method. *ASHRAE Transactions* 73(2):III.1.1.
- Stephenson, D.G., and G.P. Mitalas. 1971. Calculation of heat transfer functions for multi-layer slabs. *ASHRAE Transactions* 77(2):117-126.
- Sun, T.-Y. 1968. Computer evaluation of the shadow area on a window cast by the adjacent building. *ASHRAE Journal* (September).
- Todorovic, B. 1982. Cooling load from solar radiation through partially shaded windows, taking heat storage effect into account. *ASHRAE Transactions* 88(2):924-937.
- Todorovic, B. 1984. Distribution of solar energy following its transmittal through window panes. *ASHRAE Transactions* 90(1B):806-815.
- Todorovic, B. 1987. The effect of the changing shade line on the cooling load calculations. In ASHRAE videotape, *Practical applications for cooling load calculations*.
- Todorovic, B. 1989. *Heat storage in building structure and its effect on cooling load; Heat and mass transfer in building materials and structure*. Hemisphere Publishing, New York.
- Todorovic, B., and D. Curcija. 1984. Calculative procedure for estimating cooling loads influenced by window shading, using negative cooling load method. *ASHRAE Transactions* 2:662.
- Todorovic, B., L. Marjanovic, and D. Kovacevic. 1993. Comparison of different calculation procedures for cooling load from solar radiation through a window. *ASHRAE Transactions* 99(2):559-564.
- Wilkins, C.K. 1998. Electronic equipment heat gains in buildings. *ASHRAE Transactions* 104(1B):1784-1789.
- York, D.A., and C.C. Cappiello. 1981. *DOE-2 engineers manual* (Version 2.1A). Lawrence Berkeley Laboratory and Los Alamos National Laboratory.